5-2005

Development of an Electronic System for Field-Scale Geomorphometric Measurements

Roberto Negrão Barbosa
University of Tennessee - Knoxville

To the Graduate Council:

I am submitting herewith a dissertation written by Roberto Negrão Barbosa entitled "Development of an Electronic System for Field-Scale Geomorphometric Measurements." I have examined the final electronic copy of this dissertation for form and content and recommend that it be accepted in partial fulfillment of the requirements for the degree of Doctor of Philosophy, with a major in Biosystems Engineering.

John B. Wilkerson, Major Professor

We have read this dissertation and recommend its acceptance:

Daniel C. Yoder, H. Paul Denton, Bruce Ralston

Accepted for the Council:
Dixie L. Thompson

Vice Provost and Dean of the Graduate School

(Original signatures are on file with official student records.)

To the Graduate Council:

I am submitting herewith a dissertation written by Roberto Negrão Barbosa entitled "Development of an Electronic System for Field-Scale Geomorphometric Measurements." I have examined the final electronic copy of this dissertation for form and content and recommend that it be accepted in partial fulfillment of the requirements for the degree of Doctor of Philosophy, with a major in Biosystems Engineering.

John B. Wilkerson
Major Professor

We have read this dissertation
and recommend its acceptance:

Daniel C. Yoder

H. Paul Denton

Bruce Ralston

Accepted for the Council:

Anne Mayhew
Vice Chancellor and
Dean of Graduate Studies

(Original signatures are on file with official student records.)

DEVELOPMENT OF AN ELECTRONIC SYSTEM FOR FIELD-SCALE GEOMORPHOMETRIC MEASUREMENTS

A Dissertation
Presented for the
Doctor of Philosophy
Degree
The University of Tennessee, Knoxville

Roberto Negrão Barbosa
May 2005

DEDICATION

This dissertation is dedicated to my family:
my wife Camila, my son Kurlan,
and my daughter Mirela for their support,
love, affection, and lots of patience.
You are the true light of my life.
I love you all very much.

ACKNOWLEDGMENTS

I would like to thank everyone that helped me successfully complete this project. I want to thank Dr. Ronald E. Yoder, former head of the Biosystems Engineering Department for his support and enthusiasm in arranging me to study at The University of Tennessee. Thanks also for Dr. D. Raj Raman, current department head, for the continuation of the support.

To my major professor Dr. John B. Wilkerson, I wish to express my sincere gratitude. Due to his continuous support, friendship, and encouragement, I was able to complete all tasks while enjoying my work.

To the members of my committee, Dr. H. Paul Denton, Dr. Daniel C. Yoder, and Dr. Bruce Ralston, I wish to thank for all help available throughout the process. Your support and friendship were very important to me.

Finally I want to extend my thanks and appreciation to all BEES staff but in particular to Henry Moody, David Smith, Jeff Sowders, Margaret Taylor, and Craig Wagoner; to BEES professors Dr. William E. Hart, Dr. John T. Ammons, Dr. Joanne Logan, Dr. Al Womac and to fellow graduate students. Thanks to Drs. Schoeneberger and Wysocki (NSSC-NRCS) for allowing me to use their figure in my dissertation.

To all Brazilian citizens living in the Knoxville area, thanks for the support and friendship during the past 4 years. I really appreciate our moments together remembering our country.

ABSTRACT

Terrain attributes are among the most studied soil characteristics. Although important, in only a few areas are topographic features mapped at the field-scale level. These features play an important role in assessing the crop production potential and erosion susceptibility of agricultural fields. Therefore high-resolution mapping of terrain attributes are vital to a better management of production fields. Today, terrain attributes are derived from elevation measurement.

A more direct form of measurement was developed by Rowe and Spencer (1976), pitch and roll angles were used to derive slope gradient and vehicle attitude. Yang (1997) related vehicle attitude to slope aspect. The existing mathematical models are difficult to implement with today's low-cost micro-controllers because of existing trigonometric functions. Research conducted at the Biosystems Department of The University of Tennessee focused on the simplification of existing models and on the development of an electronic system to test two sensing techniques in dual-axial rotational measurement of a roving vehicle: a clinometer and an accelerometer. Tests were conducted in a field with a widely varying topography located on the Blount Experiment Research Unit, by mounting the electronic monitoring system on an ATV. Elevation data measured with a RTK-GPS were used to generate an accurate elevation map. Terrain attributes were calculated in 3 spatial resolutions: 4, 16, and 100 m^2.

Simplification of the mathematical models relating pitch and roll angles to terrain attributes is possible because of the existing limitations on slope gradient of arable lands. Results obtained during field tests show that slope measurement accuracy varied according to spatial resolutions. The density of points used in the calculation of the terrain attributes also contributes to measurement accuracy. In general, mean absolute error

(MAE) were less than 1° for both sensors in all resolutions tested. Data collected from pitch and roll sensors can also be used to detect field elevation changes.

In conclusion, it is possible to rely on measurements of vehicle axial rotation for the computation of field-scale terrain attributes. The sensing techniques tested were successfully used in these measurements. The application of simplified models to derive terrain measurements is possible due to the existing slope gradient limitation of arable lands. It is possible to describe terrain attributes in a scale similar to order I soil maps using the proposed electronic system and models. The system can also be used to pinpoint locations of elevation differences in the field.

TABLE OF CONTENTS

LIST OF TABLES

TABLE **PAGE**

LIST OF FIGURES

FIGURE **PAGE**

CHAPTER I

INTRODUCTION

Justification

Geomorphometry is the measurement and definition of landforms (Dehn, 1999). Terrain attributes produced by geomorphometric measurements are among the most intensively studied soil characteristics. Scientists agree that landform plays an important role in assessing the crop production potential and erosion susceptibility of agricultural fields. Although important, topographic features are mapped at the field scale level in only a few agricultural areas. Existing limitations are vast and go from the high labor cost for traditional measurement techniques to the need for highly trained personnel to operate sophisticated electronic surveying equipment.

Physical and chemical soil properties such as soil depth, organic matter content, nutrient distribution and moisture distribution are affected by terrain properties, and have been studied extensively. Since soils are inherently variable in nature, producers try to optimize crop production inputs by dividing fields into different management zones. The concept of management zones refers to the grouping of soils with similar yield potential so that soil amendments, fertilizers, crop protectors or seed population can be tailored to each zone's needs. Intensively mapping field topography may aid in the creation of management zones. Mapping topography at the field scale level can also provide information about many important yield-influencing variables such as slope gradient and curvature.

Producers and crop consultants collect spatially intensive yield and soil information to be used in an agricultural decision-making processes. However, published soil maps lack the accuracy and spatial resolution needed to be used at the field scale. The use of information sources with different scales of precision may introduce errors in the analysis of productivity factors (Moore, 1993).

Research in field topography measurement is a work in progress. Many tools are being developed and refined to improve field mapping (Renschler et al., 2002). Traditionally, topographic features such as slope gradient, slope aspect, and curvature have been derived from elevation measurements above a pre-determined datum. Such attributes are typically computed with the aid of geographic information system (GIS) technology.

Advances in the computer and electronic industries over the last decades have allowed precision farming to go from concept to reality. Today, agricultural machines are equipped with computers and on-board processors that perform a variety of functions, from estimating crop yield to controlling spray operations. Agriculturalists have become avid users of GPS equipment and electronic instruments to monitor agricultural related activities such as plant health and soil nutrient status.

Although activities such as planting, scouting, and spraying are repeated every season, there has not been an attempt to use these operations to assist in field-mapping terrain attributes. A machine-based, cost-effective system could aid field scale topography mapping, using existing mathematical models that relate vehicle axial rotational measurements to field slope. Such a system could integrate existing monitors and use scheduled field trips to record and refine measurements. This system would not depend on skilled operators or data post-processing.

Some limitations make the development of such system very challenging. The mathematical models used to calculate slope gradient and aspect from vehicle axial measurements are not readily implemented in low-cost micro-controllers because of trigonometric calculations. The challenge is amplified by the dynamic nature of the operating conditions.

Some researchers have used the principle of vehicle axial measurements, but have not attempted to map terrain attributes at the field scale level (Freeland, 1990; Yang et al., 1997; Westphalen et al., 2003). There is no documented scientific work that attempts to quantify the uncertainty associated with vehicle-derived terrain slope and curvature measurements at the field scale level.

Objectives

The goal of this study is to develop a cost-effective data approach to map terrain attributes at the field scale level. Specific objectives are to:

1. Design, fabricate, and test an electronic system to dynamically measure in-field slope gradient, aspect, and curvature;

2. Develop simplified mathematical models relating vehicle axial measurements to soil slope;

3. Evaluate the system’s ability to define landform at the field scale level (order I soil survey).

Dissertation Organization

In order to address the specific objectives listed above, this dissertation is organized in five chapters. Each chapter refers to one or more objectives. Chapter II is a literature review, Chapter III addresses the simplification of existing models, Chapter IV details the fabrication, testing of the data acquisition system, and the evaluation of its use to define landforms at the field scale level, and Chapter V lists our conclusions. Chapters III and IV include their own procedures, results and appendices.

CHAPTER II

BACKGROUND AND LITERATURE REVIEW

The Importance of Terrain Attributes

Measurements of landforms and their attributes are known by many names in the scientific community. Buol (2003) refers to the physical configuration of the land as relief, which he defines as inequalities in elevation and topographic positions of the land surface. Moore et al. (1991) classify landform attributes in two groups: primary and secondary. Primary attributes are directly calculated from elevations measured above a pre-determine datum. Secondary attributes are indices that describe the spatial variability of specific processes occurring in the landscape.

Slope is probably the most researched terrain attribute. Slope is a vector measurement of the rate of change of elevation. The magnitude of a slope measurement is its gradient, and the direction of a slope measurement is its aspect. Slope is widely studied because it affects many of the dynamic processes occurring in the soil, such as soil properties, crop yield, and water movement.

Many scientific studies relate slope gradient and slope aspect to dynamic processes occurring in the soil. Stone et al. (1985) showed corn yield differences on different slope positions. Moore et al. (1993) demonstrated that multiple soil attributes (A-horizon thickness, organic matter content, texture) could be predicted and mapped using terrain parameters such as slope gradient, slope aspect, and profile curvature. Gessler et al. (2000) showed that soil depth, productivity, and mass organic C in the soil profile could be predicted using measurements of slope, contributing area, and topographic wetness index.

Changes in slope also influence water movement. Water is probably the most important factor inducing soil variability and thus one of the most important driving forces in the processes of soil genesis and landscape evolution (Hall, 1991). Soils are expected to be different based on the movement and accumulation of water in hillslope positions (Hall, 1991). Pennock and Acton (1989) used hillslope elements to determine the relative contributions of sedimentation and hydrologic activity to soil formation. The soil characteristics they observed in the field were in accord with the water movement in the landscape.

Water movement and erosion rates are related issues. Erosion is very dependent on slope gradient, in that erosion increases as slope length increases. Soil loss increases more rapidly with slope steepness than it does with slope length. The shape of the slope affects the average soil loss and the location of the soil loss along the slope. The average soil loss from a convex slope can easily be 30% greater than that from a uniform slope with the same average steepness (Renard et al., 1997).

Slope aspect also affects soil microclimate. In the Northern hemisphere, south-facing slopes tend to be warmer and thus droughtier than north-facing slopes (Buol et al., 2003). The surface energy budget is a driving force for evaporation and transpiration processes occurring at the land surface and thus is highly dependent on topography (Moore et al., 1991).

Another important factor in soil research is landform curvature. Evans (1980) defines curvature (convexity) as the rate of change of slope. Profile curvature is the rate of change of slope gradient; plan curvature is the rate of change of slope aspect. Concavity is negative convexity. Mathematically, curvature classification depends on the second derivative of the proposed function in a given interval. A function is called concave if the second derivative is positive in the given interval; it is called convex, or concave downward, if the second derivative is negative. Linearity is defined when curvature is close to zero (Stewart, 1998).

Curvature is also commonly referred to as slope shape. The combination of shapes both across and in the direction of maximum slope yields nine possible geometric forms to describe all slopes. Figure 1 is an example of the possible combinations of slope shape. Curvature strongly influences the lateral movement of water across the surface as overland flow and internally as throughflow. Curvature redistributes moisture received by precipitation, creating distinct microenvironments on the landscape. The complementary influences of curvature on water movement and of soil moisture on landscapes control soil formation and vegetation (Wysocki et al., 2000).

Although curvature is often empirically evaluated by soil scientists in the field, a review of the literature yielded no specific parameter value to distinguish between concavity, convexity, or linearity. A study conducted by Aandahl (1948) recognized the importance of curvature and differences in fertility status and soil morphological properties. Convexity and concavity are important controls on water movement, directly related to the variability of soils in a hillslope (Hall, 1991). Sinai et al. (1981) found that yield and grain size in concave positions were significantly different from those in convex positions.

Landscape positions also influence soil variability. Low-lying slope positions tend to accumulate organic matter (Buol et al., 2003). Rhue (1968) formalized terms to describe geomorphic slope components: head slope for the concave portion, side slope for the linear portion, and nose slope for the convex portion. Hillslope positions are widely known by hillslope elements of summit, shoulder, backslope, footslope, and toeslope (Hall, 1991). A number of studies have found a relationship among soils' physical and chemical properties and hillslope position (Hall, 1991).

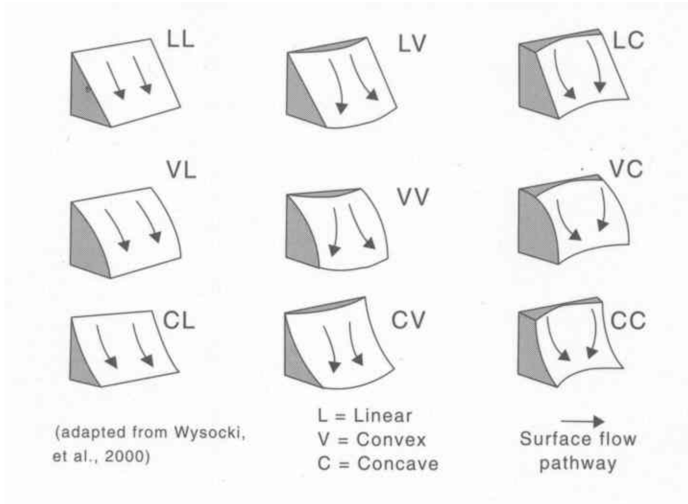

Figure 1. Possible classifications of soil curvature (Wysocki et al., 2000).

Measurement of Terrain Attributes

Elevation

Methods used to measure elevation above a pre-determined datum vary according to the size of the area to be measured. In small areas, typically field-size or even watershed-size, conventional methods such as theodolites and total station equipment yield the best, most accurate results. However, problems associated with conventional methods include high labor and equipment costs. Elevation of larger areas can be determined using digital elevation models (DEM) or triangular irregular networks (TIN) produced with remote sensing techniques such as aerial photogrammetric surveys, airborne laser scanning, or interferometric synthetic aperture radar (Renschler et al., 2002). However, these are expensive techniques and are most often used in large-scale low-resolution applications.

With the development of the Global Positioning System (GPS), highly accurate GPS receivers, often referred as survey-grade GPS, have become the standard for elevation measurement. Survey-grade GPS use a carrier-phase positioning technique to obtain higher level of accuracy (Renschler et al., 2002). Real-time kinematic survey (RTK) continuously computes accurate positional information.

Clark and Lee (1998) obtained elevation errors of 4 to 9 centimeters when using RTK GPS equipment to determine the topography of field-size areas (Renschler et al., 2002). Borgelt et al. (1996) reported errors of 12 centimeters when comparing kinematic GPS elevations to those obtained using a total station-surveying instrument (Renschler et al., 2002).

Although some GPS receivers are suited for elevation measurements, not all of them may be used for this purpose. Differential GPS receivers (DGPS) used in agricultural operations have been used to provide horizontal location information, but not to obtain elevation data, because of its relatively low accuracy (Renschler et al., 2002). Yao and Clark (2000) evaluated the efficacy of using DGPS receivers with 2 to 5 meter horizontal accuracy to develop elevation maps. They reported that this type of DGPS is not suitable for topographic mapping (Renschler et al., 2002).

The accuracy of GPS receivers influences not only measurements of elevation, but also elevation-derived information such as slope gradient. Using kinematic GPS data to calculate elevation and other topographic attributes, Wilson et al. (1998) reported that small differences in GPS-derived elevation at individual points could translate into large differences in slope gradient and catchment area (Renschler et al., 2002).

Renschler et al. (2002) compared the accuracy of six alternative topographic data sources on watershed topography and delineation. The standard measurement was a survey-grade, centimeter-accurate RTK GPS. Alternatives included the photogrammetric-survey derived TIN, the precision agriculture DGPS system, topographic maps, and the 30-m raster DEM. For elevation measurements, they concluded that DGPS receivers performed better than DEM-derived or aerial photogrammetric-derived measurements. In slope measurements however, TIN-derived measurements performed better than DGPS or DEM measurements.

Slope

Slope is a terrain attribute estimated from measured elevation. Burrough (1986) defined slope gradient as the maximum rate of change of elevation and aspect as the compass direction of this maximum change. Using elevation values (z) defined in East (x) and North (y) directions, slope is determined as:

$$Gradient = \tan^{-1}\sqrt{\left(\frac{\partial Z}{\partial X}\right)^2 + \left(\frac{\partial Z}{\partial Y}\right)^2} \qquad [2\text{-}1]$$

and

$$Aspect = \tan^{-1}\left(\frac{-\partial Z / \partial Y}{\partial Z / \partial X}\right) \qquad [2\text{-}2].$$

Evans (1980) used a regular-spaced elevation matrix for the derivation of topographic indices such as slope gradient, aspect, and curvature. A second-order polynomial was used to define the change in elevation in a sub-matrix composed of 9 cells. Elevations of each cell were used to compute the parameters of the polynomial equation (Zevenbergen and Thorne, 1987).

Zevenbergen and Thorne (1987) modified Evan’s method by using a partial quadratic equation passing exactly through the nine elevation points of the 3 by 3 sub matrix:

$$Z = Ax^2y^2 + Bx^2y + Cxy^2 + Dx^2 + Ey^2 + Fxy + Gx + Hy + I \qquad [2\text{-}3].$$

The equation parameters were found using the elevation values of the nine grid cells and Lagrange polynomials. Topographic indices were then computed using arithmetic operations of the equation parameters:

$$Slope\_Gradient = -\sqrt{G^2 + H^2} \qquad [2\text{-}4]$$

$$Slope\_Aspect = \tan^{-1}\left(\frac{-H}{-G}\right) \qquad [2\text{-}5]$$

where:

$$G = \frac{-z_4 + z_6}{2l} \qquad [2\text{-}6]$$

and

$$H = \frac{z_2 - z_8}{2l} \qquad [2\text{-}7].$$

Parameters *z* and *l* in [2-6] and [2-7] are elevation and grid distance respectively. Subscripts on *z* refer to grid position. With some modifications, this is the method used to compute slope and other terrain attributes in most geographic information system (GIS) software today (ESRI, 2005; Srinivasan and Engel, 1991).

Deriving Slope from Vehicle Measurements

Rowe and Spencer (1976) proposed the measurement of two angles of a tractor, pitch (α) and roll (β), as a mean of measuring maximum slope (θ) and heading angle (Ψ). According to Euler's rotation theorem, any rotation may be described using three angles: pitch, roll, and yaw (Weisstein, 1999). Rotations about an imaginary axis crossing the vehicle's longitudinal direction are defined as roll angles. Pitch angles can be defined as rotations about the pitch axis, perpendicular to the roll axis. Refer to Figure 2 for an illustration of pitch and roll.

Rowe and Spencer (1976) defined maximum slope (θ) and heading angle (Ψ) thus:

$$\sin\theta = \sqrt{\sin^2\alpha + \sin^2\beta} \qquad [2\text{-}8]$$

$$\sin\psi = \frac{\sin\beta}{\sqrt{\sin^2\alpha + \sin^2\beta}} \qquad [2\text{-}9].$$

Yang et al. (1997) showed that when measuring pitch and roll angles, if either one of the angles are different than zero, then the one being measured concurrently is not the actual pitch or roll. Yang proposed the following models to calculate ground slope (θ) and vehicle attitude (ψ) based on pitch and roll angles:

$$\cos\theta = \sqrt{\frac{1}{1+\tan^2\alpha + \tan^2\beta}} \qquad [2\text{-}10]$$

$$\tan\psi = \frac{\left(\tan\beta / \tan\alpha\right) \times \left(1+\tan^2\beta\right) + \tan\alpha \times \tan\beta}{\sqrt{1+\tan^2\alpha + \tan^2\beta}} \qquad [2\text{-}11].$$

Yang et al. (1997) also showed that slope aspect could be derived from vehicle heading by determining the vehicle’s orientation and taking into account the vehicle’s driving direction.

Freeland (1990) measured pitch and roll angles of a lawn and garden tractor using electronic clinometers. Measurements were made at three different speeds. Freeland concluded that the sensors were able to

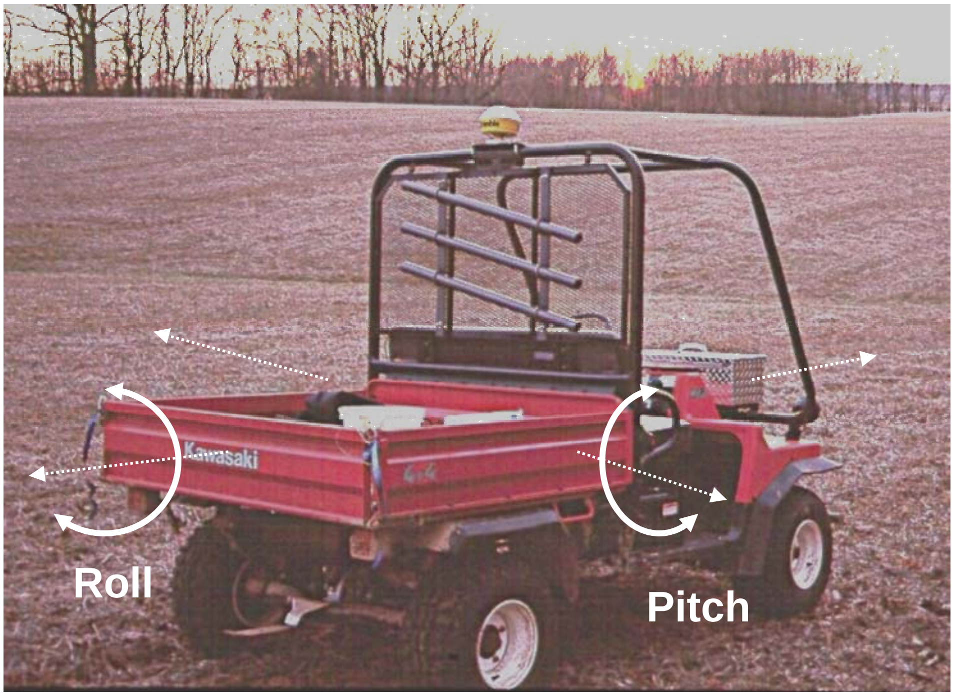

Figure 2. Pitch and roll angles of a vehicle.

produce acceptable results. There is no literature on the measurement of curvature or other terrain attributes using dynamic vehicle data.

Sensors Used in Dynamic Measurements

Sensors are defined as elements capable of converting a change in quantity to a change, usually proportional, in electrical energy (voltage or current) (Rizzoni, 2000). For physical quantities, the active part of a sensor is the transducer (Alciatore, 2003). The sensing technique used by a particular sensor involves the engineering aspects of how the conversion from a physical quantity to electrical energy is made.

Electronic sensors are part of a measurement system that involves sensing the physical quantity, sampling at a desired rate, conditioning and transforming the signal, and storing the sampled signal in digital format. Electronic sensors are widely used in measuring systems to describe, define, or classify soil attributes. Soil attributes are commonly measured with many different sensing techniques.

Recent developments of the electronic industry include micro-electrical-mechanical systems (MEMS). MEMS are the result of the integration of mechanical elements, sensors, actuators and electronics on a common silicon substratum through micro-fabrication technology (Memsnet, 2004). Accelerometers are probably the most widely used MEMS sensors. They are designed to measure acceleration using a variety of sensing techniques such as capacitive, thermal, and piezoelectric. The utilization of accelerometers by the automotive industry has proven to be revolutionary, reducing airbag costs from hundreds of dollars to less than $30 dollars in 1998 (Analog, 2003). Accelerometers are present in common technologies from personal digital assistants (PDA) to washing machines.

A survey of research indicates that accelerometers have had a wide range of applications in agricultural research such as monitoring vibrations, tilt, and accelerations:

- Powers et al. (2000) used accelerometers to monitor pitch and roll angles to prevent tractor overturns and to deploy an automatic rollover protection structure (ROPS). They concluded that accelerometers were able to safely predict tractor overturn.
- Yule et al. (1999) developed an in-field tractor performance monitor equipped with transducers for engine monitoring, a GPS receiver, and a field slope sensor. Pitch and roll angles were measured using a pendulum-type sensor. They concluded that engine and field monitoring

provide invaluable spatial information that could be used to increase operation efficiency.

- Guo et al. (2002) proposed the fusion of GPS and dead reckoning to provide consistent and accurate position measurement. An inertial measurement unit (IMU) composed of three accelerometers and three gyros was used to measure angular rates and accelerations in three orthogonal directions. Kalman filters were used to integrate GPS and IMU readings. The system proved to be efficient in increasing position sampling rate and improving heading angle measurements.
- Westphalen et al. (2003) equipped a self-propelled sprayer with four RTK-GPS receivers and an IMU to measure vehicle attitude and field elevation. The IMU unit was capable of measuring pitch and roll angles, angular velocities and accelerations. They found that the addition of an IMU could improve field elevation measurements.
- Vellidis et al. (2001) used accelerometers to evaluate the harmonic vibration noise present in a peanut combine operation. Based on their sampled data, analog anti-aliasing filtering techniques were also developed.
- Anthonis et al. (2000) used two accelerometers to measure horizontal boom vibrations on a self-propelled sprayer, to operate an active suspension.
- Jeon et al. (2004) built on-board instrumentation with 12 accelerometers for a sprayer to measure vibration inputs, boom acceleration response, height response and sprayer position. Intentionally placed track bumps showed correspondent measurement signals by the accelerometers. According to Jeon, the instrumentation may aid in the design of future sprayers.
- Accelerometers have also been successfully used to experimentally measure the magnitude of raindrop energy at impact (Guzel and Barros, 2001).

In summary, terrain attributes are shown to affect different soil properties, as well as different dynamic processes occurring in the field. Several methods are used to estimate terrain attributes, and vehicle-derived measurements using current electronic technology show promise as a low-cost but still accurate form of estimation. The mathematical models used to relate vehicle pitch and roll measurements to soil slope are not easily programmable in low-cost microprocessors and there is potential gain in the minimization of such models, as shown in Chapter III.

CHAPTER III

MODEL SIMPLIFICATION FOR DYNAMIC SLOPE DETERMINATION USING VEHICLE MEASUREMENTS

Justification

The mathematical models developed by Rowe and Spencer (1976) and Yang et al. (1997) relate axial measurements to slope gradient and vehicle attitude. These models use trigonometric and inverse trigonometric functions as explained in Chapter II. Implementing such models using state-of-the-art micro-controller technology can be challenging since trigonometric calculations require repetitive calculations. For some micro-controllers, the calculation of inverse trigonometric functions is not an option (Parallax, 2000). Most micro-controllers have limited ability to carry out floating-point mathematical calculations.

Since the soil slopes of croplands have a relatively small range, the definition of boundary limits may make it possible to reduce mathematical models to simplified versions. However, it is first necessary to determine if an error term associated with the simplified model can be regarded as negligible according to the usual expression of slope gradient and aspect results measurements in soil science.

Expression of Slope in Soil Science

Measurements of slope gradient are usually expressed in percentages (%) and often rounded to the nearest integer value. According to the USDA-NRCS soil survey manual, slope gradient is defined in classes as shown in Table 1 (All Tables for this Chapter are listed in Appendix A). Slopes can be classified differently depending on their classification as simple or complex. Complex slopes have definite breaks in several directions and in most cases markedly different slopes within the areas delineated (Soil Survey Division Staff, 1993).

Slope aspect classification divides the possible 360° circumference in 8 groups of 45 degrees as shown in Table 2. Slope aspect can be calculated from vehicle attitude if the vehicle heading is known. Several GPS receivers on the market today record heading direction, or “course over ground” (COG).

Boundary Limits of Soil Slope

The National Resources Inventory lists non-federal rural cropland use by capability classification (USDA, 2000). The grouping of soils by capability is primarily for agricultural purposes. Arable soils are grouped according to their potentials and limitations for sustained production of the commonly cultivated crops. Arable soils are divided in classes I through IV according to three categories: capability unit, capability class, and capability subclass. Limitations are progressively greater from I to IV (USDA, 1961). According to the 1997 National Resources Inventory, 376,997,900 acres of non-federal rural land are used as cropland (USDA, 2000). The cropland area classification by capability classes is listed in Table 3.

It is estimated that 94.7% of the cropland of the United States is located in areas where the slope gradient is less than 30% (16.7°). The remaining 19,940,300 acres (5.3%) of cropland are located in soils classified in groups V, VI, VII, or VIII, and labeled not suited for cultivation (USDA, 1961). Generally other limitations contribute to the classification of an area as not suited for agricultural production.

The fact that the majority of cropland area is located in low sloping ground is reinforced by the Land Capability Classification of the British

Society for Soil Science. In this system, 11 to 15° is the assumed upper limit for agricultural equipment operations such as combines and 2-wheel drive tractors (Bibby et al., 1991). Therefore slope gradient of 16.7° can be regarded as a boundary limit that very seldom will be exceeded when machines are used in agricultural operations.

Model Simplification

Slope Gradient

Taking into account this boundary limit for croplands, ground slope (θ) determination based on pitch (α) and roll (β) angles can be estimated using a simplified model. The model is based on the square root of the vector sum of the roll and pitch angles. An error term (ε) has been added to represent the difference between this model and the other two published models, as shown:

$$\theta \cong \underbrace{\sin^{-1}\sqrt{\sin^2\alpha + \sin^2\beta}}_{\text{I}} \cong \underbrace{\cos^{-1}\sqrt{1 \Big/ 1 + \tan^2\alpha + \tan^2\beta}}_{\text{II}} \cong \underbrace{\sqrt{\alpha^2 + \beta^2} + \varepsilon}_{\text{III}} \qquad [3\text{-}1]$$

where I represents the model proposed by Rowe and Spencer, II represents the model proposed by Yang, and III is the simplified model developed to meet the objectives of this research.

Vehicle Attitude

It is also possible to develop a simplified model to calculate vehicle attitude (ψ) based on pitch (α) and roll (β) angles. The simplified model is the inverse tangent of the ratio of roll and pitch angles. An error term (ε) has been added to represent the difference between this model and the other two published models, as shown:

$$\underbrace{\psi \cong \sin^{-1}\frac{\sin\beta}{\sqrt{\sin^2\beta+\sin^2\alpha}}}_{\mathrm{I}} \cong \underbrace{\tan^{-1}\frac{\left(\tan\beta/\tan\alpha\right)\times\left(1+\tan^2\beta\right)+\tan\alpha\times\tan\beta}{\sqrt{1+\tan^2\alpha+\tan^2\beta}}}_{\mathrm{II}}$$

$$\underbrace{\cong \tan^{-1}\frac{\beta}{\alpha}+\varepsilon}_{\mathrm{III}} \qquad [3\text{-}2]$$

where I represents the model proposed by Rowe and Spencer, II represents the model proposed by Yang, and III is the simplified model developed to meet the objectives of this research.

Vehicle attitude results are expressed in radians. The results are the combinations of positive and/or negative axial measurements. The measurement puts the vehicle in one of four possible quadrants, always in reference to the direction of travel. To convert vehicle attitude results to degrees, a correction algorithm has to be used. The assumed convention is

- 1^{st} quadrant: Negative pitch, positive roll
- 2^{nd} quadrant: Positive pitch, positive roll
- 3^{rd} quadrant: Positive pitch, negative roll
- 4^{th} quadrant: Negative pitch, negative roll.

The applied algorithm varies according to models. In the first and fourth quadrants, Rowe and Spencer's model yields negative results only when the roll angle is negative. Yang's model and the simplified model yield negative results in both first and third quadrants. The algorithm developed is listed in Table 4.

Error Term Determination

To determine if the magnitude of the error term created when using simplified models in the calculation of slope is acceptable, a Matlab® program was used. This program simulates the calculation of slope gradient and vehicle attitude from pitch and roll angles. The pitch and roll angles were limited to ±15°[1]. Results obtained from the simplified models were compared with results obtained from the published models. Surfaces showing the distribution of the differences between models according to pitch and roll angles were calculated. Indices used in the assessment of the error term were

- Mean Absolute Deviation (MAD) between models. MAD is calculated as:

$$MAD = \frac{1}{n}\sum_{i=1}^{n} ABS\left(X_i - XX_i\right) \qquad [3\text{-}3]$$

  where $X_i - XX_i$ represents the difference between models. MAD expresses the overall deviation between results of different models.

- The correlation coefficient (r) between results of different models. The correlation coefficient expresses the linear relationship of results obtained with different models.

[1] Pitch and roll angles of 15° will yield a slope gradient of 21.2°, therefore greater than the proposed boundary limit of 16.4°.

Test Results

Slope Gradient

Small differences arose when computing slope gradient using the proposed simplified models. Mean absolute differences in slope gradient calculation bound by ±15° pitch and roll angles were less than 0.12°. The mean absolute deviation (MAD) results are shown in Table 5. Difference between models increased with the increase in slope gradient as shown in Figures 3, 4 and 5 (All figures for this Chapter are listed in Appendix B). The maximum difference between models occurred when both pitch and roll measurements were maximized. The maximum difference between Rowe and Spencer's model and Yang's model was 0.717°. The maximum difference between the simplified model and Rowe and Spencer's model was 0.257°. The maximum difference between the simplified model and Yang's model was 0.460°.

Correlation coefficients between results of different models calculated by Matlab® were greater than 0.999 ($p<0.05$). The error term (ε) introduced with the simplified model can therefore be assumed to be negligible for slope gradient up to 20 degrees (36.4%).

Vehicle Attitude

Vehicle attitude results computed with different models, when using ±15° pitch and roll angles were very similar. The differences between models were less than 0.51°. Results of the mean absolute deviation (MAD) between models are shown in Table 6. Differences increased with the increase in pitch and roll values, as shown in Figures 6, 7 and 8. The difference was maximized when both pitch and roll measurements were at a maximum. The maximum difference between Rowe and Spencer's model and Yang's model was 1.921°. The maximum difference between the simplified model and Rowe and Spencer's model was 0.197°. The maximum difference between the simplified model and Yang's model was 1.921°.

Correlation coefficients between results of different models calculated by Matlab® were also greater than 0.999 ($p<0.05$). In vehicle attitude calculations based on pitch and roll angles, the error term (ε) introduced with the simplified model can be assumed to be negligible for slope gradient up to 20 degrees (36.4%).

Elimination of Trigonometric Functions

Nearly all trigonometric functions were eliminated with the adoption of the simplified models. The only remaining trigonometric function was in the vehicle attitude determination. To eliminate all trigonometric operations from the simplified models, the result of an inverse tangent calculation can be approximated with the Maclaurin series. The Maclaurin series is a special case of the Taylor series, named after the Scottish mathematician Colin Maclaurin, defined thus:

$$f(x)=\sum_{n=0}^{\infty}\frac{f^{(n)}(0)}{n!}x^{n} \qquad [3\text{-}4]$$

where n is the number of terms used in the calculation.

To prove that calculations of vehicle attitude using Maclaurin series are equivalent to those achieved using an inverse tangent function, 2 surfaces were created using ±15° pitch and roll angles, one with each calculation method. The mean absolute deviation and the maximum deviation between surfaces were evaluated.

Surface Comparison

The resultant surface showing the difference between the inverse tangent and the Maclaurin series calculations is shown in Figure 9. The mean absolute deviation was $2.9 \times 10^{-6\circ}$ and the maximum difference $9.5 \times 10^{-5\circ}$. In this comparison, a *n* value equal to 7 was used in the Maclaurin series calculation. The difference between methods is dependent of the number of terms used in the Maclaurin series computation. The greater the number of terms used, the more accurate the result. To speed up calculations for example, a small *n* could have been used. Using *n* equals 2 yields a maximum difference between surfaces of 0.304°. For each additional term included in the Maclaurin series, the maximum difference decreases approximately fivefold, as shown in Table 7.

The logical principle of parsimony, often called “Occam’s Razor”, states that one should not make more assumptions than the minimum needed (Heylighen, 2004). We can use this principle to acknowledge that due to existing slope gradient limitations in agricultural areas, simplified models yield comparable results to existing models in the calculation of slope gradient and aspect. The Maclaurin series can be used to replace an inverse trigonometric function if the selected microprocessor does not support trigonometric calculations. The definition of number of terms to use in the series calculation depends on the accuracy and speed of calculation needed.

CHAPTER IV

DEFINITION OF TERRAIN ATTRIBUTES USING VEHICLE MEASUREMENTS

System Development and Calibration

Concept

The data acquisition system (DAS) discussed below uses vehicle-mounted sensors to monitor axial rotations as a means of mapping terrain attributes and field-scale elevation changes. The assumption is that axis rotations are a function of differences in terrain elevation and vibrations resulting from the vehicle's motor and suspension activities. Therefore, by measuring and filtering axial variations, details of field scale elevation can be mapped.

Circuit Design

Two sensors were used to measure vehicle axial rotation in two planes: a dual-axis clinometer (Schaevits Sensors, model Accustar II/DAS 20) and a dual-axis accelerometer (Analog Devices, model ADXL202E). The clinometer is a proven technology used in similar applications (Freeland, 1990; Yang, 1997), while the accelerometer is a new low-cost technology (MEMS). Both sensors are capacitance-based, measuring angular position with respect to the gravity vector, the most stable external reference force. This is one of the most popular uses for an accelerometer, since an output force is recorded when the axis are moved away from a perpendicular position to the force of gravity, i.e. parallel to the earth's surface.

The clinometer is composed of two hermetically sealed domes spaced 1/8" apart. The lower polyester-plastic dome has 4 capacitive plates while the aluminum upper dome acts as a ground. A fluid with a high dielectric constant is sealed within the dome sandwich, leaving an air bubble between the two domes. Movement of the bubble is related to tilt (Schaevitz Sensors, 2005). The accelerometer is a micro-machined polysilicon structure built on top of a silicon wafer. This structure provides resistance against acceleration forces. Deflection of the structure is measured using a differential capacitor (Analog Devices, 2003).

A signal-conditioning circuit was designed to condition the sensor output signal before it is sampled by the analog-to-digital (A/D) board, and to filter out high frequency components of the output signals. The measurement range was limited to ± 20° based on boundary limitations of field slope, as explained in Chapter III. This limitation was introduced by the amplification of the corresponding portion of the signal to match the A/D input range.

A first-order low-pass filter with a 16-Hz cut-off frequency was designed to attenuate the high frequency component of the accelerometer's output signal (6 KHz at -3db). The cut-off frequency of 16-Hz was chosen on the assumption that at defined traveling speeds (3 ~ 4 m/s), higher-frequency signal components result from vehicle dynamics rather than from elevation changes. The clinometer has a built in low-pass filter (0.25 Hz at -3 db); therefore no additional filter was required.

Four single supply rail-to-rail instrumentation amplifiers (Analog Devices, model AD627) were used in the circuit. Among other features, these amplifiers have the ability to set a variable gain with only one resistor. The sensor output included a bias term of one-half the supply voltage. The output bias was eliminated by biasing the input signal with variable potentiometers. Appendix F lists the circuit schematic and electronic components specifications.

A 12-bit PCMCIA A/D card (Measurement Computing, model PCM-DAS08) was used for sampling and conversion of the amplified sensor outputs. Common characteristics of this A/D are ±5-volt input range, 8 single-ended analog input channels, 2 digital input channels, 3 digital output channels, and 1 input external trigger.

System Calibration

A static calibration procedure was implemented to define sensor sensitivity to slope change after signal amplification and to develop linear equations relating sensor output to axial rotation. During calibration, the circuit was placed on a static tilt test stand. Rotations were applied to the stand while a custom Visual Basic® program sampled the signal from each sensor. True values were found by measuring distances to a referenced position on the test unit.

Linear equation models in SAS® were used to relate the measured voltage to the angle of rotation. These models are listed in Table 8 along with the axis sensitivity of each sensor (All tables for this Chapter are listed in Appendix C).

The accelerometer relates sensor output to force (g) rather than tilt. The following equation was used to convert changes in acceleration to angles of rotation:

$$Rotation\_Angle(\theta) = \sin^{-1}\left(\frac{Force(g)}{1g}\right) \qquad [4\text{-}1].$$

Local Coordinate System Definition

The rotation of sensors in a plane yields positive and negative readings as a vehicle pitches and rolls. A local coordinate system is needed to define sensor output directions as positive or negative and also to match dual-axis output with defined pitch and roll directions. The coordinate system was defined so that pitch rotation matched the x-axis sensor output and roll rotation matched the y-axis sensor output. Clockwise rotations were defined as positive and counterclockwise rotations as negative.

Field Test

Field Overview

A 4.4-ha pasture field (field # 9) on the University of Tennessee Blount Experiment Research Unit (35° 50' N, 83° 57' W) was the testing site. The Blount County soil survey (USDA, 1959) describes this field as having great differences in soils due to topography and parent material. Field # 9 is formed of deep, well-drained soils with varying slopes, in a Cumberland-Dewey-Huntington soil series association. Figure 10 is a reproduction of an aerial photograph showing the field's soil survey (All figures for this Chapter are listed in Appendix D). Descriptions of the soil units, erosion phase, and slope gradient range, based on the 1959 survey, are found in Table 9.

Data Acquisition and Sampling

The DAS was mounted on a bracket attached to the roll cage cross-member of an all-terrain vehicle (Kawasaki Mule, model 2510). A custom Visual Basic® program and a laptop computer were used to sample the hardware filtered signals at 500 Hz and record the average value every 2 Hz.

Prior to data collection, the ATV was placed on flat ground and sensor data was collected to identify bias. The bias was removed before data processing.

A GPS receiver with WAAS (Wide Area Augmentation System) differential correction codes was used only to record horizontal coordinate information (latitude and longitude) during data collection (Trimble, model AG-132). A centimeter-accuracy, dual-frequency RTK-GPS (Trimble, model AgGPS 214) was used to collect high-resolution elevation data. A second dual-frequency RTK-GPS receiver (Trimble, model MS 750) was used as a base station to compute error correction codes. Error correction codes were transmitted to the rover unit via a 900 MHz radio link (Trimble, model Trimtalk 900) while data collected with the RTK-GPS receiver were stored in a different laptop computer on the ATV. Figure 11 illustrates the hardware setup for the field data collection.

To simulate data collection as it would occur during agricultural operations, the ATV was driven perpendicular to the field's slope lines. Speed of operation was similar to the speed of agricultural machinery (3 ~ 4 m/s) normally used. In order to collect spatially intensive data, an average distance of 2 meters was kept between passes.

Data Processing

Dual-axis sensor data collected during field testing represented the variations in pitch and roll angles of the vehicle as it traveled the field surface. A time-domain filter was applied during data collection. A Visual Basic® program was used to average and sample raw data at a 2 Hz frequency. After data were collected, a spatial-domain filter was applied. To compute field-scale terrain attributes, data points were averaged in 3 spatial resolutions: 4 m^2 (2m x 2m), 16 m^2 (4m x 4m), and 100 m^2 (10m x 10m).

Data collected within 10 meters of the field boundary were excluded from the analysis to avoid the introduction of errors caused by vehicle steering and rapid acceleration changes. All measurements were referenced to the same direction to comply with the local coordinate system defined for the DAS.

Simplified models were used to calculate slope gradient and vehicle attitude from the filtered data. These models were shown to yield results comparable to both Rowe and Spencer's (1976) and Yang's (1997) models, as defined in Chapter III.

Slope Aspect Calculation

To calculate slope aspect based on vehicle attitude measurement, it is necessary to know vehicle heading direction. The GPS data collected during the test did not include course-over-ground (COG) information, so linear regression models were used to determine the average heading direction during data collection (Yang, 1997). Ten ten-second samples were used to compute the average heading direction, which was found to be 137°. Data used in the average heading calculation are listed in Appendix H. Slope aspect was calculated according to the following rules:

If vehicle attitude < (360 – heading direction)
Then
Slope Aspect = vehicle attitude + heading direction

If vehicle attitude > (360 – heading direction)
Then
Slope Aspect = vehicle attitude + heading direction – 360.

Curvature Calculation

Curvature results were calculated for the Easting (x) and Northing (y) directions. The results expressed the degree of curvature (°/m) of the grid cell. Curvature is generally classified as linear, concave, or convex, although extensive literature review yielded no single quantitative parameter for this classification. One of the possible reasons for this lack of supporting data may be the imprecision of the empirical and manual processes often used in curvature classification for soil mapping purposes.

An average curvature difference (ACD) value was computed for each spatial resolution. ACD was computed as the average difference in slope gradient between the center-most cell and the eight surrounding cells. The equation used was an adaptation of the surface curvature (Cs) equation defined by Blaszczynski (1997) (Park et al., 2001). In the Cs equation, an average elevation difference is calculated by subtracting the elevation of the centermost cell and the surrounding cells. ACD is defined thus:

$$ACD = \frac{1}{n}\sum_{x=1}^{n}\left(s_i - s_x\right) \qquad [4\text{-}2]$$

where n is the number of cells, s_i is the slope value for the centermost cell and s_x is the slope value for the surrounding grid cell. The ACD value represents the average difference between the slope of a cell and its surrounding cells.

Standard Topographic Measurements

In order to evaluate the accuracy of the geomorphometric data derived from the electronic sensors and the mathematical models, RTK-GPS data were used to create an elevation surface. Terrain attributes of this surface were computed using standard equations defined in Chapter II. Equally-spaced points were extracted from the surface using the same spatial resolutions previously applied to field data. Slope and curvature were computed in Matlab®. Elevation values were also used in slope calculations obtained with GIS software (ESRI ArcView®) as an added standard for assessment, since GIS derived measurements are almost always referred as true measurement values.

The elevation surface was interpolated using Universal Kriging, a statistical interpolation method. A total of 32,564 elevation points collected with RTK-GPS were used for the interpolation process, one half of which were used in the interpolation method. The other half were used in a jackknife procedure to verify the quality of the interpolation. In this procedure, estimated elevation values are compared to measured ones left out of the interpolation. The mean absolute error (MAE) of prediction was 0.0279 meters. Terrain attributes derived from this elevation surface were used as the standard (i.e. the truth) to compared sensor-derived measurements.

Calculating True Slope

The average elevation differences in Easting (x) and Northing (y) directions were calculated thus:

$$\frac{\partial z}{\partial x} = \frac{\left(E_{i,j+1} - E_{i,j}\right) + \left(E_{i+1,j+1} - E_{i+1,j}\right)}{2d} \qquad [4\text{-}3]$$

$$\frac{\partial z}{\partial y} = \frac{\left(E_{i+1,j} - E_{i,j}\right) + \left(E_{i+1,j+1} - E_{i,j+1}\right)}{2d} \qquad [4\text{-}4]$$

where E represents the estimated elevation at each grid corner, i and j represent the upper-left corner of the grid cell, i is the subscript representing a row change, j is the subscript representing column change, and d is the grid distance. Therefore for each of the spatial resolutions tested, the change in elevation in Northing and Easting directions for a grid cell was calculated as the average elevation difference between estimated elevation values at each corners of a grid cell. Elevation values used in this calculation are from the interpolated surface based on RTK-GPS points.

Slope gradient and slope aspect were calculated using [2-1] and [2-2]. Because slope aspect results are bounded by $\pm\pi$ radians, a conversion algorithm is needed to express aspect in degrees. The algorithm used was based on the elevation difference in the Easting direction. If the difference was positive, 270° was added to the result; otherwise 90° was added.

Calculating Slope Using GIS

Slope calculation can be performed in various ways using GIS software (Srinivasan, 1991). ArcView® uses a method derived by Horn (ESRI, 2005): elevations of raster-based cells in a 3-by-3 window are used to compute elevation differences of the center cell, in Easting (x) and Northing (y) directions. Using a center cell (E_5) as an example, elevation differences can be computed thus:

$$\frac{\partial z}{\partial x} = \frac{(E_3 + 2E_6 + E_9) - (E_1 + 2E_4 + E_7)}{8d} \qquad [4\text{-}5]$$

$$\frac{\partial z}{\partial y} = \frac{(E_7 + 2E_8 + E_9) - (E_1 + 2E_2 + E_3)}{8d} \qquad [4\text{-}6]$$

where the subscript in E refers to the cell position. E_1 is the upper-left corner cell. Subscript numbers increase to the right and down. These values are then used to compute slope gradient and slope aspect using [2-1] and [2-2]. Elevation values derived from the interpolated surface created using RTK-GPS points were used to calculate slope gradient and aspect using GIS algorithms.

True Curvature Calculation

Easting and Northing curvature surfaces and ACD surface were calculated using the same process described in the previous section.

Measurement Comparisons

The slope gradient results were compared to the true slope gradient and GIS-derived slope gradient using the following indices:

- Coefficient of determination (r^2).

- Mean Absolute Error (MAE).

- Model Efficiency (ME). The ME method developed by Nash and Sutcliffe is used to compare model results to observed values (Renschler, 2002). ME values can range from $-\infty$ to 1. The closer the value is to 1, the better the model representation is. ME is calculated as

$$ME = 1 - \frac{\sum_{i=1}^{n}(x_i - y_i)^2}{\sum_{i=1}^{n}(y_i - \overline{y})^2} \qquad [4\text{-}7]$$

where x is the observed slope gradient value, y is the true slope gradient and $\overline{y}$ is the mean gradient value.

- Group Classification, GC: Slope gradient is often expressed and mapped in slope groups (Appendix A, Table 1). The frequency of correct group classification by each sensor was calculated as a function of spatial resolution.

As explained in Chapter III, when analyzing slope gradient, soil scientists often group results in classes. These classes are general guidelines of how slope gradients should be grouped; groupings can vary slightly depending on the region of interest. Table 10 shows a representative soil gradient class for East Tennessee according to experts at The University of Tennessee (Denton, 2005).

For comparison of slope aspect results, the index used was the correct group classification. In curvature comparisons, direction-dependent mean absolute differences between calculated, GIS, and sensor-derived surfaces were computed. ACD surfaces were also calculated and compared.

Test Results

Overall Operating Conditions

The field used for this analysis has the maximum measured slope gradient of 15.6° and the minimum value of 0°[2]. The average slope gradient was 3.5° with a standard deviation of 2.3°. The The average slope gradient value and the maximum value were within the tested range for the application of the simplified models discussed in Chapter III.

The average absolute acceleration during the field test was 0.26 g and 0.22 g for the direction of travel and perpendicular to the direction of travel, respectively. The maximum and minimum measured accelerations were 3.5 g and –2.3 g in the direction of travel , and 3.5 g and –2.4 g perpendicular to the direction of travel. The average velocity during data collection was 1.3 meters per second.

Slope Gradient

Results of slope gradient measurement varied according to spatial resolution, when compared to the surface-derived results. Overall, lower resolution data (100 m^2) yielded better gradient results than higher resolutions (4 and 16 m^2). An average of 73.5 points were used to compute results for 100 m^2 resolution (0.735 points per m^2), 12.9 points for 16 m^2 (0.806 points per m^2), and 3.6 points for 4 m^2 resolution (0.9 points per m^2). All indices used in this comparison (r^2, MAE, model efficiency, percent group classification) improved when larger spatial resolutions were evaluated.

---

[2] Values obtained with Matlab calculations using surface-derived measurements in 4m^2 resolution.

Complete slope gradient results are shown in Table 11. Figures 12, 13, and 14 are scatter plots of calculated versus estimated slope gradient using different methods. The figures also show the error distribution as a function of method of measurement. In all resolutions, the error distribution for both sensors is concentrated within ±1°. Figures 15, 16, and 17 are composite maps of slope gradient results by measurement method.

Analysis of the error term distribution as shown in Appendix J show that sensor calibrations can be improved since they show a tendency to under predict slope gradient in high sloping areas. This trend is more noticeable on the accelerometer. Due to the nature of the test conducted, lower resolutions (16 and 100 m^2) included more than just one pass of the vehicle when collecting data. Multiple passes in different directions may have helped attenuate systematic errors present in the sensor's calibration.

To determine the role of the spatial resolution and point density in determining slope gradient, results for the 16 m^2 resolution were calculated using different number of points collected with the sensors, as shown in Table 12. Results show that both the distribution and the density of the points affect slope gradient estimation.

At higher resolutions, the clinometer and the accelerometer presented very similar results in all indices. Decreasing spatial resolution impacted more positively the results from the clinometer than the results of the accelerometer. In lower resolutions, indices presented by the clinometer were very close to indices calculated by the GIS.

GIS-derived results showed an artificial smoothness introduced in the gradient results, especially in high resolutions. This smoothness is resultant of the utilization of elevation data of nearby cells in the calculation of terrain attributes as explained in Chapter II. All indices improved in lower resolutions. The calculation of terrain attributes from surfaces derived from high accuracy GPS equipment is still prone to error depending on the method and resolution used.

Slope Aspect

Results of the slope aspect calculations followed the same logic presented in the slope gradient results section. There was a great improvement in results going from the highest resolution ($4m^2$) to the intermediate resolution (16 m^2). The rate of improvement decreased when going from 16 to 100 m^2. Table 13 presents the results obtained for different resolutions. Figures 18, 19, and 20 are composite maps of slope aspect results by resolution, showing all measurement methods.

Comparing results from 4 m^2 and 100 m^2 resolutions, the accuracy of slope aspect classification increased from 53.9% to 85.1% for the clinometer and from 48.4% to 77.7% for the accelerometer. The clinometer and the accelerometer presented very similar results at all resolutions. At the lowest resolution (100 m^2), indices presented by both sensors were very close to the indices calculated by the GIS.

Curvature

Curvature results were computed in respect to Easting and Northing directions. The results expressed the degree of curvature (°/m) of the surface in the direction of increasing coordinates. Negative curvatures were assumed to be concave, whereas positive curvatures were assumed to be convex. No published data exists suggesting what curvature threshold should be used to differentiate between concave, linear and convex; therefore there is no easy way to show an overall curvature for a field. A vector sum of Easting and Northing curvatures eliminates the signs of the curvature results and simply expresses the degree of curvature of the terrain. With no positive and negative differences in the surface results, there is no way to show concavity, linearity, or convexity.

Curvature surface differences were computed for all methods of measurements, and the mean absolute difference (MAD) was calculated for each resolution. Curvature surfaces calculated with GIS, clinometer, and accelerometer data were compared to calculated curvature surfaces. The results are shown in Table 14. Decreasing areal resolution also decreased differences between sensor-derived and RTK-derived curvatures. Sensor results at 16 m^2 resolution were comparable to the results obtained with GIS software.

Figures 21, 22, and 23 are composite maps of the ACD surfaces. Thresholds of –0.25° and 0.25° were chosen to classify the surfaces, based on personal experience. High resolution ACD surfaces like the one shown in Figure 21 appear very fuzzy, whether calculated or sensor-derived. The GIS-derived surface in the same resolution introduced an artificial smoothness to the data. In general, sensor-derived surfaces tended to over-predict curvatures, even at lower resolutions, as shown in Figures 22 and 23.

Landform Punctual Measurements

This system has a potential use as a punctual landform indicator. Earlier tests have indicated that changes in sensor signal are closely related to field elevation changes (Barbosa et al., 2004). Thus, one may hypothesize that the signal may be used to pinpoint elevation changes, according to vehicle traveling direction.

To test this hypothesis, raw sensor data were selected from the field test. A total of twenty field passes were selected, evenly distributed in the field. Ten passes were selected in the direction of travel, and ten perpendicular to the direction of travel. Data from both sensors were compared to changes in elevation as measured by the RTK-GPS. The coefficient of correlation (r) was used to measure the strength of the linear relation between variables.

Noise was inherently introduced in the data due to the vehicle's traveling dynamics. Pitch results are noisier than roll results, since pitch measurements are in the traveling direction. Digital filters were applied to the data to attenuate the effect of this noise. Digital filters are mathematical operators used on discrete data, often divided between finite impulse response (FIR) and infinite impulse response (IIR) filters (Durrance et al, 1997). The filter applied in this study was a direct-form II transposed-implementation of the standard difference equation, which can be used to find running averages (The Matworks Inc., 2002). Filter sizes used were 5, 10, 15, and 20 points.

Strong correlations were found between sensor axial data and changes in field elevation, as measured by RTK GPS. Linear coefficient correlation (r) results are shown on Tables 15 and 16 as functions of the absolute elevation difference between points and of the filter size. Results showed that the higher the elevation difference between points, the higher the correlation coefficient. Digital filtering of the data increased the correlation coefficient between the sensor output and the rate of change of elevation. Pitch results presented a higher correlation when a higher filter size was used (i.e. 20 points). Roll results presented high correlation coefficients even with lower filter sizes. From the high correlation coefficients obtained in this test, a conclusion can be drawn that monitoring the axial signal output can help identify locations where there is an inversion of the elevation trend. Appendix E graphically shows pitch and roll results of all 20 passes, along with the RTK-GPS elevation and the calculated rate of change of elevation.

The coefficient of variation (cv) can be used to pinpoint elevation inversion trends. Examples are shown in Figures 24 and 25. The sensor data used in the graphs of Figure 24 are filtered versions of the raw data, using a 20-point filter. This feature can be useful to mark field locations such as drainage points and ridges.

This system can potentially be used to map soil curvature using punctual pitch and roll signals. The measured rate of change of elevation is closely followed by the variation of the sensor output, as verified in Appendix E. A negative or positive rate of change of elevation yielded similar response from the sensors. Therefore, spatially-variable soil curvature measurements can be defined by monitoring sensor output changes from positive to negative and vice-versa. Peak rates of change and their associated location can also be pinpointed. Sensor output value close to zero means no difference in surface elevation; therefore no curvature radius can be defined.

Further testing should be done on this hypothesis. The results shown here confirm the hypothesis that angle-measuring sensors can detect the rate of change of elevation in field conditions and that minimal signal conditioning is needed in order to use this signal.

CHAPTER V

SUMMARY AND CONCLUSIONS

Summary

The specific objectives of this work were to design, fabricate, and test an electronic system to dynamically measure field-scale geomorphometric features. The computed attributes were slope gradient, slope aspect, and curvature. Other objectives were to simplify existing mathematical models relating vehicle axial measurements to soil slope and to evaluate the system's ability to define landform at the field scale level.

An electronic system was built using the concept that data obtained by monitoring the axial rotations of a roving vehicle can be used to map in-field topography. This method rests on the assumption that axis rotations are a function of differences in terrain elevation and vibrations, resulting from the vehicle's motor and suspension activities. Therefore measuring and filtering axial variations can help to detail field scale elevation.

Two sensing techniques were evaluated for their ability to measure in-field topography changes, a dual-axis clinometer and a dual-axis accelerometer. Both sensing techniques are capacitance-based, measuring angular position with respect to the gravity vector, the most stable external reference force. A signal-conditioning circuit was designed to provide regulated energy for the sensors, to condition the output signal to be sampled by an analog-to-digital (A/D) board, and to filter high frequency signal components.

A field test was conducted in field # 9 of the Blount Experiment Research Unit of the Knoxville Experiment Station. The electronic system was mounted on an ATV and driven through the field mimicking a regular work trajectory. Simplified models were used to compute slope gradient and slope aspect. Simplified slopes were shown to yield similar results to published models by both Rowe and Spencer (1976) and Yang (1997).

Elevation data measured with a RTK-GPS were used to generate a highly accurate elevation map for the field. Terrain attributes were calculated based on elevation points in 3 areal resolutions: 4 m^2, 16 m^2, and 100 m^2. Computed terrain attributes were used as standard measurements for sensor result comparison. GIS-derived measurements computed using Arcview® were used as an added standard for comparisons.

The mean slope gradient of field # 9 is 3.5°, with a maximum gradient computed as 15.6°. It was found that slope gradient accuracy measured with electronic sensors varied with terrain resolution. The spatial resolution used to aggregate the data and the density of points collected are important issues in the estimation of terrain attributes. In general, lower resolutions (larger areas) provided better estimations of slope, as shown in Tables 11 and 13. Higher density of points also contributed positively for the slope estimation as shown in Table 12.

Slope aspect was evaluated by assessing the system's ability to correctly classify a cell into one of eight groups (N, NE, E, SE, S, SW, W, NW). Classification rates of 85.1% were achieved for the clinometer and 77.7% for the accelerometer in the 100 m^2 resolution. GIS-derived measurements had 87.8% accuracy in the same resolution.

Curvature results were calculated for Easting and Northing directions. The mean absolute difference between calculated surfaces and sensor-derived ones were computed. Differences varied greatly among resolutions tested for both sensors. High-resolution results ($4m^2$) presented a higher MAE than lower resolution results (100 m^2) for both sensors, as shown in Table 14. An average curvature difference (ACD) was computed for each sensing technique and for GIS data. The sensor-derived data had a tendency to over-predict curvature results, whereas the GIS-derived data had a tendency to under predict curvature results.

Vehicle axial data can be used to detect field elevation changes. Digital filtering of the data increases the correlation coefficient between sensor data and changes in field elevation. The correlation is also positively affected by increases in mean absolute elevation differences. Monitoring the axial signal output can help identify locations where there is an inversion of the elevation trend. This feature can be useful to mark field locations such as drainage points and ridges.

Conclusions

Based on the results obtained in the study, the following conclusions can be made:

- It is possible to rely on measurements of vehicle axial rotation for the computation of field-scale terrain attributes. Slope gradient, slope aspect, and landform curvature are among the terrain attributes that can be derived from such measurements.

- Sensing techniques such as the ones represented by the clinometer and accelerometer can be successfully used in such measurements. The simplicity in their use, ruggedness, and low cost are key marks for their application in the agricultural environment.

- Simplified mathematical models based on pitch and roll measurements can be used for slope gradient and aspect results. Such results are comparable to those obtained with published models.

- It is possible to accurately measure terrain attributes in a scale equivalent to an Order I soils map. Accuracy is dependent on the spatial resolution and density of points collected.

- Vehicle axial data can also be used to pinpoint elevation changes in the field. The correlation of rate of change of elevation and axial data were above 0.9 when filtered points were used. Correlation rates increase with increases in the mean absolute elevation difference between points.

- Digital filtering of pitch and roll data is necessary to attenuate noise introduced by vehicle dynamics. The signal-to-noise ration is lower in the pitch direction than in the roll direction.

Suggestions for Future Work

Field mapping of important yield-influencing attributes such as terrain attributes is vital for the progress of precision farming. Monitoring axial rotations in agricultural vehicles may be an easy and cheap way to map such important variables in high resolution. However, the sensors and system developed in this study were prototypes. More research is required before this technique can be made commercially available. I hope the Biosystems Engineering Department of the University of Tennessee will secure the necessary funds for the continuation of this research.

I suggest that future research be intensified in the utilization of the accelerometer as a potential sensor for this measurement due to its volume-oriented price and product quality. Improving filtering algorithms will give the system the necessary accuracy. Calibration procedures must also be improved to reflect differences in vehicle dynamic.

Disclaimer

Mentions of commercial products are solely for the purpose of providing specific information and should not be construed as product endorsements by the author or The University of Tennessee.

BIBLIOGRAPHY

BIBLIOGRAPHY

Aandahl A.R. 1948. The Characterization of Slope Positions and Their Influence on the Total Nitrogen Content of a Few Virgin Soils in Western Iowa. Soil Science Society of America Journal. 52:1076-1081.

Alciatore D.G., Histand M.B. 2003. Introduction to Mechatronics and Measurements Systems. Second Edition. McGraw-Hill.

Analog Devices. Accelerometer Design and Applications. Available at: www.analog.com. Accessed on: September 20, 2003.

Anthonis J., Ramon H., De Baerdemaeker J. 2000. Implementation of an Active Horizontal Suspension on a Spray Boom. Transactions of the ASAE. Vol 43(2): 213-220. ASAE.

Bakhsh A., Colvin T.S., Jaynes D.B, Kanwar R.S., Tim U.S. 2000. Using Soil Attributes and GIS for Interpretation of Spatial Variability in Yield. Transactions of the ASAE. Vol. 43:819-828. ASAE

Barbosa R.N., Wilkerson J.B., Yoder D.C., Denton H.P. 2004. Evaluating Slope Sensing and Surface Modeling Techniques to Map Topography Changes Within a Field. Proceedings of the 7th International Conference on Precision Agriculture. July, 2004. Minneapolis, MN.

Bibby J.S., Douglas H.A., Thomasson A.J., and Robertson J.S. 1991. Land Capability Classification for Agriculture. MLURI, Aberdeen. ISBN.: 0 7084 0508 8.

Buol S.W., Southard R.J., Graham R.C., McDaniel P.A. 2003. Soil Genesis and Classification. Fifth Edition. Iowa State Press.

Burrough P.A. 1986. Principles of Geographical Information Systems for Land Resources Assessment. Oxford Science Publications. Monographs on Soil and Resources Survey No. 12.

Dehn M., Gartner H., Dikau R. 1999. Principles of Semantic Modeling of Landform Structures. Geocomputation 99. Available at: www.geovista.psu.edu/sites/gecomp99/Gc99/067/gc_067.htm. Acessed on February 22, 2005.

Denton H.P. 2005. Interview by the author, Knoxville, TN. January, 2005.

Durrence J.S., Hamrita T.K., Vellidis G.V., Perry C.D., Thomas D.L., Kvien C.K. 1997. Digital Signal Processing Techniques for Optimizing a Load Cell Peanut Yield Monitor. ASAE Paper No. 97-3009. ASAE.

Elder J.A., SCS, and Springer M.E. 1959. Soil Map of The University of Tennessee Blount Farm. Soil Science Department of The University of Tennessee. Scale 1” = 660’.

ESRI. 2005. Knowledge Base, Technical Articles. Article ID: 21345. Available at: www.esri.com. Acessed on February, 11, 2005.

Evans I.S. 1972. General Morphometry Derivatives of Altitude and Descriptive Statistics. In: Spatial Analysis in Geomorphology by Richard J. Chorley. London.

Evans I.S. 1980. An Integrated System of Terrain Analysis and Slope Mapping. Zeitschrift fur Geomorphologie. Suppl.-Bd 36. 274-295.

Florinsky I.V. 1998. Accuracy of Local Topographic Variables Derived from Digital Elevation Models. International Journal of Geographical Information Science. Vol. 12, No. 1, 47-61.

Florinsky I.V. 1998. Combined Analysis of Digital Terrain Models and Remotely Sensed Data in Landscape Investigations. Progress in Physiscal Geography. 22, 1 (1998) pp. 33-60.

Freeland R.S. 1990. Instrumentation for Tractor Pitch and Roll Angle Measurement. Applied Engineering in Agriculture. Vol. 6(5): 548-552. ASAE.

Fridgen J.J., Kitchen N.R., Sudduth K.A., Drummond S.T., Wiebold W.J., Fraisse C.W. 2004. Management Zone Analyst (MZA): Software for

Subfield Management Zone Delineation. Agronomy Journal. 96:100-108 (2004). American Society of Agronomy. Madison, WI.

Gessler P.E., Chadwick O.A., Chamran F., Outhouse L., Holmes K. 2000. Modeling Soil-Landscape and Ecosystems Properties Using Terrain Attributes. Soil Science of America Journal. 64:2046-2056.

Guo L.S., Zhang Q., Han S., 2002. Position Estimate of Off-Road Vehicles Using a Low Cost GPS and IMU. ASAE Paper Number 021157. ASAE.

Guzel H., Barros A.P. 2001. Using Acoustic Emission Testing to Monitor Kinetic Energy of Raindrop and Rainsplash Erosion. Proceedings of the International Symposium in Soil Erosion Research for the 21st Century. Pp 525-528. ASAE.

Hall G.F., Olson C.G. 1991. Predicting Variability of Soils from Landscape Models. In: Spatial Variabilities of Soils and Landforms. SSSA Special Publication no. 28. Soil Science Society of America. Madison, WI.

Heylighen F. Occam's Razor. Principia Cibernetica Web. Available at: http://pespmc1.vub.ac.be/OCCAMRAZ.html Acessed on: December 10, 2004.

Horn B.K.P. 1981. Hill Shading and the Reflectance Map. Proceedins of the IEEE. Vol. 69(1) 14-47.

Jaynes D.B., Kaspar T.C., Colvin T.S., James D.E. 2003. Cluster Analysis of Spatiotemporal Corn Yield Patterns in an Iowa Field. Agronomy Journal. 95:574-586 (2003). American Society of Agronomy. Madison, WI.

Jeon H.Y., Womac A.R., Wilkerson J.B., Hart W.E., 2004. Spray Boom Instrumentation for Field Use. Transactions of the ASAE. Vol. 47(3): 659-666. ASAE.

Memsnet. 2004. MEMS and Nanotechnology Clearinghouse. Available at: www.memsnet.org. Accessed on: February 09, 2004.

Moore I.D., Gessler P.E., Nielsen G.A., Peterson G.A. 1993. Soil Attribute Prediction Using Terrain Analysis. Soil Science Society of America Journal. 57:443-452 (1993). Madison, WI.

Moore I.D., Grayson R.B., Ladson A.R. 1991. Digital Terrain Modeling: A Review of Hydrological, Geomorphological, and Biological Applications. Hydrological Processes. Vol. 5, 3-30 (1991).

Ott R.L. 1993. An Introduction to Statistical Methods and Data Analysis. Fourth Edition. Duxbury Press. Belmont, CA.

Parallax, Inc. 2000. BASIC Stamp Programming Manual. Parallax, Inc.

Park S.J., McSweeney K., Lowery B. 2001. Identification of the Spatial Distribution of Soils Using a Process-Based Terrain Characterization. Geoderma. 103 (2001) 249-272.

Pennock D.J., Acton D.F. 1989. Hydrological and Sedimentological Influences on Boroll Catenas, Central Saskatchewan. Soil Science Society of America Journal. 53:904-910.

Powers J.R., Harris J.R., Etherton J.R.,Snyder K.A., Ronaghi M., Newbraugh B.H. 2000. Performance of an Automatic Deployable ROPS on ASAE Tests. Journal of Agricultural Safety and Health. Vol. 7(1): 51-61. ASAE.

Renard K.G., Foster G.R., Weesies G.A., McCool D.K., Yoder D.C. (coordinators). 1997. Predicting Soil Erosion by Water: A Guide to Conservation Planning With the Revised Universal Soil Loss Equation (RUSLE). USDA. Agricuture Handbook No. 703, 403 pp.

Renschler C.S., Flanagan D.C., Engel B.A., Kramer L.A., Sudduth K.A. 2002. Site-Specific Decision-Making Based on RTK GPS Survey and Six Alternative Elevation Data Sources: Watershed Topography and Delineation. Transactions of the ASAE. Vol. 45(6):1883-1895. ASAE.

Rizzoni, G. 2000. Principles and Applications of Electrical Engineering. Third Edition. McGraw-Hill.

Rowe E.P.H., Spencer H.B. 1976. An Instrumented Tractor for Use in Motion Behaviour Studies on Sloping Ground. Journal of Agricultural Engineering Research. (1976) 21, 355-360.

Ruhe R. V., Walker P.H. 1968. Hillslope Models and Soil Formation: I. Open Systems. Transactions of the 9th International Congress of Soils Science. 4:551-560.

Schmidt J., Evans I.S., Brinkmann J. 2003. Comparison of Polynomial Models for Land Surface Curvature Calculation. International Journal of Geographical Information Science. Vol. 17, No. 8, 797-814.

Schaevitz Sensors, 2005. Sensor Datasheet. Available at: www.msiusa.com/schaevitz. Acessed on March, 2005.

Schoeneberger P.J., Wysocki D.A., Benham E.C., Broderson W.D. (editors). 2002. Field Book for Describing and Sampling Soils. Version 2.0. Natural Resources Conservation Service, National Soil Survey Center. Lincoln, NE.

Sinai G., Zaslasvsky D., Golany P.1981. The Effect of Soil Surface Curvature on Moisture and Yield – Beer Sheba Observation. Soil Science Society of America Journal. 132:367-375.

Soil Science Society of America. 1991. Spatial Variabilities of Soils and Landforms. Special Publication N° 28. Madison, WI.

Soil Survey Division Staff. 1993. Soil Survey Manual. United States Department of Agriculture.

Srinivasan R., Engel B.A. 1991. Effect of Slope Prediction Methods on Slope and Erosion Estimates. ASAE. Vol. 7(6): 779-783. November 1991. ASAE.

Stewart J. 1998. Calculus: Concepts and Contexts. Brooks Cole Publishing Company. Pacific Grove, CA.

Stone J.R., Gilliam J.W., Cassel D.K., Daniels R.B., Nelson L.A., Kleiss H.J. 1985. Effect of Erosion and Landscape Position on Productivity of Piedmont Soils. Soil Science Society of America Journal. 49:987-991.

The Mathworks Inc. 2002. Filter Design Toolbox. Available at: www.mathworks.com. Acessed on February 17, 2005.

Tomer M.D., James, D.E. 2004. Do Soil Surveys and Terrain Analyses Identify Similar Priority Sites for Conservation? Journal of the Soil Science Society of America. 68:1905-1915 (2004). Soil Science Society of America. Madison, WI.

USDA. Natural Conservation Service. 2000. Summary Report. 1997 Natural Resources Inventory (Revised December, 2000). Washington, DC.

USDA. Soil Conservation Service. 1959. Blount County Soil Survey. Series 1953, No. 7.Issued in July, 1959.

USDA. Soil Conservation Service. 1961. Land-Capability Classification. Agriculture Handbook N° 210. Washington, DC.

Vellidis G., Perry C.D., Durrance J.S., Thomas D.L., Hill R.W., Kvien C.K., Hamrita T.K., Rains G. 2001. The Peanut Yield Monitoring System. Transactions of the ASAE. Vol. 44(4): 775-785. ASAE.

Weisstein E.W. 1999. Euler Angles. Mathworld – A Wolfram Web Resource. Available at: www.mathworld.wolfram.com/EulerAngles.html. Acessed on February, 11, 2005.

Westphalen M.L., Steward B.L., Han S. 2003. Topographic Mapping Through Measurement of Vehicle Attitude. ASAE Paper Number: 031008. ASAE.

Wysocki D.A., Schoeneberger P.J., Garry H.E. 2000. Geomorphology of Soil Landscapes. In: Sumner, M.E. (ed.). 2000. Handbook of Soil Science. CRC Press LLC, Boca Raton, FL. ISBN: 0-8493-3136-6.

Yang C., Shropshire G.J., Peterson C.L. 1997. Measurement of Ground Slope and Aspect Using Two Inclinometers and GPS. Transactions of the ASAE. Vol. 40(6): 1769-1776. ASAE.

Yule I.J., Kohnen G., Nowak M. 1999. A Tractor Performance Monitor with DGPS Capability. Computer and Electronics in Agriculture. Vol. 23(1999) 155-174.

Zeleke T.B., Si B.C. 2004. Scaling Properties of Topographic Indices and Crop Yield: Multifractal and Joint Multifractal Approaches. Agronomy Journal. 96:1082-1090 (2004). American Society of Agronomy. Madison, WI.

Zevenbergen L.W., Thorne C.R. 1987. Quantitative Analysis of Land Surface Topography. Earth Surface Processes and Landforms. Vol. 12, 47-56.

APPENDICES

APPENDIX A
Chapter III Tables

Table 1. Classes used in slope gradient classification, by percent.

Simple Slopes	Complex Slopes	Limits (%)	
		Lower	**Upper**
Nearly Level	Nearly Level	0	3
Gently Sloping	Undulating	1	8
Strongly Sloping	Rolling	4	16
Moderately Steep	Hilly	10	30
Steep	Steep	20	60
Very Steep	Very Steep	> 45	

Table 2. Classes used in slope aspect classification, in degrees.

Direction	**Limits**	
	Lower	**Upper**
North	337.5°	22.5°
Northeast	22.5°	67.5°
East	67.5°	112.5°
Southeast	112.5°	157.5°
South	157.5°	202.5°
Southwest	202.5°	247.5°
West	247.5°	292.5°
Northwest	292.5°	337.5°

Table 3. Non-federal rural cropland distribution according to capability class.

Class	Area (acres)	% Of Total	Slope Gradient
I	26,566,800	7.0	Nearly Level (0-3%)
II	174,950,400	46.4	Gentle Slopes (1 to 8%)
III	114,963,000	30.5	Moderately Steep Slopes (10 to 30%)
IV	40,577,400	10.8	Steep Slopes (20 to 30%)
Total	357,057,600	94.7	-

Table 4. Algorithm used for vehicle attitude correction.

Quadrants	(I)	(II)
First	ψ	ABS (ψ)
Second	180 – ψ	180 – ψ
Third	180 – ψ	180 – ψ
Fourth	360 + ψ	360 – ψ

where:

(I) – Rowe and Spencer model

(II) – Yang and Simplified models

ψ – vehicle attitude.

Table 5. Comparison of slope gradient mean absolute deviation between different models, in degrees. Bounded by ±15°.

	Rowe	**Yang**	**Simplified**
Rowe	-	0.113	0.039
Yang	0.113	-	0.074
Simplified	0.039	0.074	-

Table 6. Comparison of vehicle attitude mean absolute deviation between different models, in degrees. Bounded by ±15°.

	Rowe	**Yang**	**Simplified**
Rowe	-	0.502	0.066
Yang	0.502	-	0.502
Simplified	0.066	0.502	-

Table 7. Difference between surfaces calculated using inverse trigonometric function or Maclaurin series, as a function of the number of terms in the Maclaurin series.

Number of Terms (n)	Maximum Difference (degrees)
2	0.3045°
3	0.0536°
4	0.0103°
5	0.0021°
6	0.00044°
7	0.000095°

APPENDIX B

Chapter III Figures

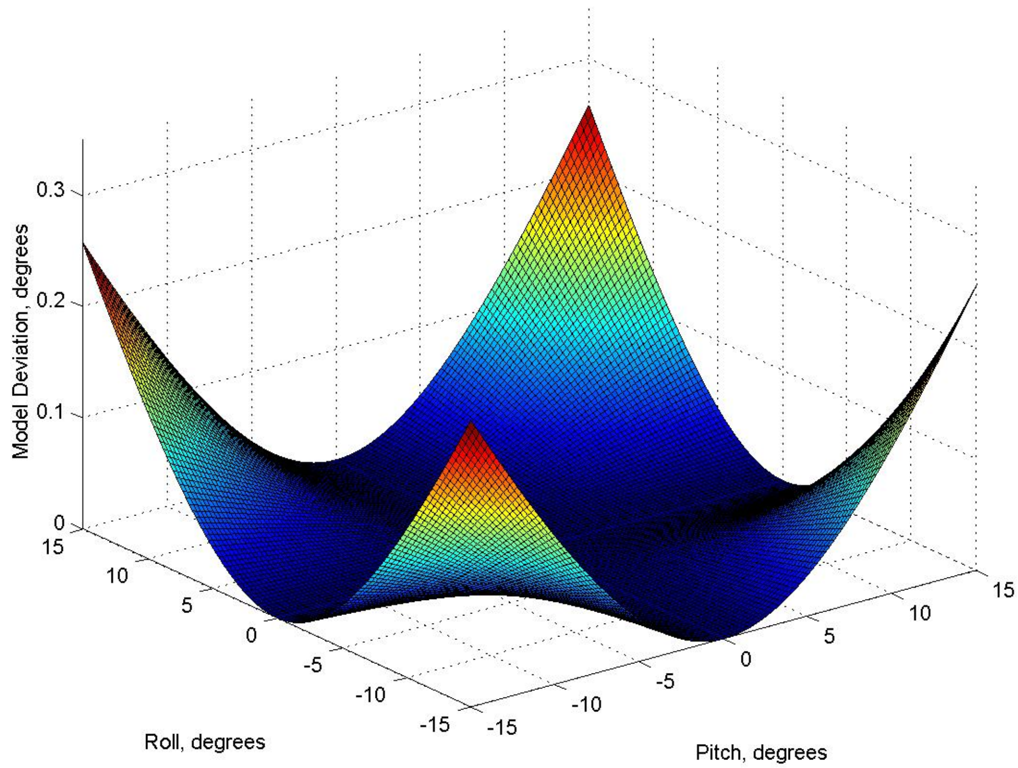

Figure 3. Surface representing the difference in slope gradient calculation between Rowe and Spencer's model and the simplified model as a function of pitch and roll angles.

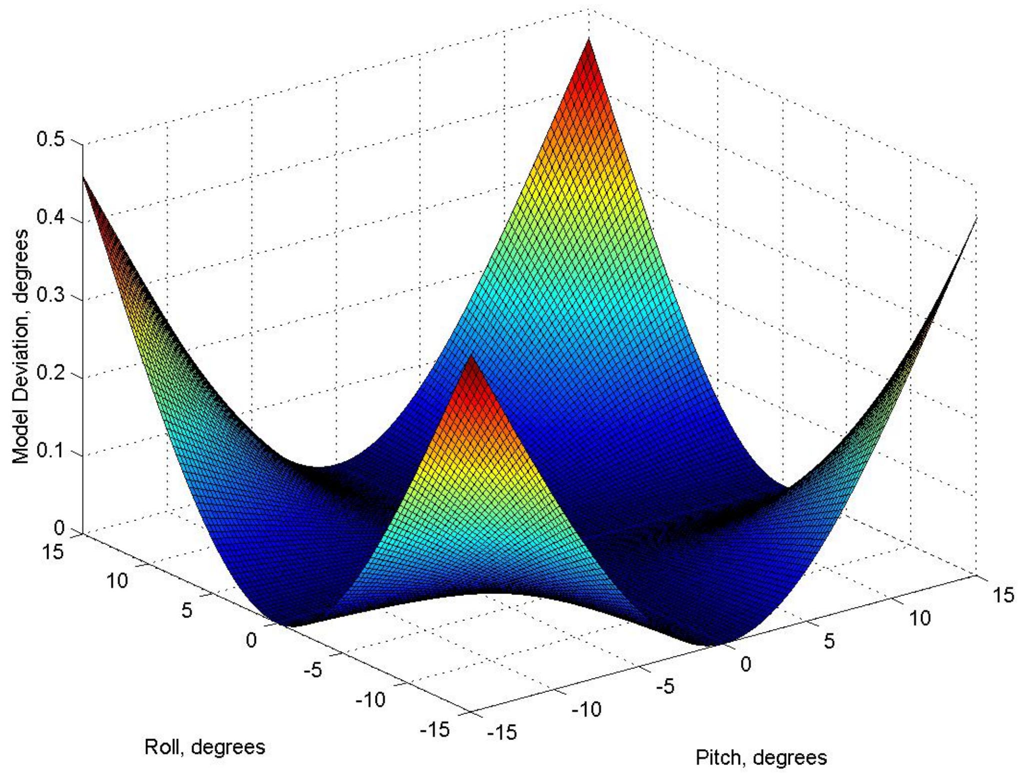

Figure 4. Surface representing the difference in slope gradient calculation between Yang’s model and the simplified model as a function of pitch and roll angles.

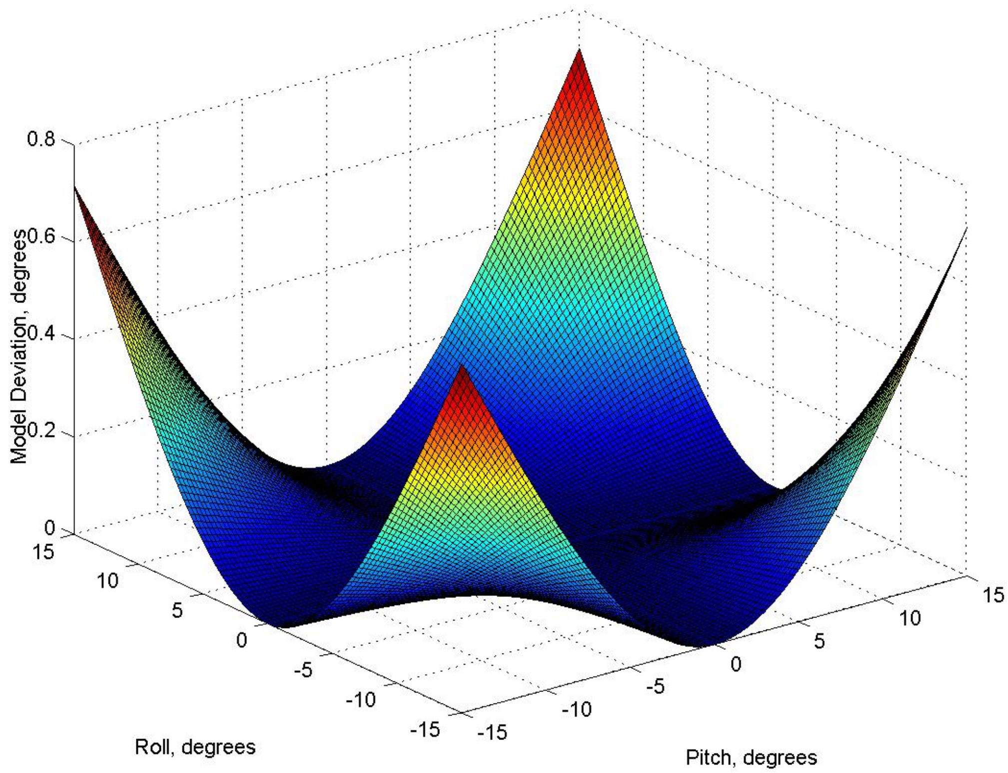

Figure 5. Surface representing the difference in slope gradient calculation between Rowe and Spencer's model and Yang's model as a function of pitch and roll angles.

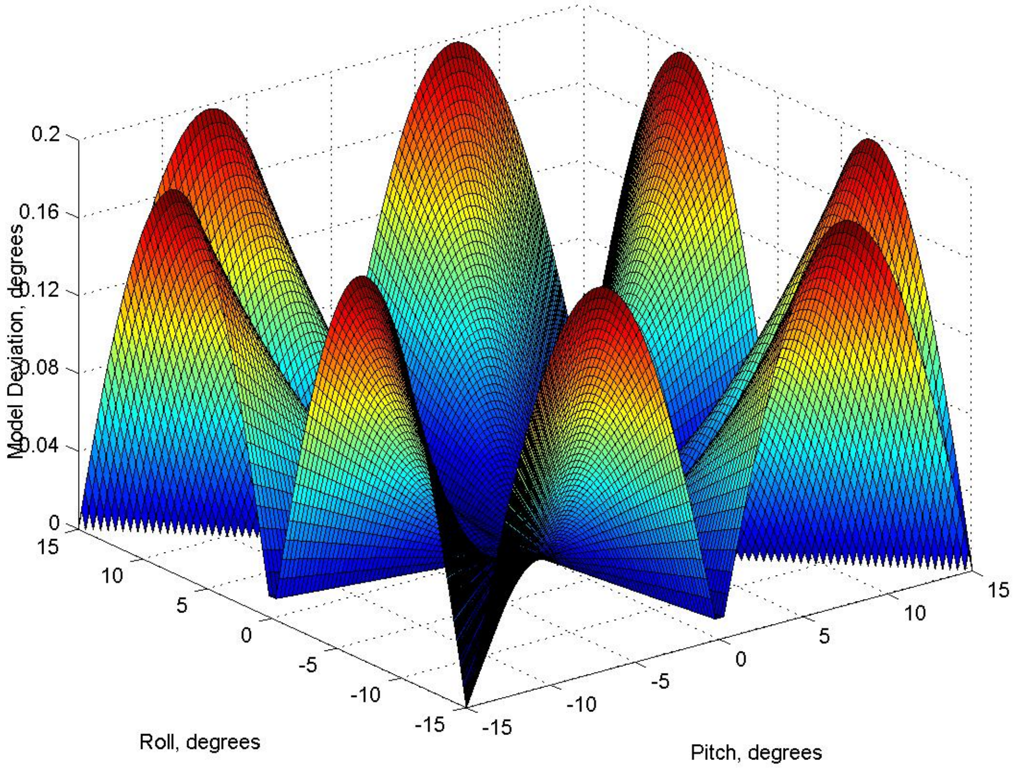

Figure 6. Surface representing the difference in vehicle attitude between Rowe and Spencer's model and the simplified model as a function of pitch and roll angles.

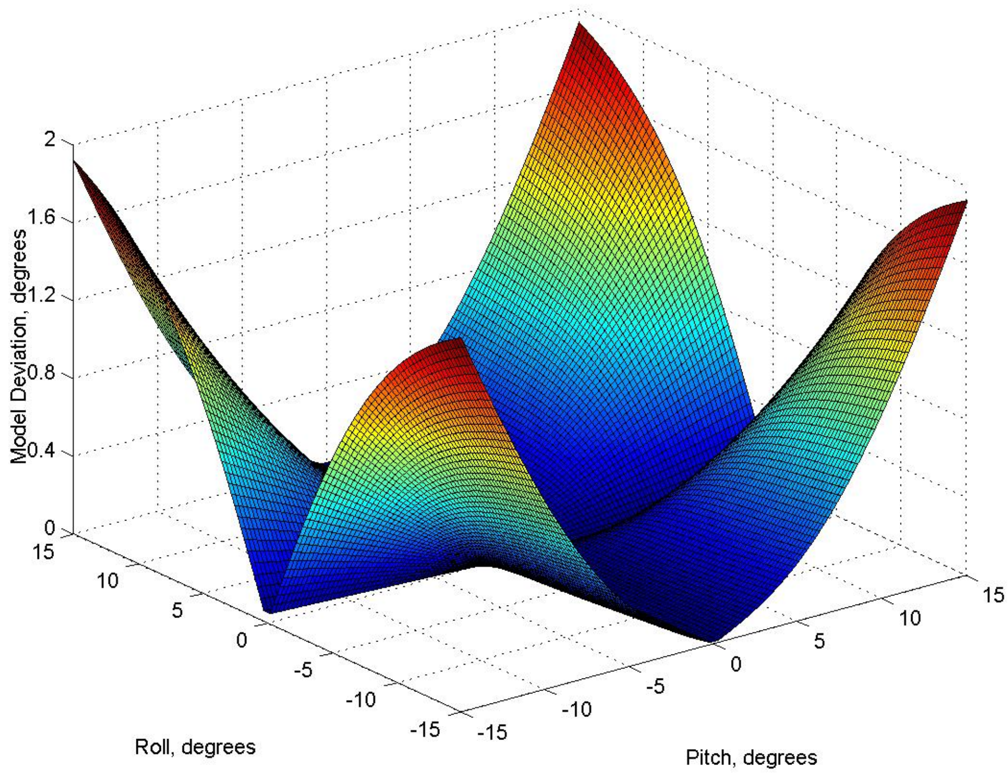

Figure 7. Surface representing the difference in vehicle attitude between Yang's model and the simplified model as a function of pitch and roll angles.

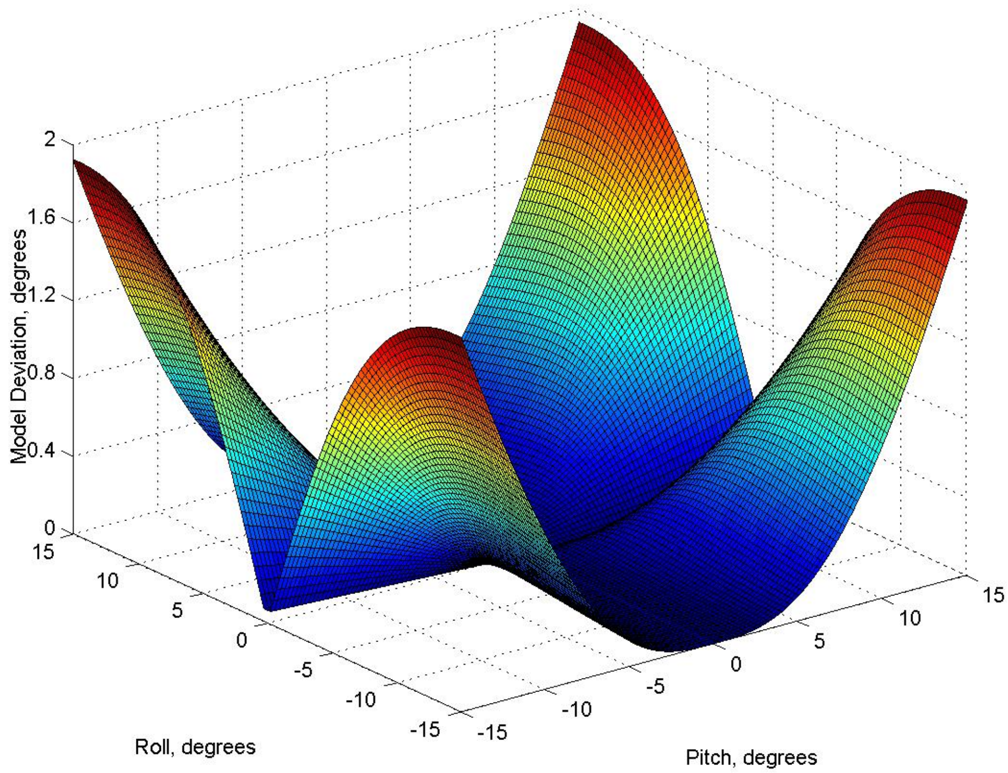

Figure 8. Surface representing the difference in vehicle attitude between Rowe and Spencer's model and Yang's model as a function of pitch and roll angles.

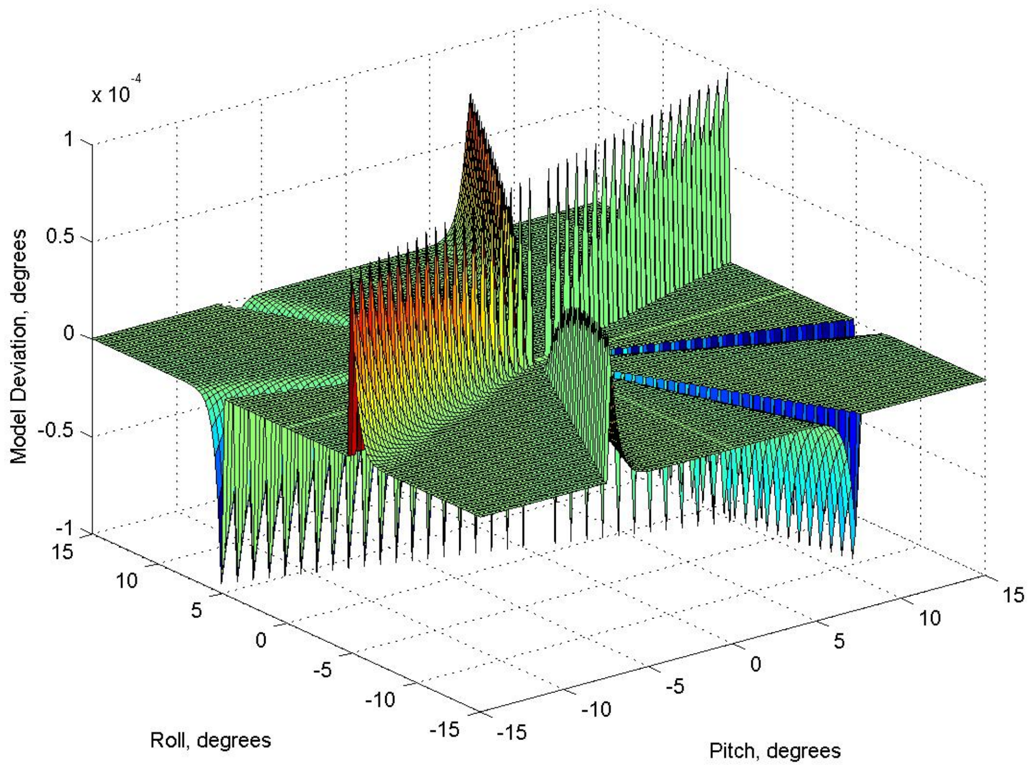

Figure 9. Surface representing the differences between vehicle attitude calculations using an inverse tangent function and the Maclaurin series as a function of pitch and roll angles.

APPENDIX C

Chapter IV Tables

Table 8. Linear equation models, coefficient of determination (r^2), and axis sensitivity (millivolt * $degree^{-1}$) after sensor calibration.

	Clinometer		Accelerometer	
Axis	X	Y	X	Y
Model r^2	0.9976	0.999	0.998	0.999
Sensitivity	258	296	220	186
Linear Equations	0.02201+0.00378*Vs	-0.067+0.0036*Vs	1.4E-03+7.294E-05*Vs	4.3E-03+7.053E-05*Vs

Table 9. Soil series description of field # 9 of the Blount experiment station unit.

Legend	Soil Series	Erosion Phase	Slope Gradient
2	Huntington Silt Loam	-	0 – 2%
20B1	Hermitage Silt Loam	Uneroded	2 – 5%
42C2	Cumberland Clay Loam	Moderately Eroded	5 – 12%
42C3	Cumberland Clay Loam	Severely Eroded	5 – 12%
63C3	Dewey Silty Clay Loam	Severely Eroded	5 – 12%
63D3	Dewey Silty Clay Loam	Severely Eroded	12 – 20%

Table 10. Slope gradient classes generally used in East TN.

Class Number	Limits (%)	Limits (degrees)
I	0 – 2	0 – 1.14
II	2 – 5	1.14 – 2.86
III	5 – 12	2.86 – 6.84
IV	12 – 20	6.84 – 11.31
V	20 – 30	11.31 – 16.7
VI	> 30	> 16.7

Table 11. Coefficient of determination (r^2), mean absolute error (MAE), model efficiency (ME), and group classification (GC) results of slope gradient evaluation using different resolutions when compared to RTK-GPS derived measurements.

	n	r^2	MAE (degrees)	ME	GC (%)
		4 m^2			
GIS	9347	0.730	0.715	0.724	75.6
Clinometer	9347	0.506	1.475	0.305	48.7
Accelerometer	9347	0.396	1.438	0.292	51.4
		16 m^2			
GIS	2272	0.910	0.400	0.905	84.2
Clinometer	2272	0.869	0.539	0.854	78.6
Accelerometer	2272	0.685	0.753	0.670	71.3
		100 m^2			
GIS	336	0.974	0.249	0.969	88.4
Clinometer	336	0.945	0.385	0.931	84.2
Accelerometer	336	0.739	0.634	0.729	74.7

Table 12. Slope gradient results calculated with multiple density of points in a 16 m^2 resolution.

	r^2	MAE (degrees)	ME	GC (%)
All points				
Clinometer	0.869	0.539	0.854	78.6
Accelerometer	0.685	0.753	0.670	71.3
Half the points				
Clinometer	0.717	0.866	0.647	66.4
Accelerometer	0.549	1.016	0.517	63.0
One-fourth of the points				
Clinometer	0.652	0.970	0.545	64.9
Accelerometer	0.485	1.125	0.424	59.5

Table 13. Group classification (GC) results of slope aspect evaluation using different resolutions when compared to RTK-GPS derived measurements.

	n	GC(%)
	4 m^2	
GIS	9347	76.0
Clinometer	9347	53.9
Accelerometer	9347	48.4
	16 m^2	
GIS	2272	83.2
Clinometer	2272	77.4
Accelerometer	2272	71.1
	100 m^2	
GIS	336	87.8
Clinometer	336	85.1
Accelerometer	336	77.7

Table 14. Mean absolute difference in curvature results using different resolutions, when compared to RTK-GPS derived measurements. Results in degrees.

	Easting	Northing
	4 m^2	
GIS	0.435	0.424
Clinometer	0.877	0.852
Accelerometer	0.752	0.727
	16 m^2	
GIS	0.117	0.117
Clinometer	0.142	0.138
Accelerometer	0.146	0.144
	100 m^2	
GIS	0.029	0.027
Clinometer	0.049	0.046
Accelerometer	0.057	0.056

Table 15. Linear correlation coefficient (r) and filter size effect between sensor raw data and elevation differences as measured by RTK-GPS. Normal to the direction of travel.

Rep	No Filter	5 Points	10 Points	15 Points	20 Points	Abs Elevation Difference (m)
			Clinometer			
I	0.72	0.93	0.96	0.96	0.97	0.117
II	0.72	0.89	0.95	0.96	0.97	0.109
III	0.77	0.95	0.97	0.98	0.98	0.112
IV	0.70	0.93	0.96	0.97	0.98	0.109
V	0.66	0.90	0.95	0.97	0.98	0.118
VI	0.84	0.96	0.98	0.98	0.98	0.120
VII	0.77	0.96	0.97	0.99	0.99	0.112
VIII	0.77	0.96	0.98	0.99	0.99	0.110
IX	0.76	0.95	0.97	0.98	0.98	0.101
X	0.67	0.93	0.95	0.96	0.98	0.099
			Accelerometer			
I	0.72	0.87	0.92	0.95	0.96	0.117
II	0.69	0.84	0.88	0.91	0.94	0.109
III	0.68	0.85	0.89	0.92	0.94	0.112
IV	0.62	0.85	0.91	0.94	0.96	0.109
V	0.60	0.82	0.89	0.93	0.95	0.118
VI	0.78	0.90	0.93	0.95	0.96	0.120
VII	0.76	0.92	0.96	0.97	0.98	0.112
VIII	0.79	0.96	0.98	0.98	0.98	0.110
IX	0.75	0.93	0.96	0.97	0.98	0.101
X	0.71	0.90	0.93	0.95	0.96	0.099

Table 16. Linear correlation coefficient (r) and filter size effect between sensor raw data and elevation differences as measured by RTK-GPS. Direction of travel.

Rep	No Filter	5 Points	10 Points	15 Points	20 Points	Abs Elevation Difference (m)
			Clinometer			
I	0.93	0.95	0.96	0.97	0.98	0.032
II	0.95	0.97	0.98	0.99	0.99	0.035
III	0.94	0.97	0.98	0.99	0.99	0.036
IV	0.87	0.91	0.95	0.97	0.97	0.023
V	0.63	0.78	0.88	0.92	0.94	0.011
VI	0.15	0.17	0.50	0.82	0.83	0.010
VII	0.39	0.48	0.62	0.70	0.74	0.006
VIII	0.25	0.41	0.56	0.64	0.66	0.008
IX	0.28	0.42	0.52	0.58	0.64	0.008
X	0.85	0.93	0.96	0.98	0.98	0.021
			Accelerometer			
I	0.94	0.96	0.97	0.98	0.98	0.032
II	0.93	0.96	0.98	0.99	0.99	0.035
III	0.93	0.97	0.98	0.99	0.99	0.036
IV	0.86	0.93	0.97	0.98	0.98	0.023
V	0.62	0.82	0.92	0.95	0.95	0.011
VI	0.09	0.30	0.67	0.85	0.86	0.010
VII	0.52	0.68	0.78	0.83	0.85	0.006
VIII	0.34	0.54	0.67	0.73	0.75	0.008
IX	0.35	0.46	0.53	0.60	0.68	0.008
X	0.85	0.93	0.96	0.97	0.98	0.021

APPENDIX D

Chapter IV Figures

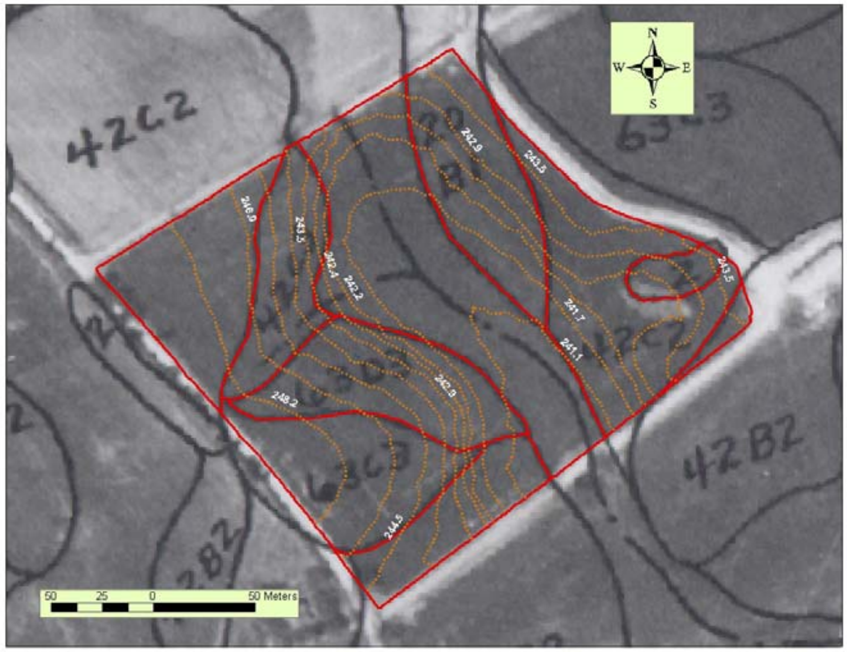

(a)

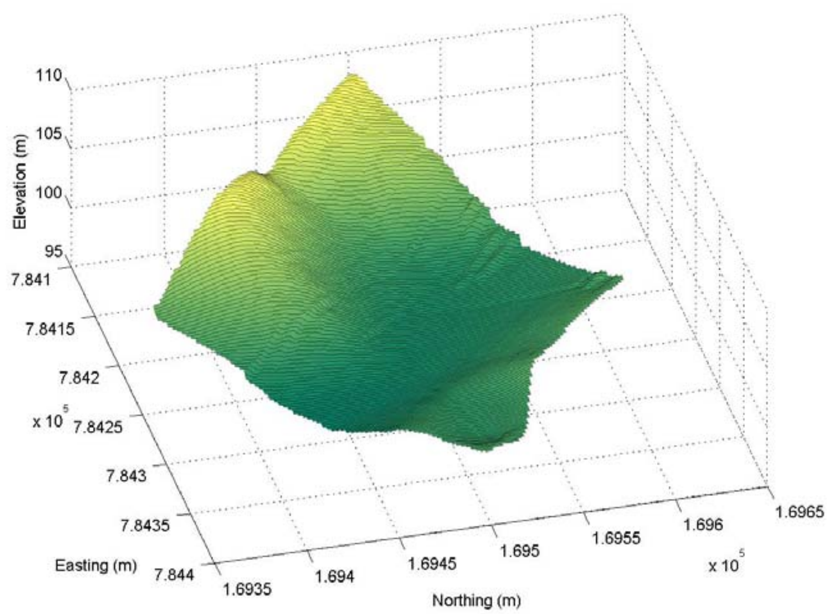

(b)

Figure 10. Overview of field # 9 of the Blount Experiment Research Unit of The University of Tennessee. (a) Soil survey (captions) and elevation contour lines. (b) 3-D representation of landform curvature.

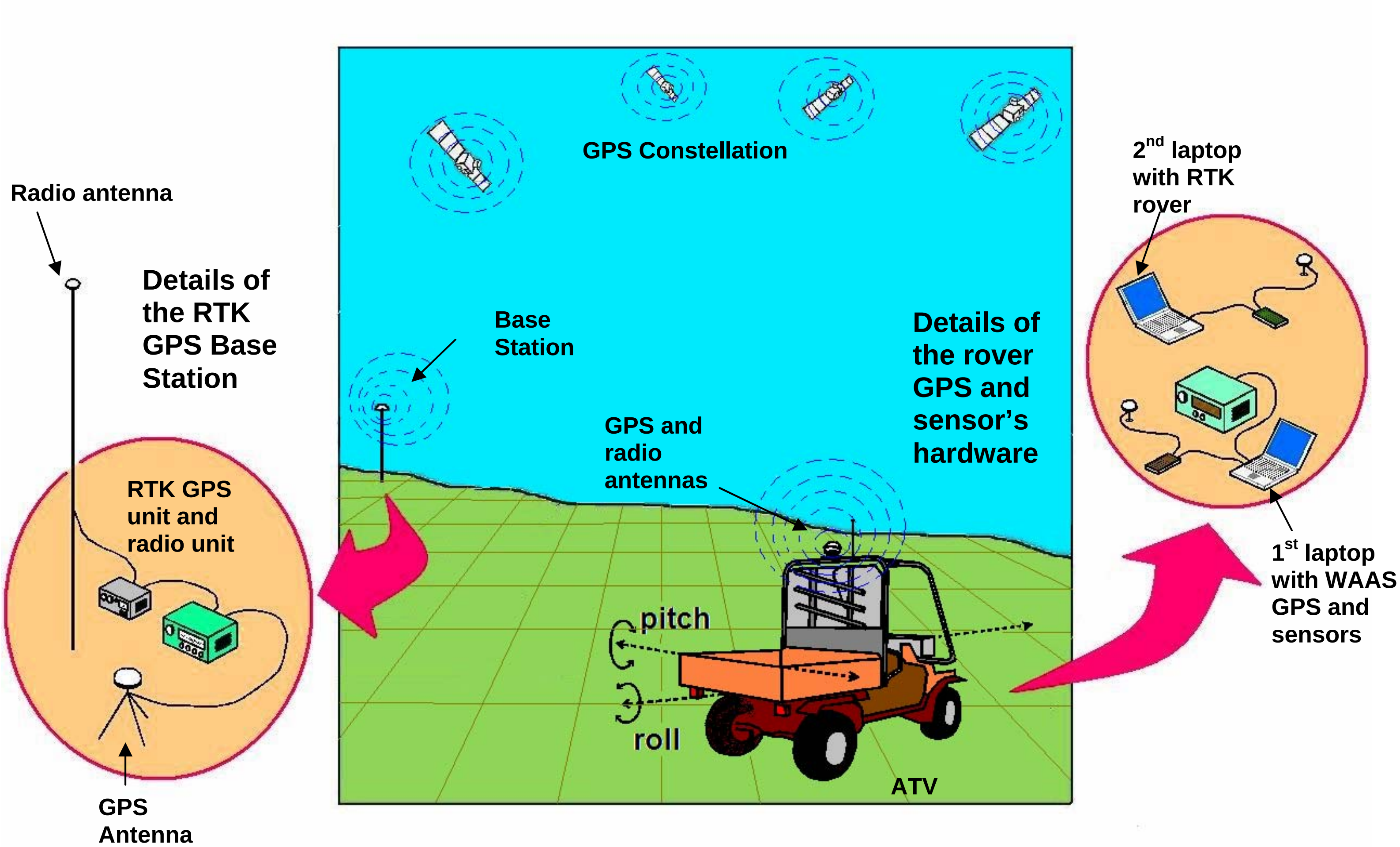

Figure 11. Illustration of the equipment used during field data collection.

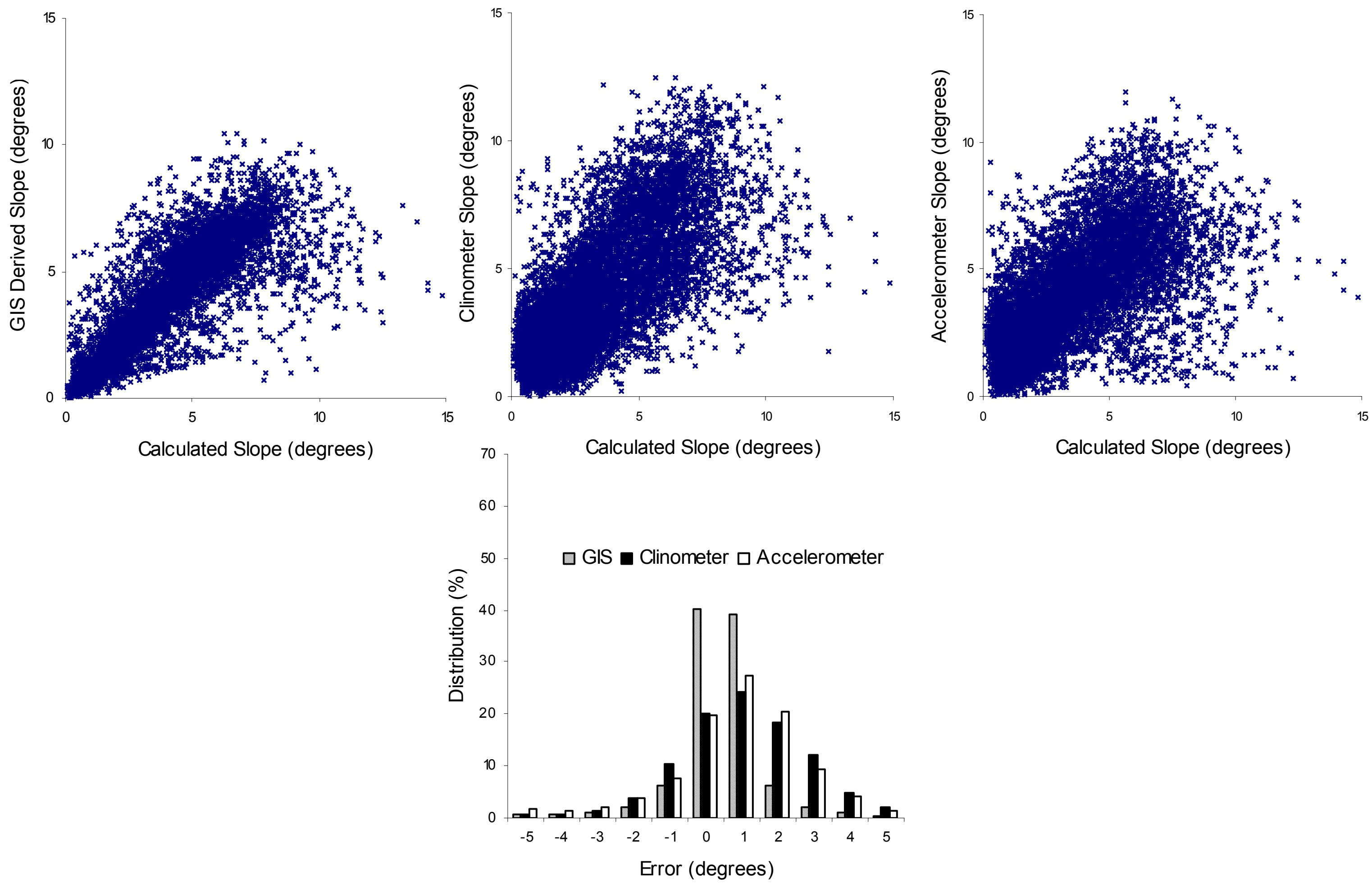

Figure 12. Calculated versus estimated slope gradient using different methods. Error distribution as a function of measurement method. Resolution of 4 m^2.

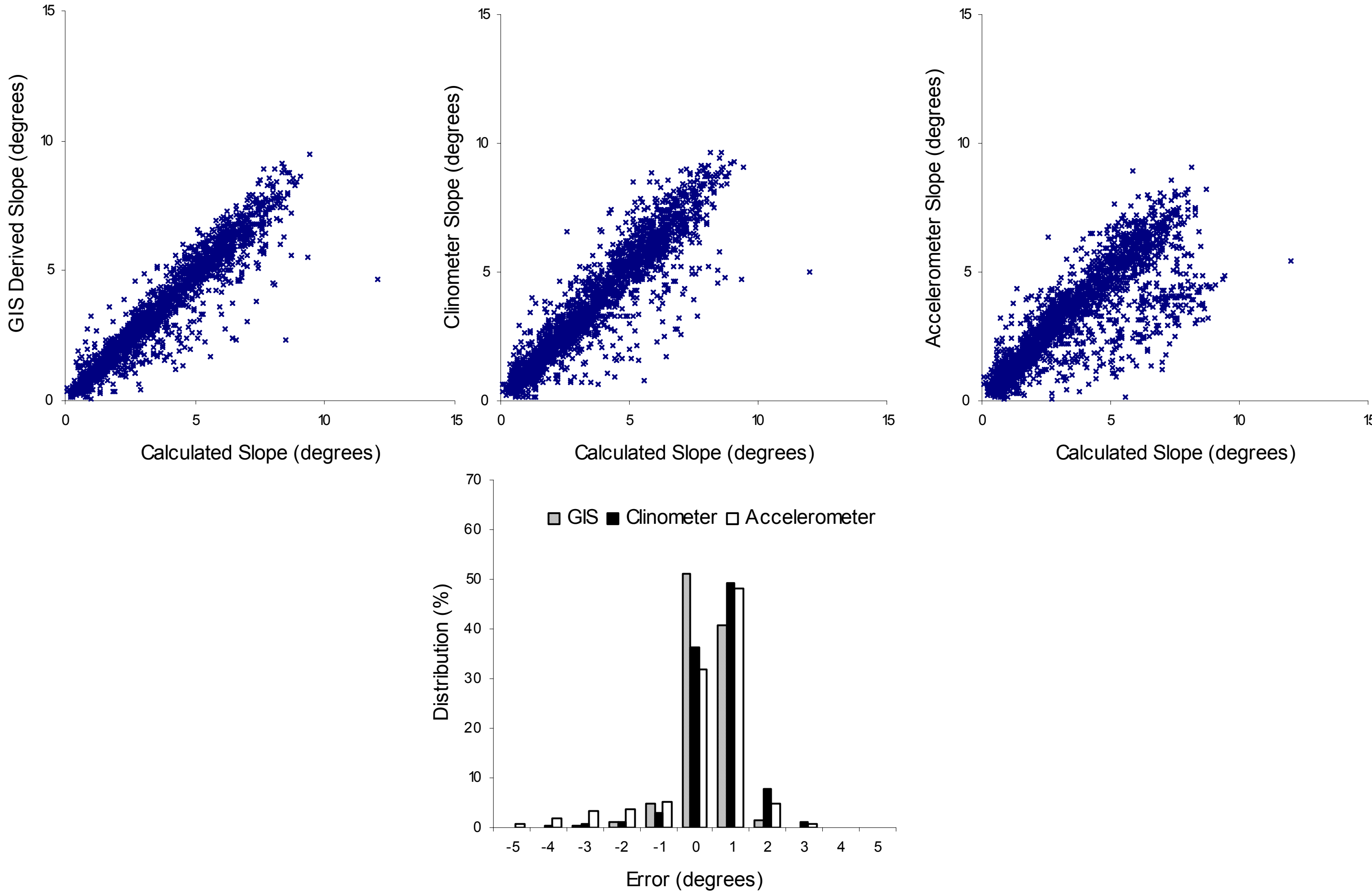

Figure 13. Calculated versus estimated slope gradient using different methods. Error distribution as a function of measurement method. Resolution of 16 m^2.

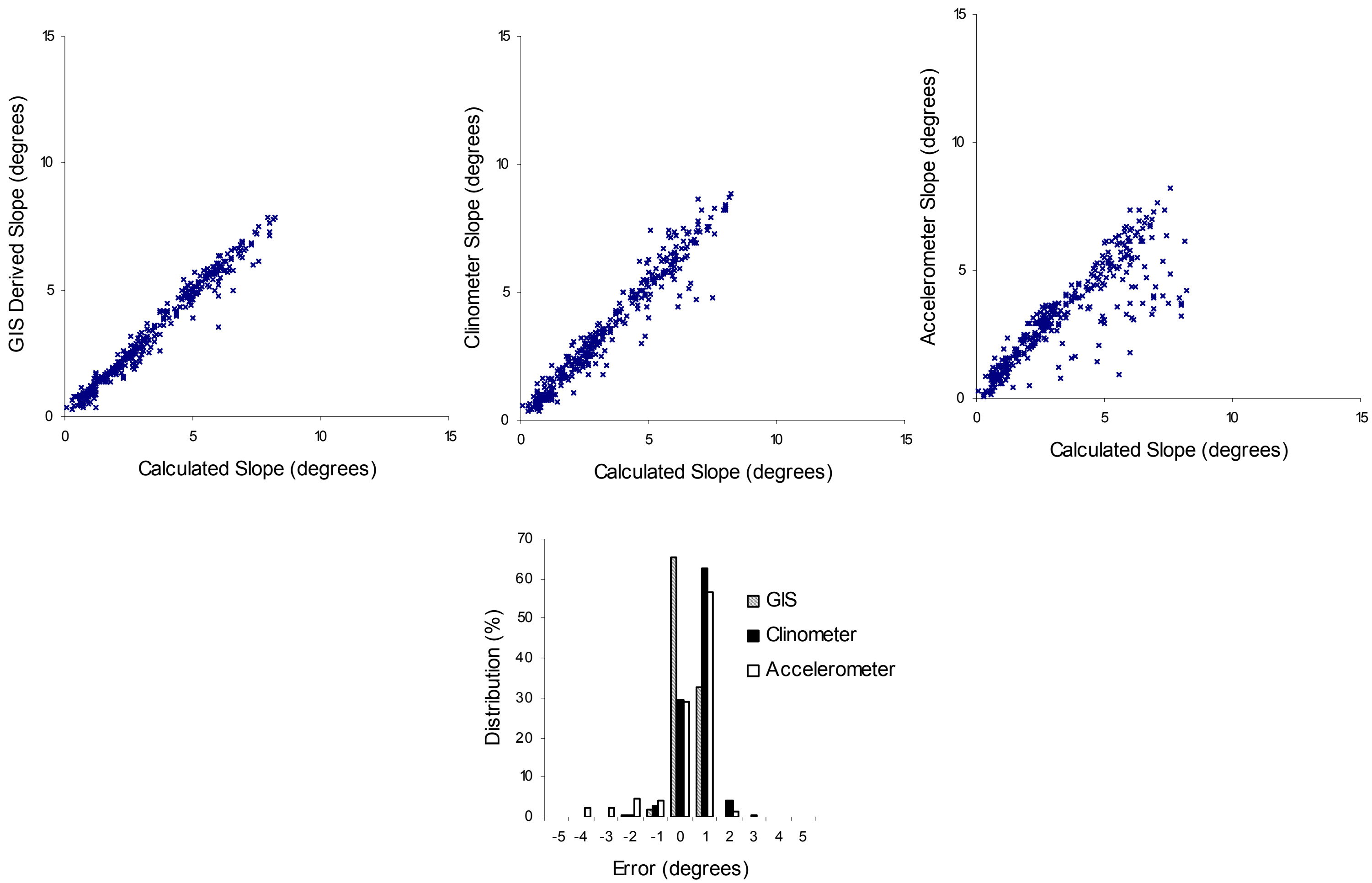

Figure 14. Calculated versus estimated slope gradient using different methods. Error distribution as a function of measurement method. Resolution of 100 m^2.

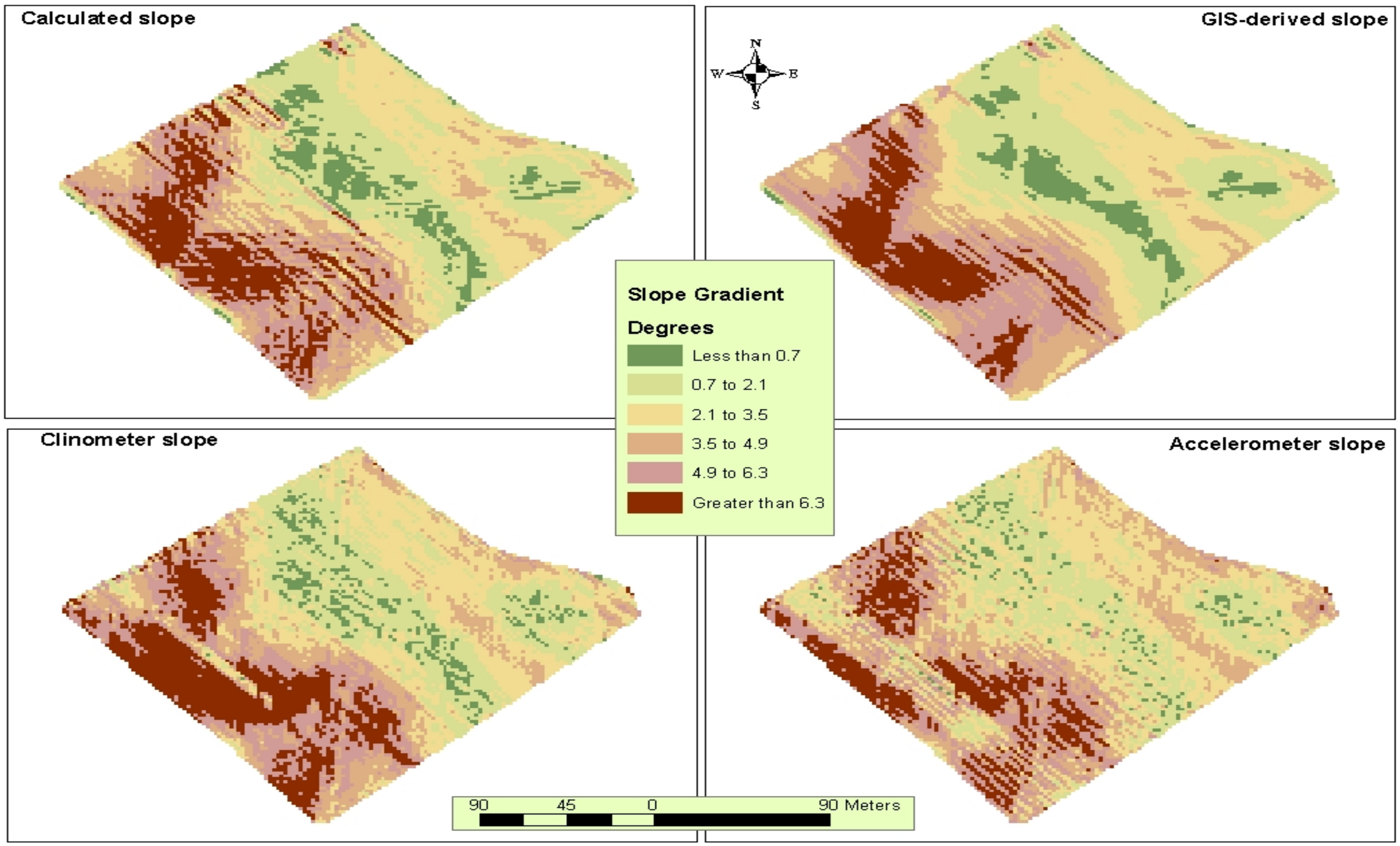

Figure 15. Composite map showing results of different measurement methods of slope gradient for field # 9. Resolution of 4 m^2.

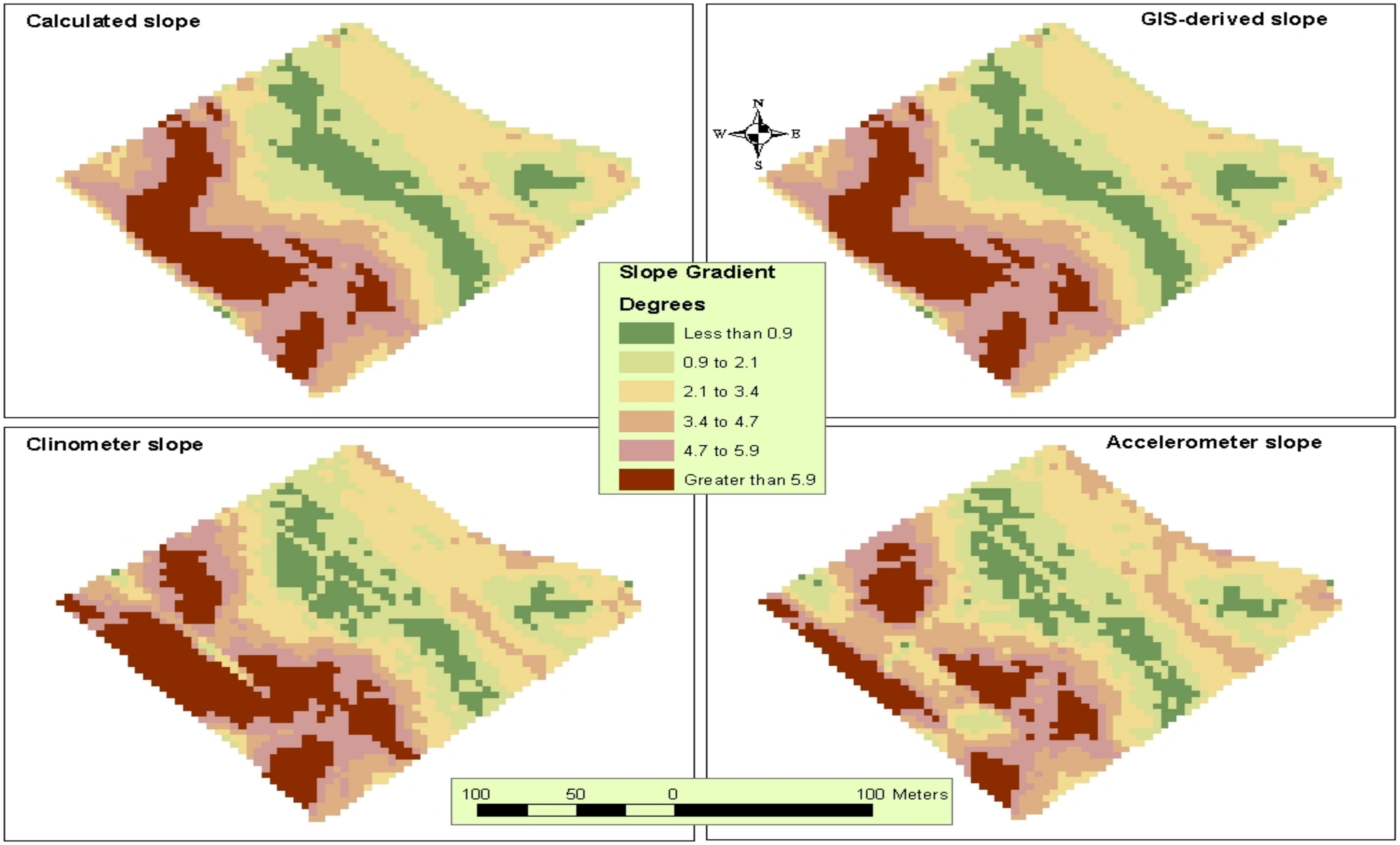

Figure 16. Composite map showing results of different measurement methods of slope gradient for field # 9. Resolution of 16 m^2.

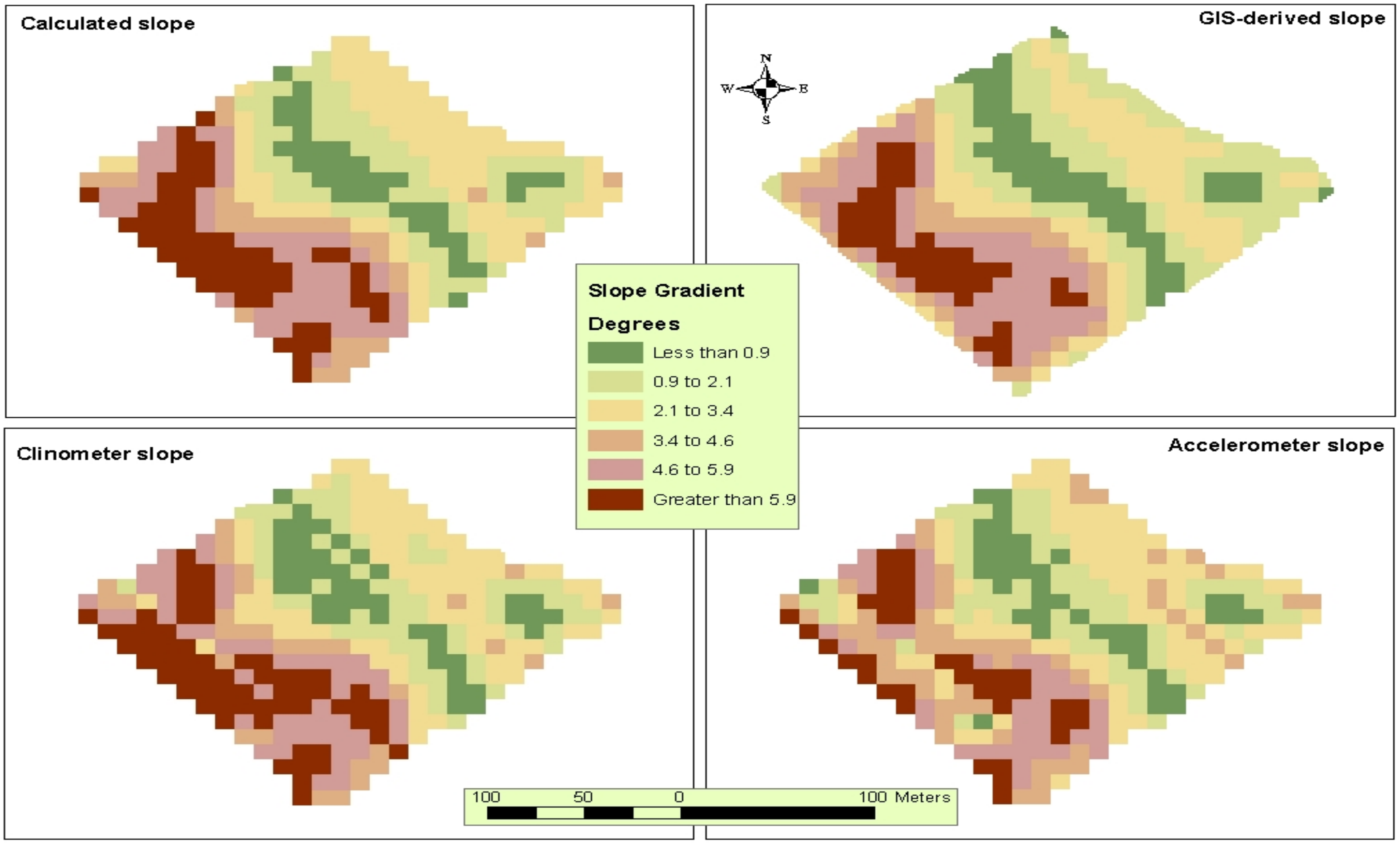

Figure 17. Composite map showing results of different measurement methods of slope gradient for field # 9. Resolution of 100 m^2.

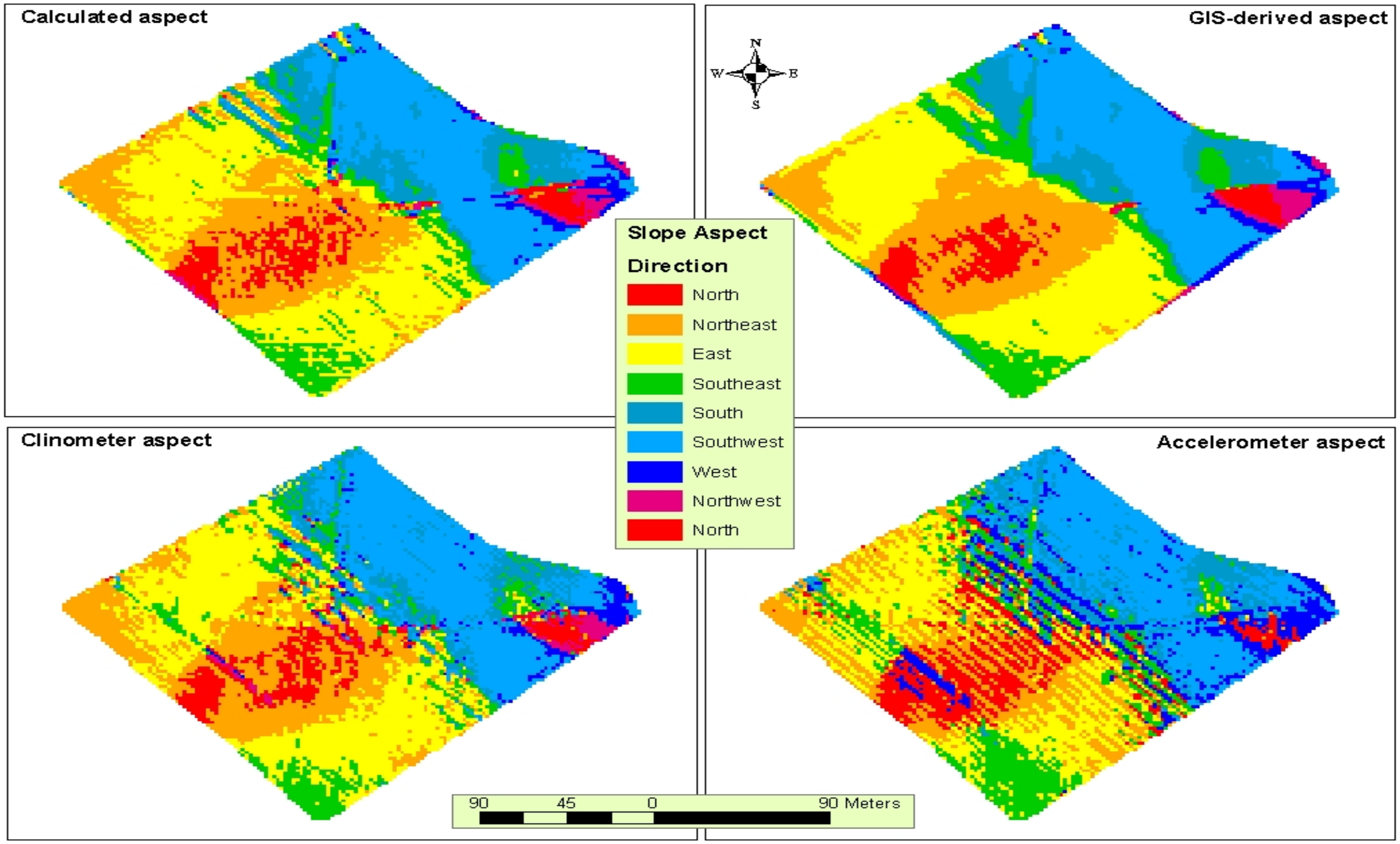

Figure 18. Composite map showing results of different measurement methods of slope aspect for field # 9. Resolution of 4 m^2.

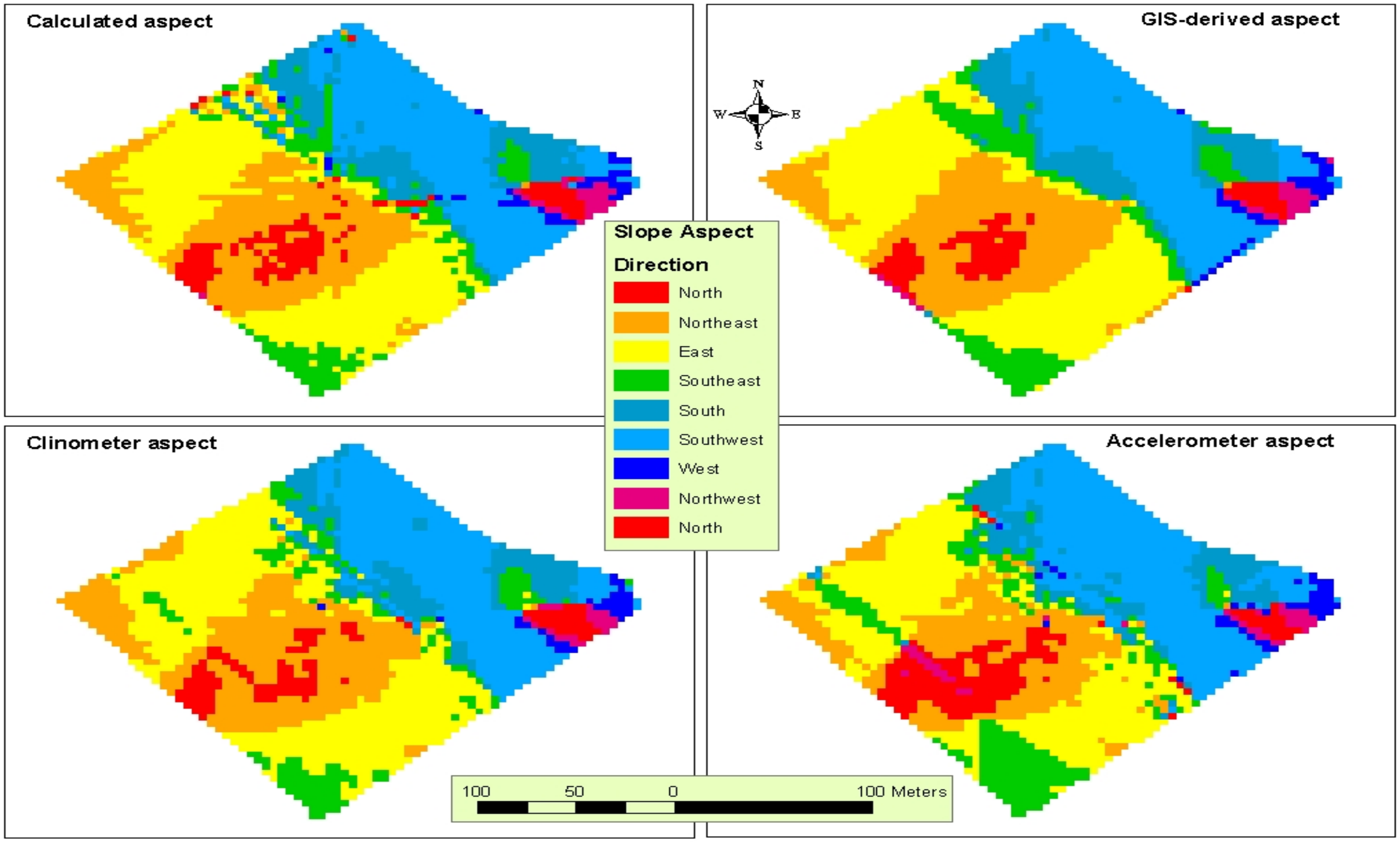

Figure 19. Composite map showing results of different measurement methods of slope aspect for field # 9. Resolution of 16 m^2.

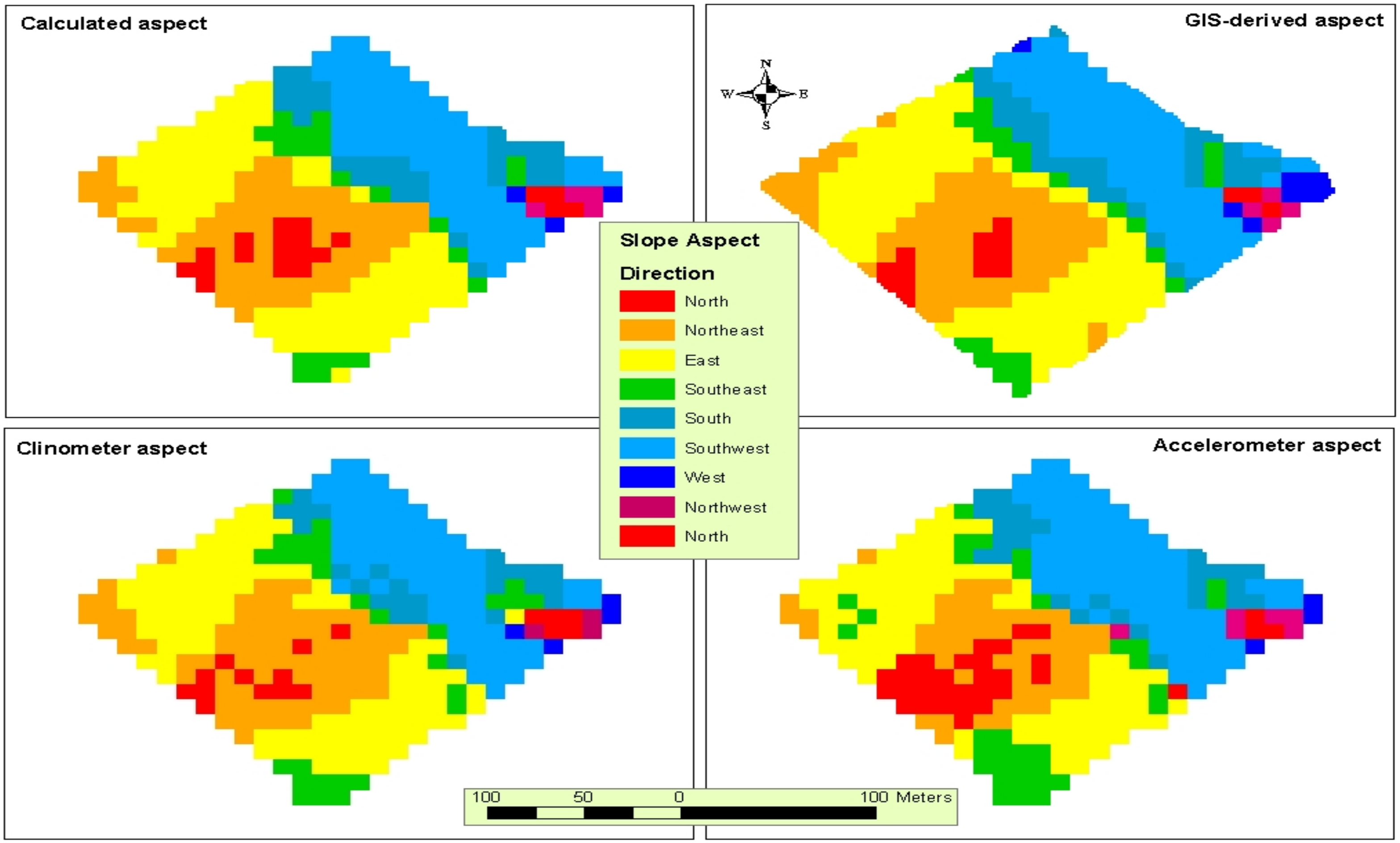

Figure 20. Composite map showing results of different measurement methods of slope aspect for field # 9. Resolution of 100 m^2.

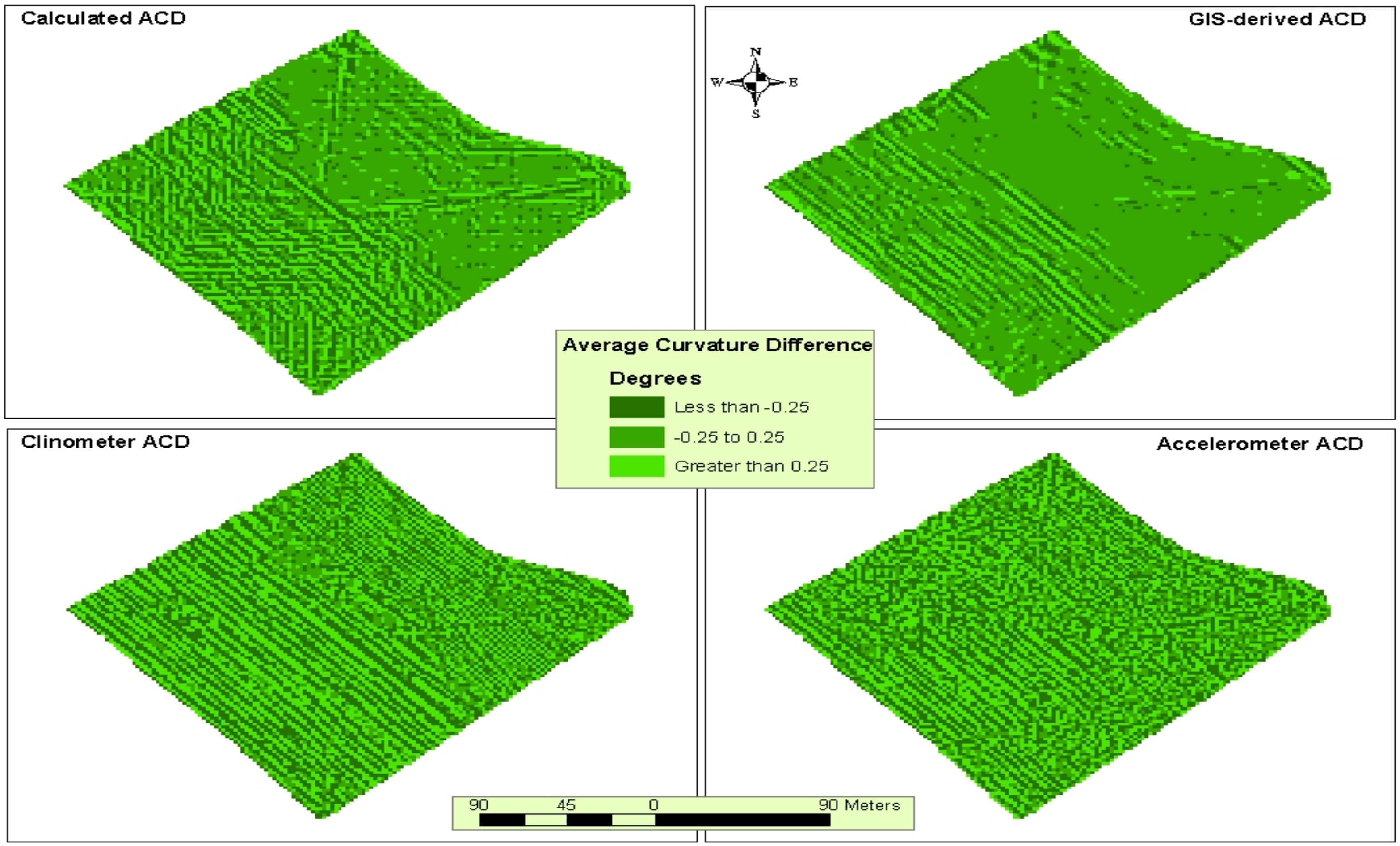

Figure 21. Composite map showing results of different measurement methods of the average curvature difference for field # 9. Resolution of 4 m^2 .

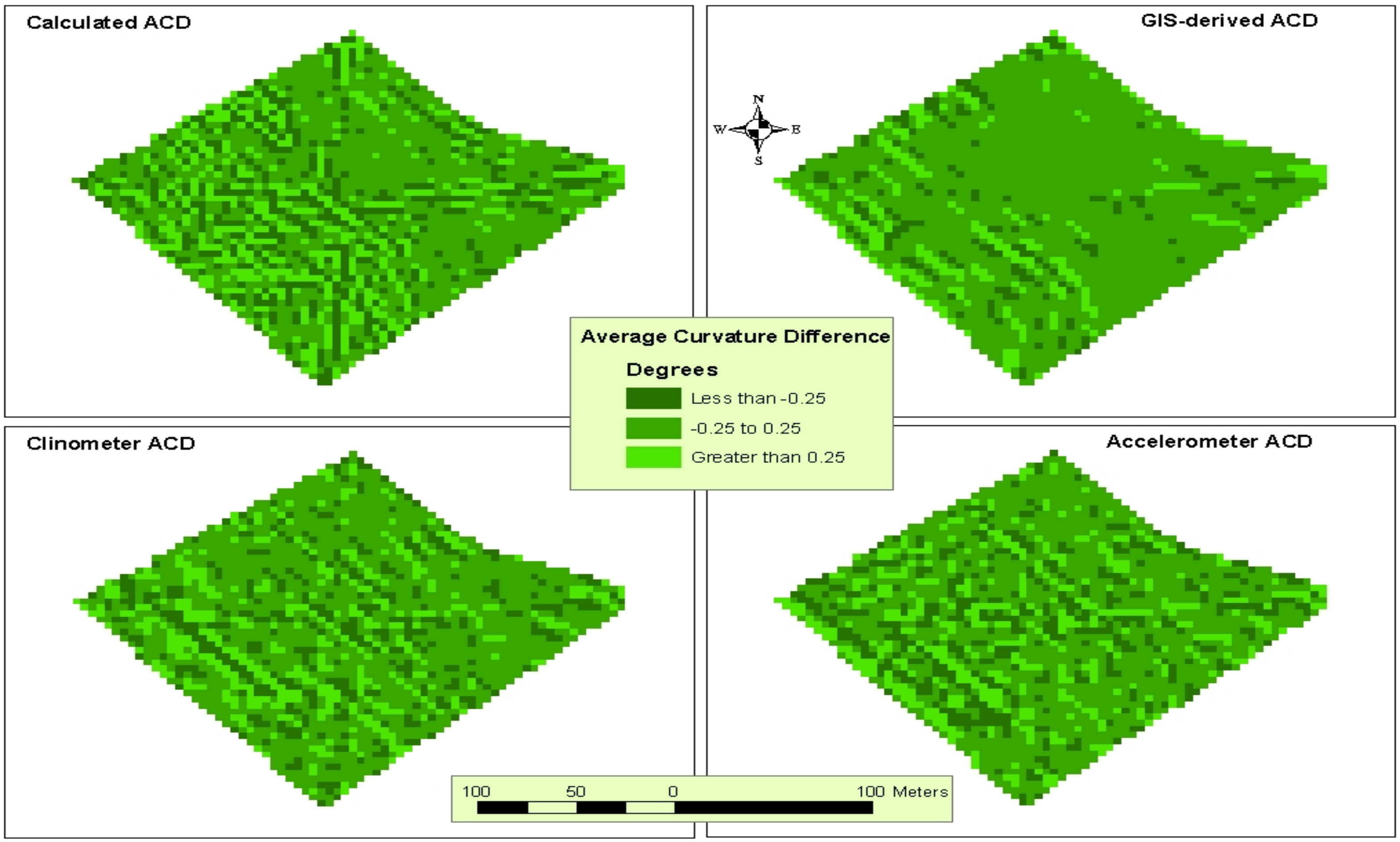

Figure 22. Composite map showing results of different measurement methods of the average curvature difference for field # 9. Resolution of 16 m^2 .

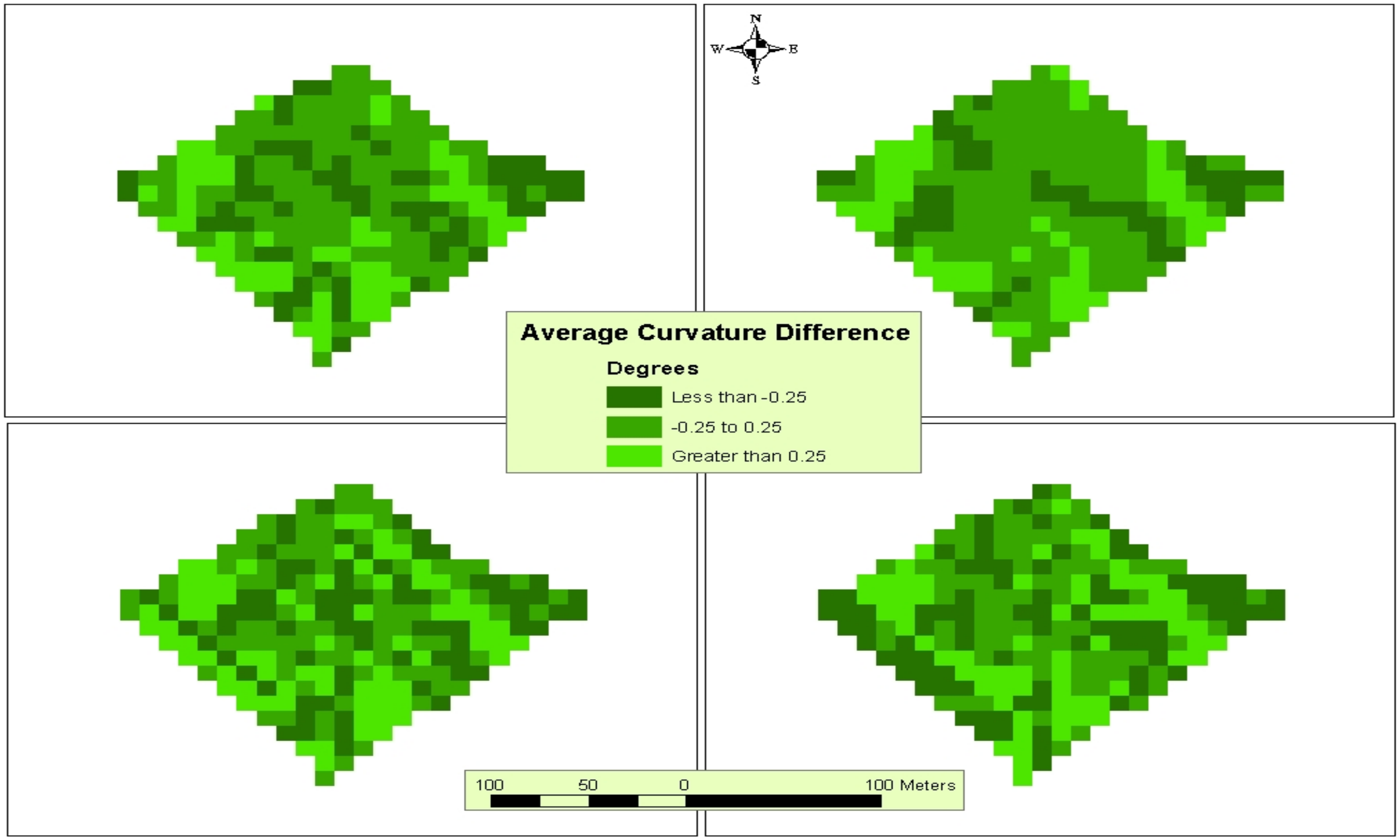

Figure 23. Composite map showing results of different measurement methods of the average curvature difference for field # 9. Resolution of 100 m^2 .

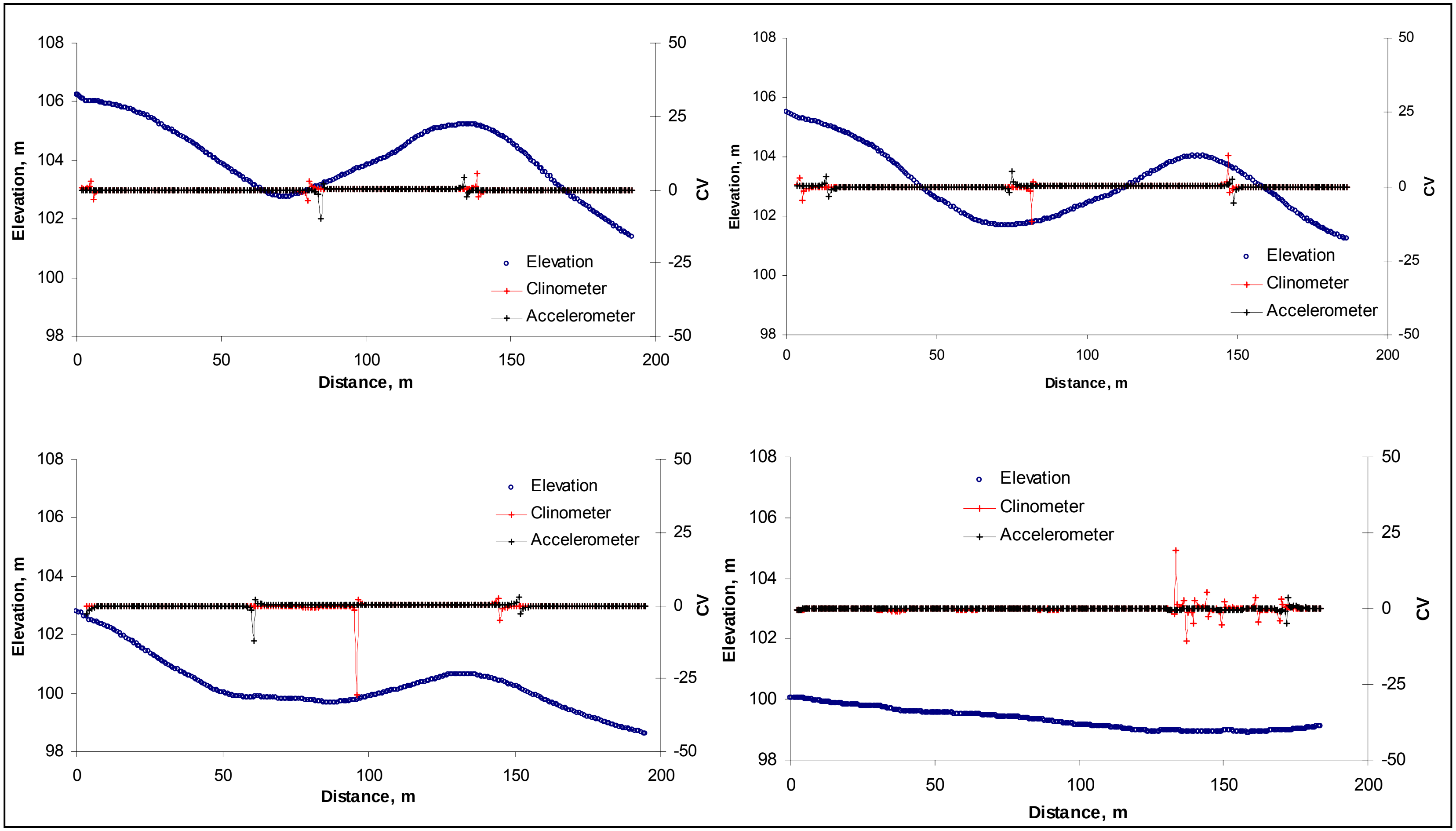

Figure 24. Coefficient of variation (%) used to indicate changes in elevation in the direction of travel.

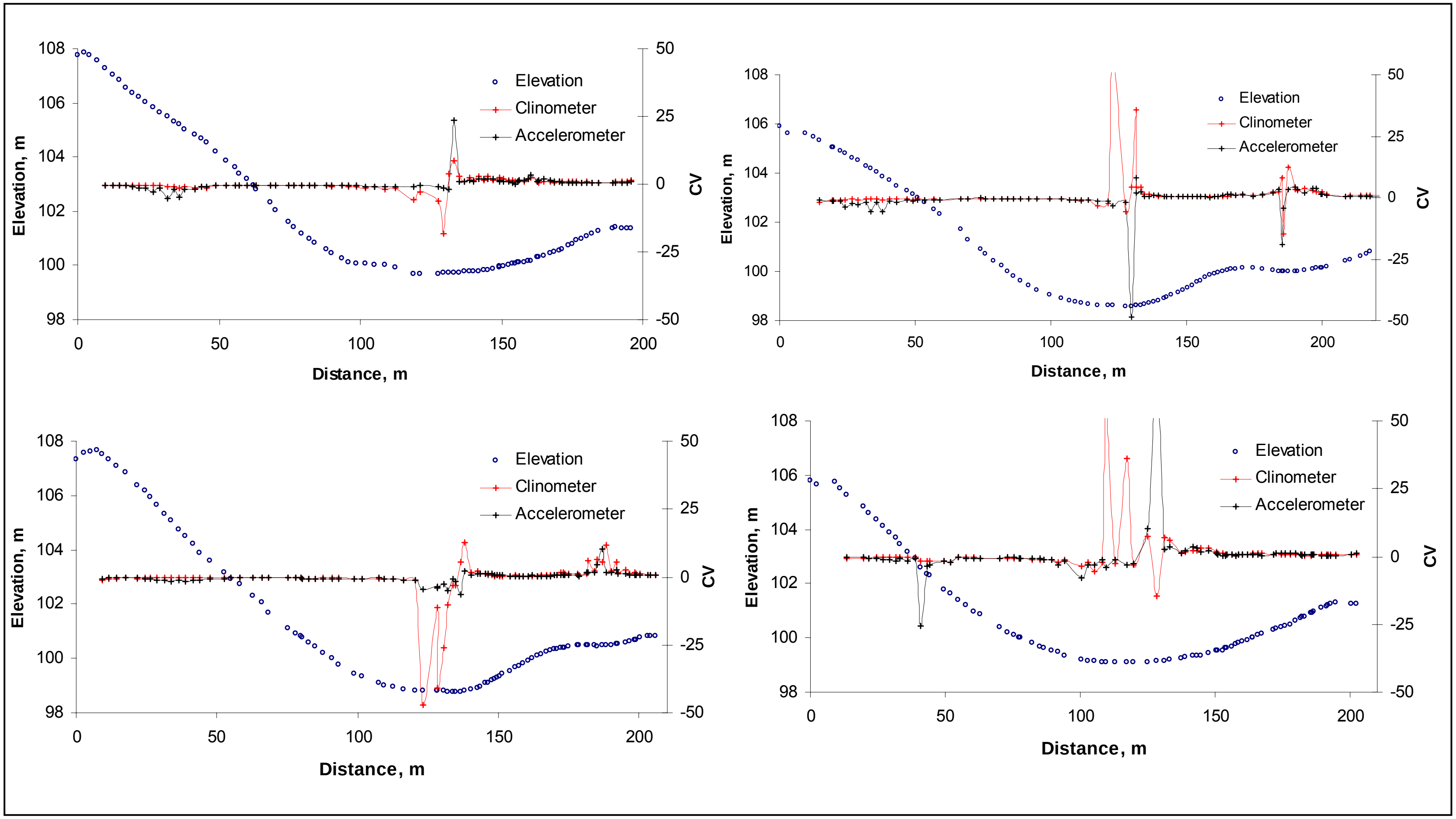

Figure 25. Coefficient of variation (%) used to indicate changes in elevation normal to the direction of travel.

APPENDIX E

Additional Graphics

Graphical representation of RTK-GPS elevation, rate of change of elevation, and sensor output variation, in the direction of travel.

I

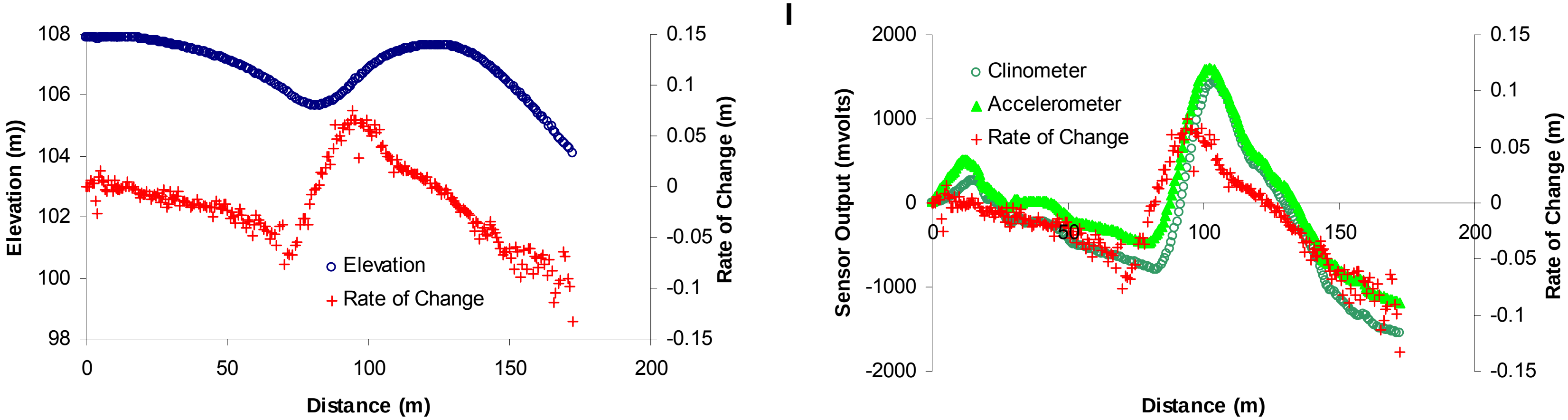

II

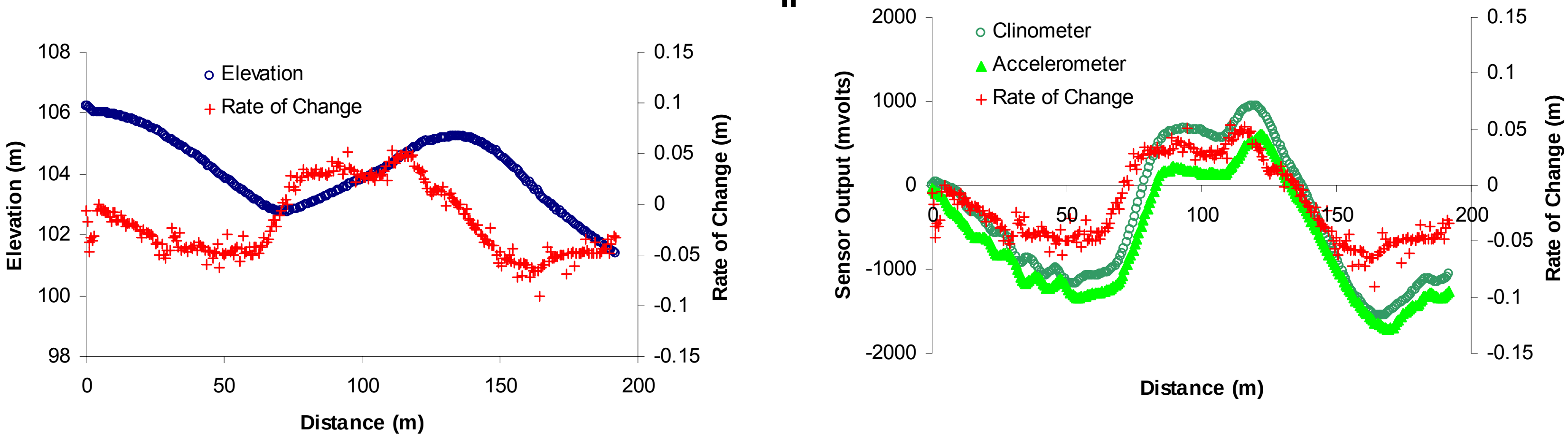

Graphical representation of RTK-GPS elevation, rate of change of elevation, and sensor output variation, in the direction of travel.

III

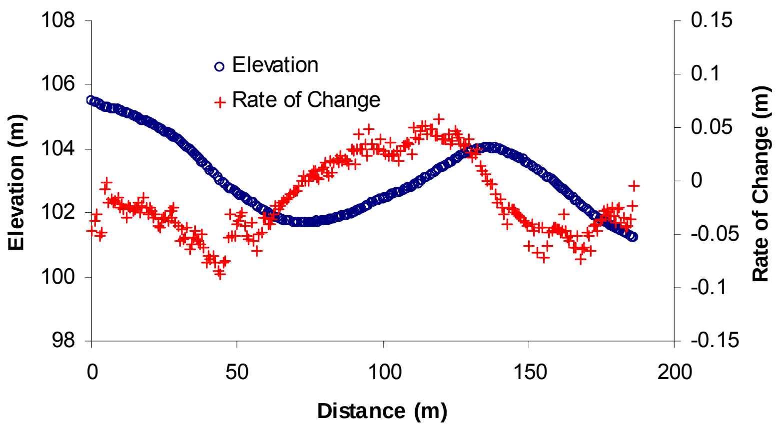

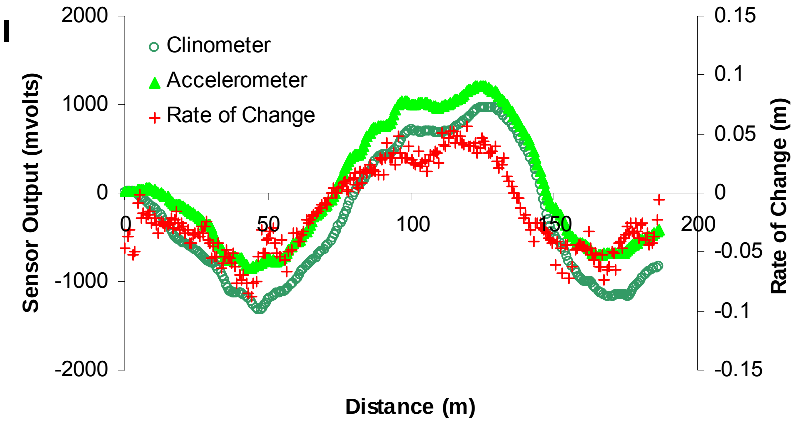

IV

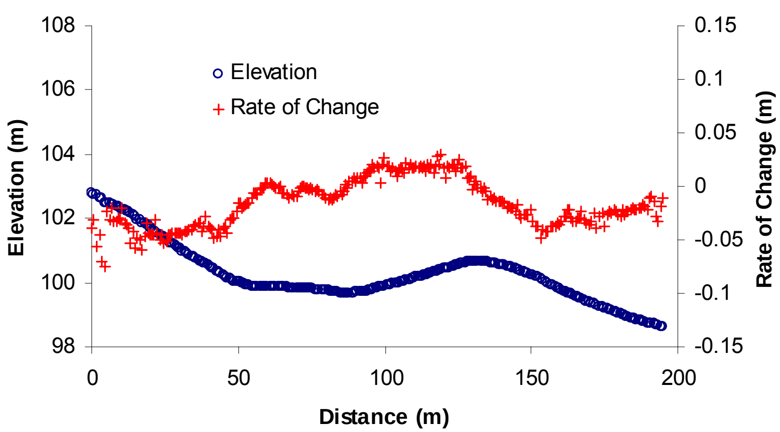

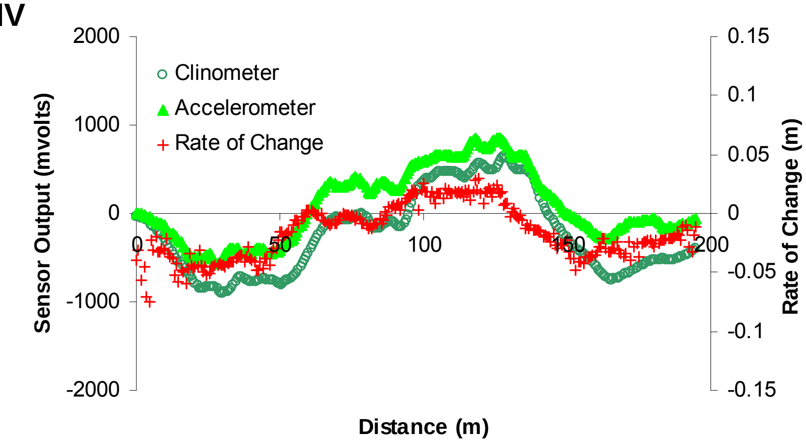

Graphical representation of RTK-GPS elevation, rate of change of elevation, and sensor output variation, in the direction of travel.

V

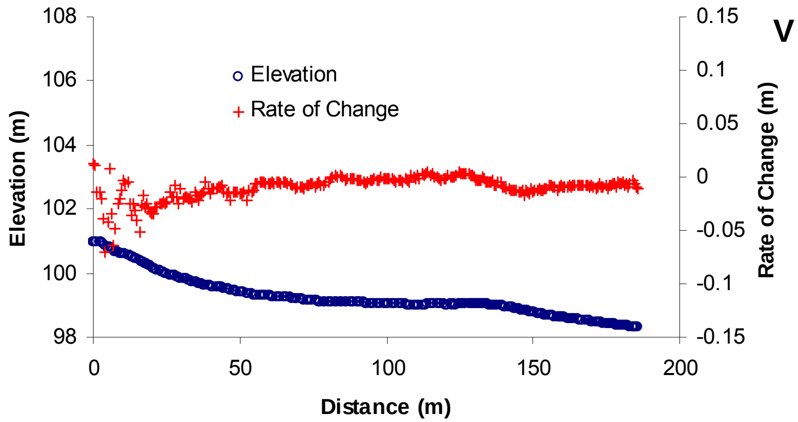

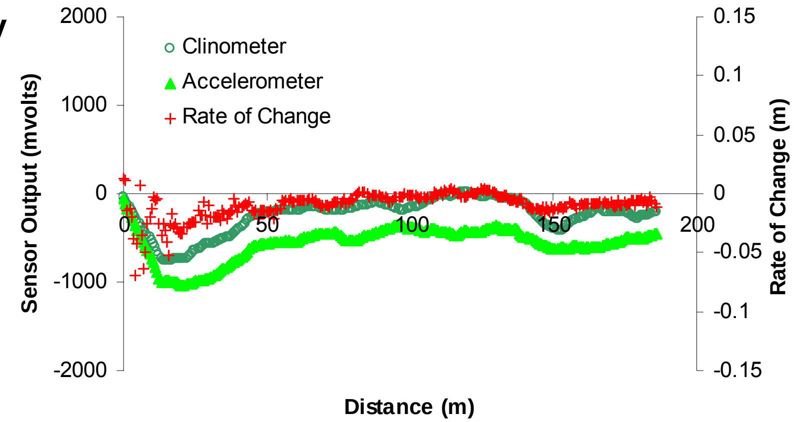

VI

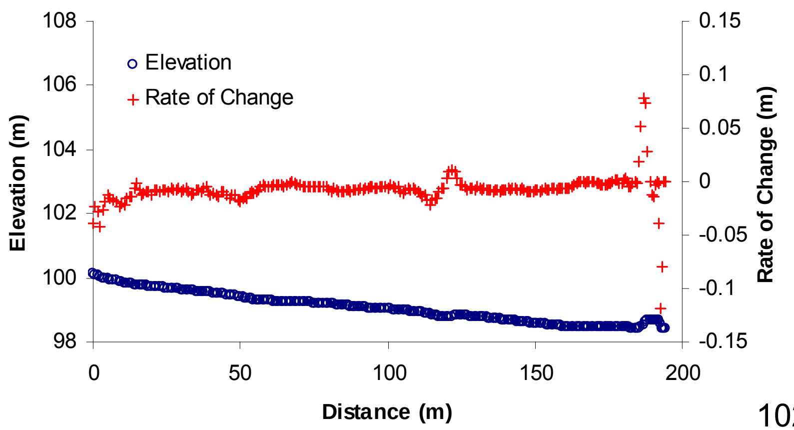

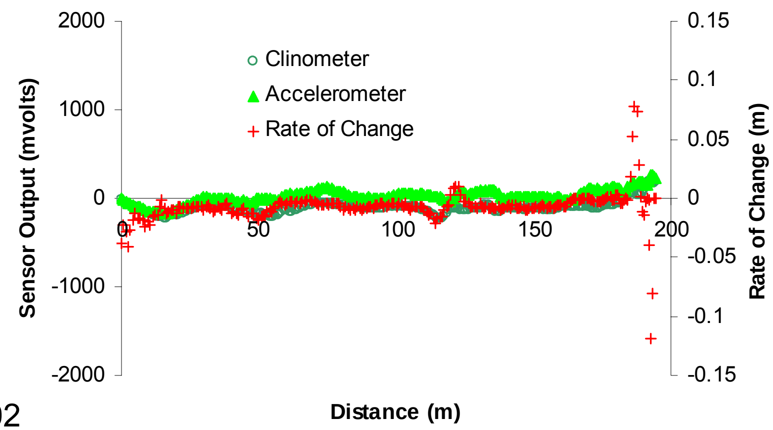

Graphical representation of RTK-GPS elevation, rate of change of elevation, and sensor output variation, in the direction of travel.

VII

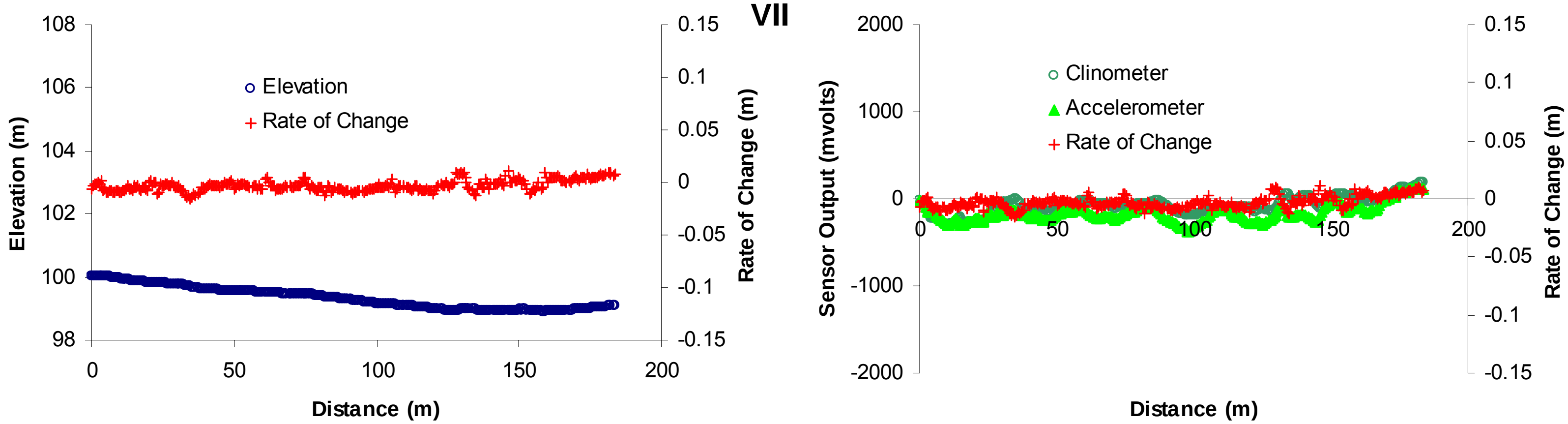

VIII

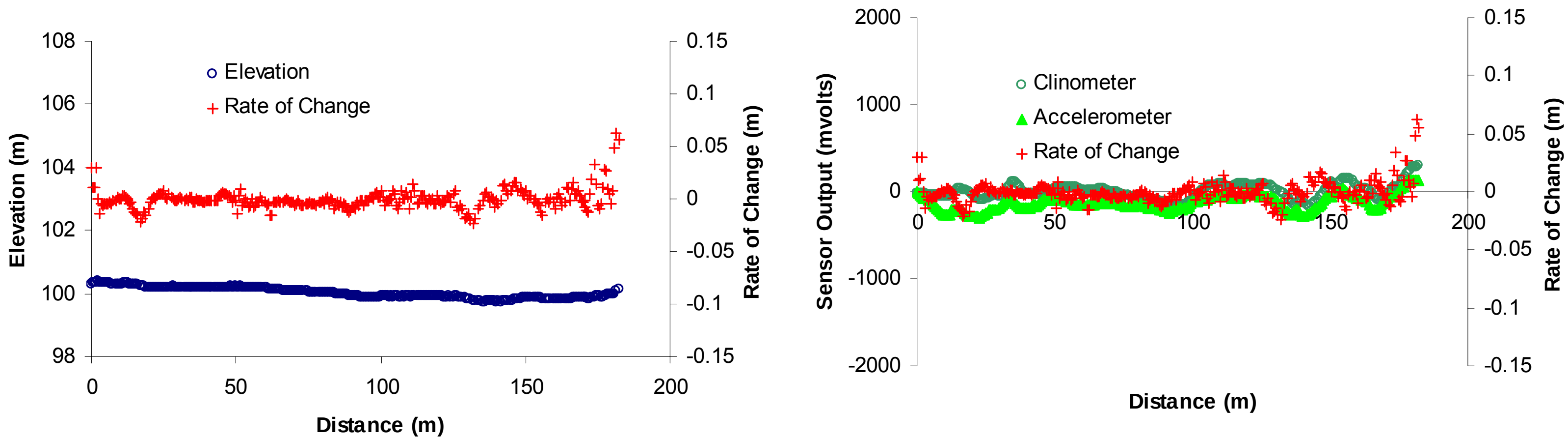

Graphical representation of RTK-GPS elevation, rate of change of elevation, and sensor output variation, in the direction of travel.

IX

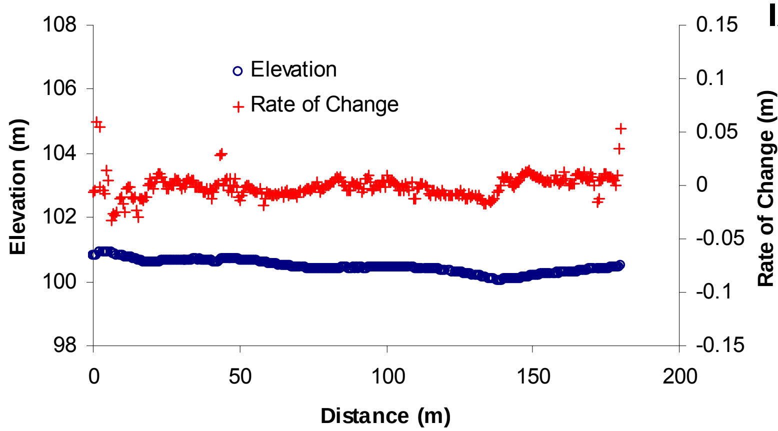

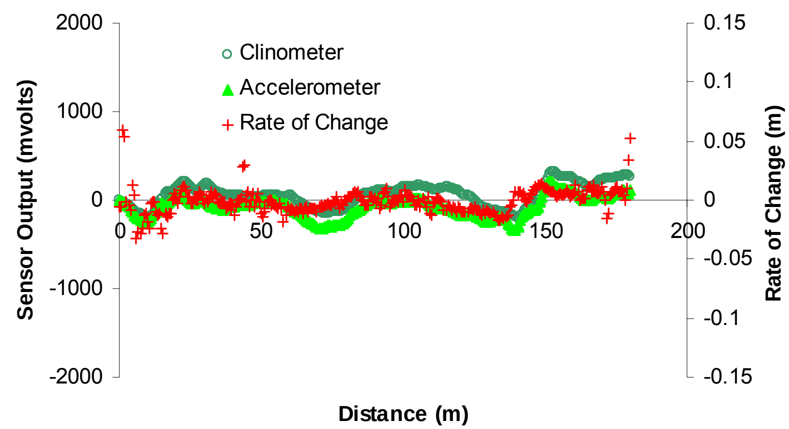

X

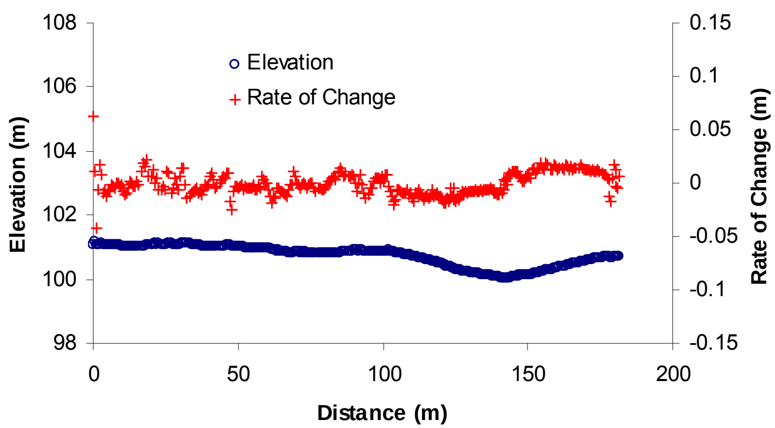

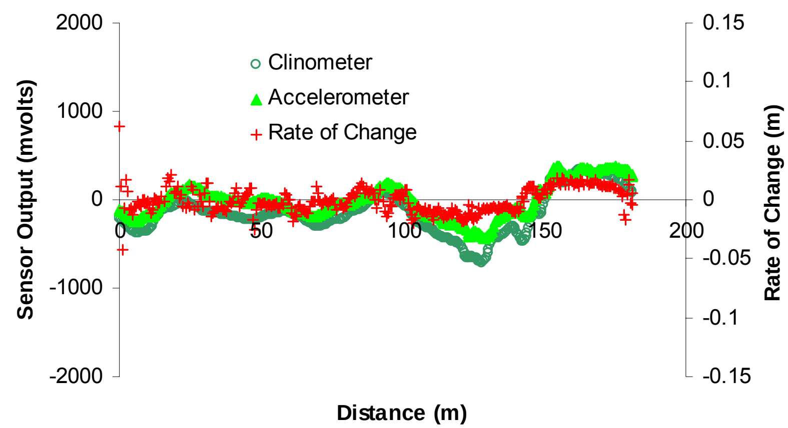

Graphical representation of RTK-GPS elevation, rate of change of elevation, and sensor output variation, perpendicular to the direction of travel.

I

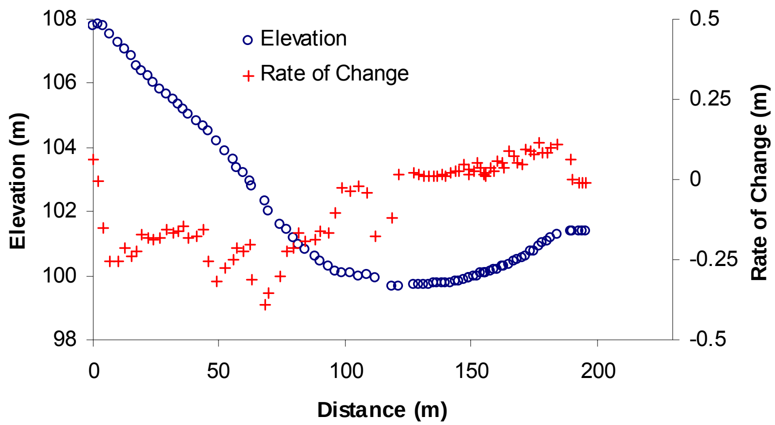

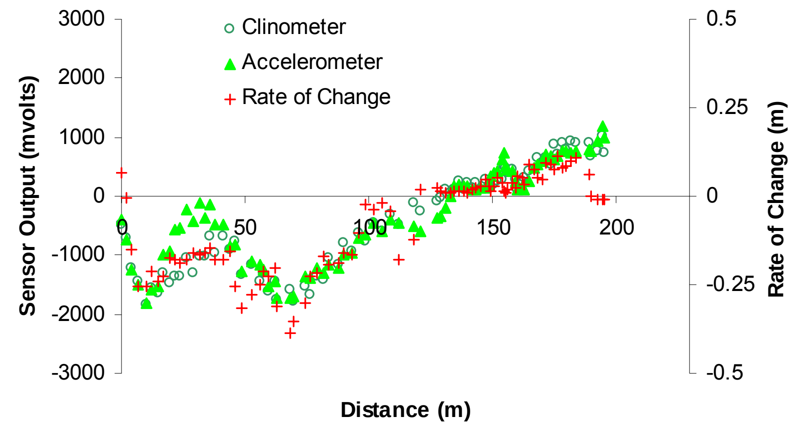

II

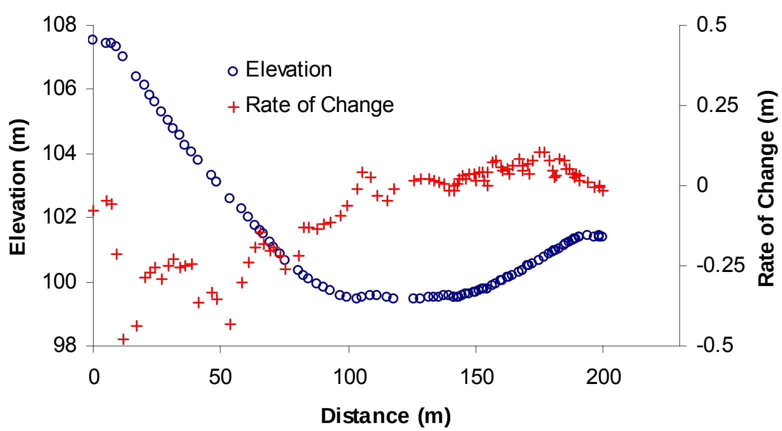

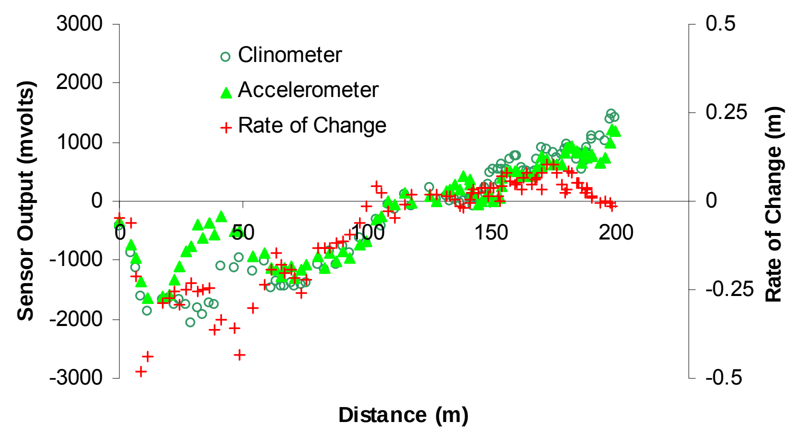

Graphical representation of RTK-GPS elevation, rate of change of elevation, and sensor output variation, perpendicular to the direction of travel.

III

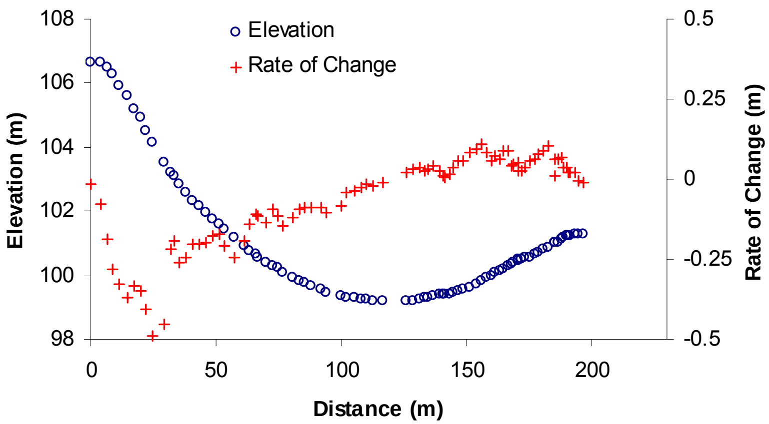

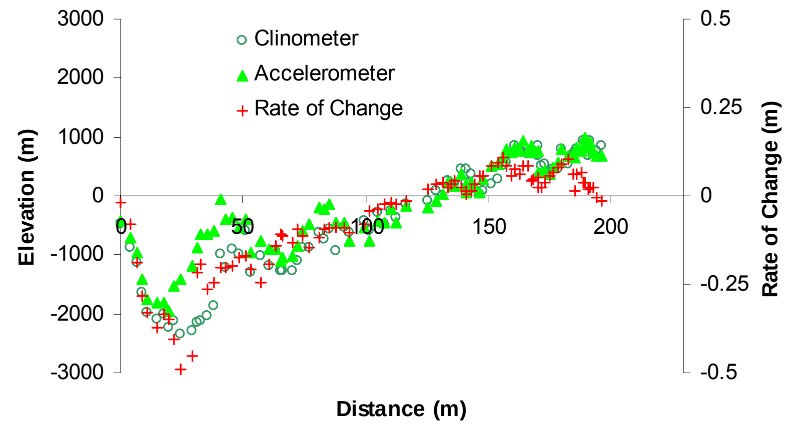

IV

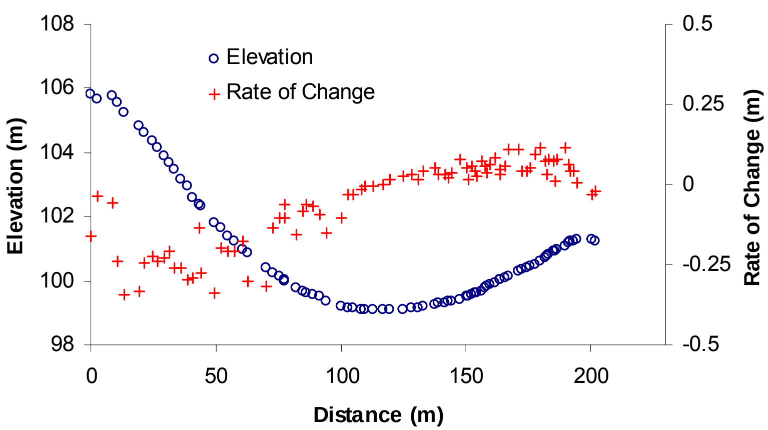

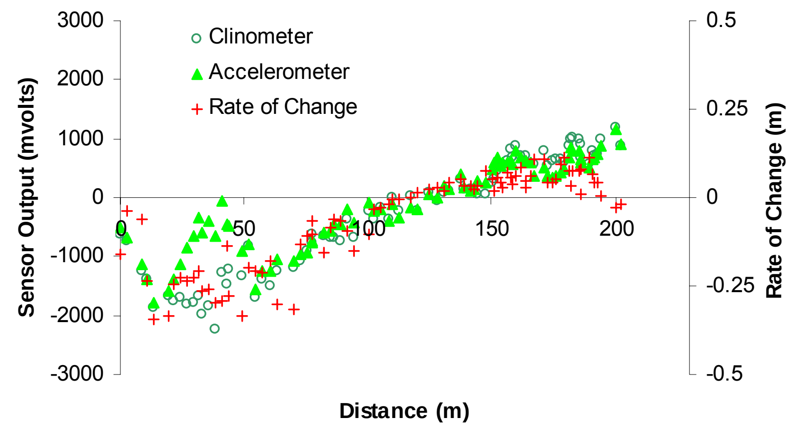

Graphical representation of RTK-GPS elevation, rate of change of elevation, and sensor output variation, perpendicular to the direction of travel.

V

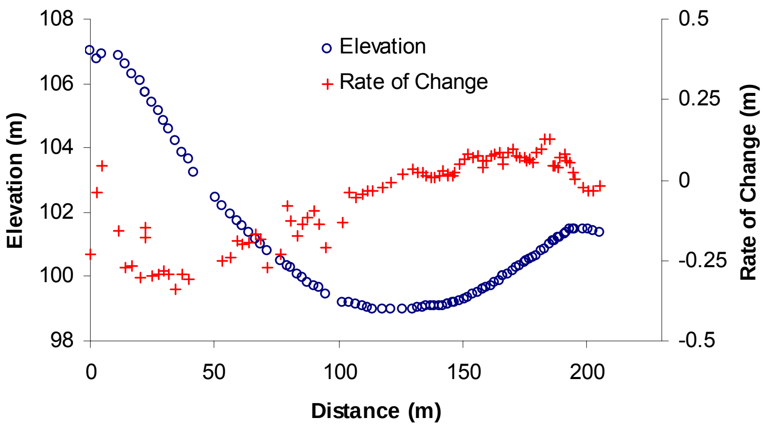

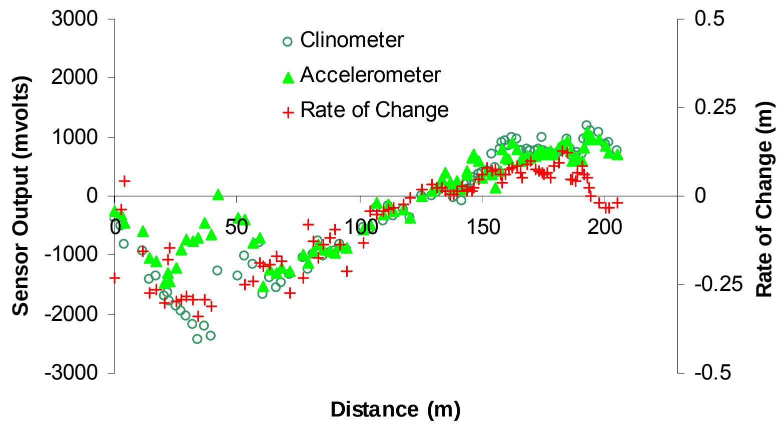

VI

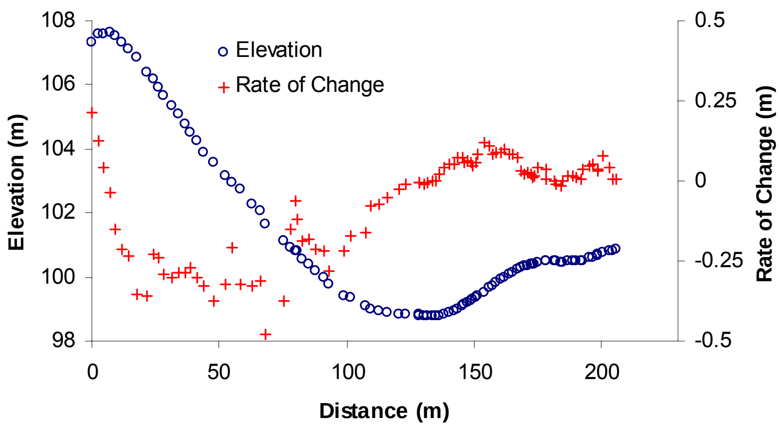

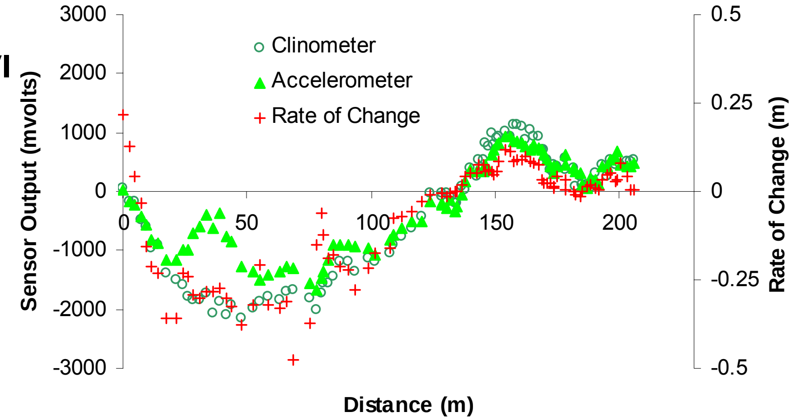

Graphical representation of RTK-GPS elevation, rate of change of elevation, and sensor output variation, perpendicular to the direction of travel.

VII

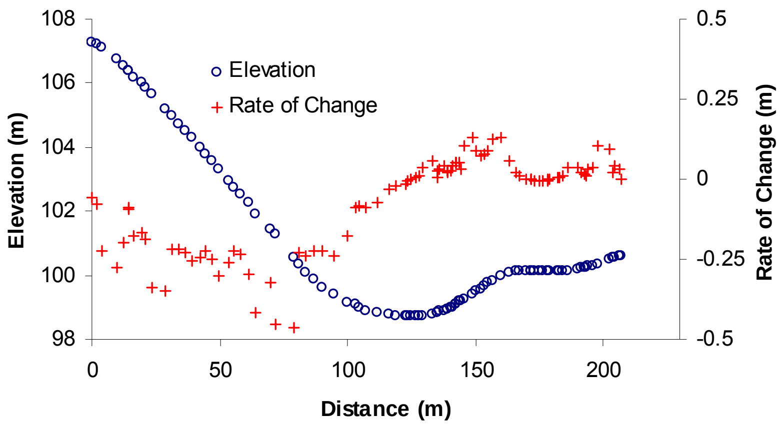

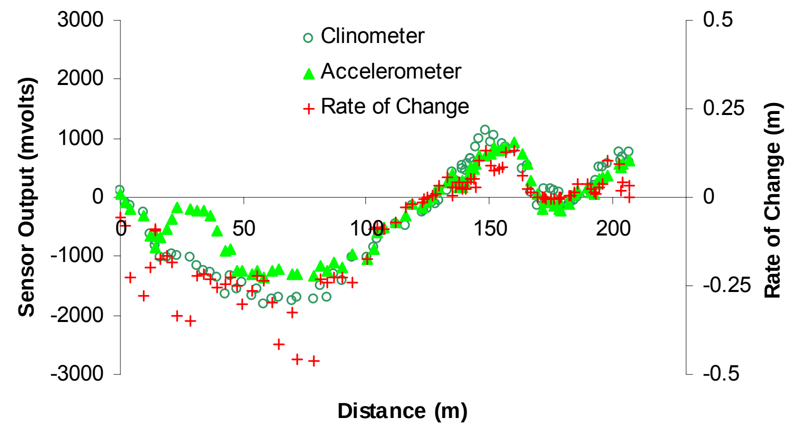

VIII

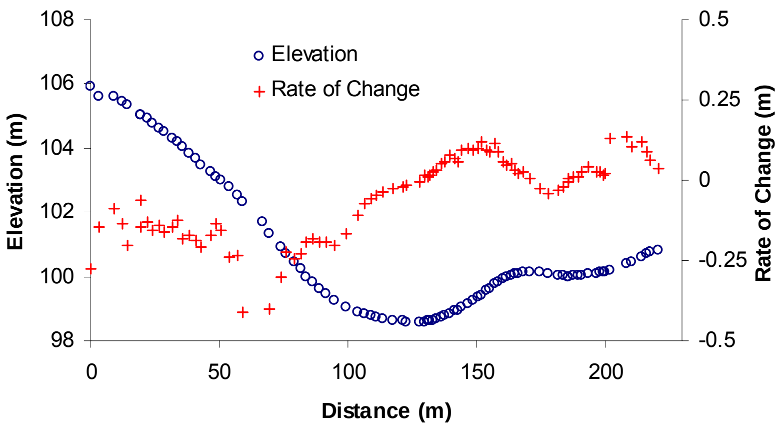

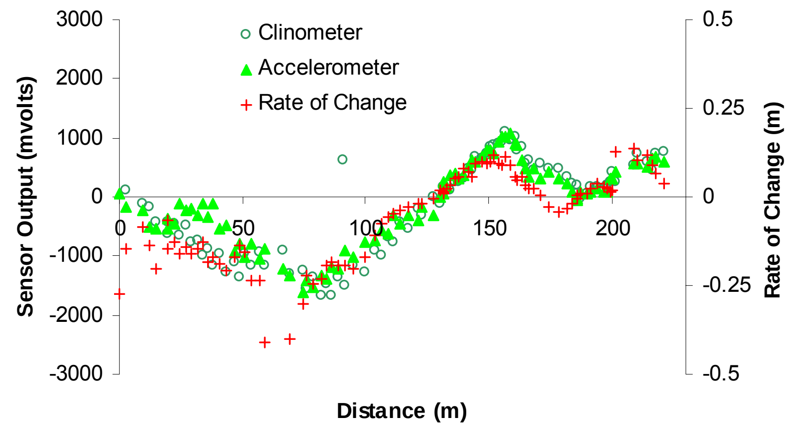

Graphical representation of RTK-GPS elevation, rate of change of elevation, and sensor output variation, perpendicular to the direction of travel.

IX

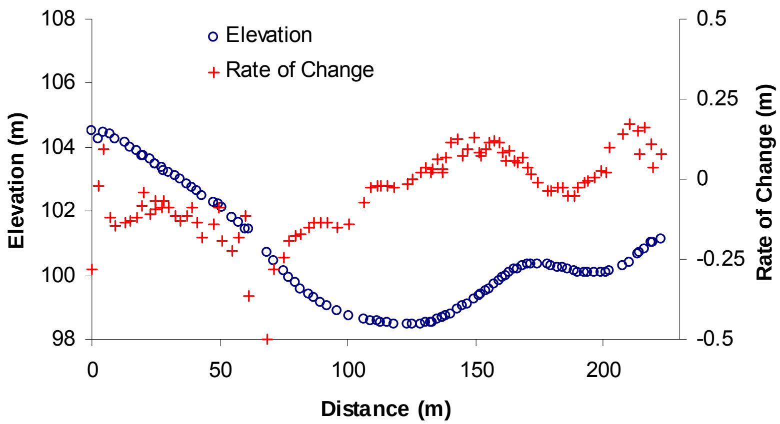

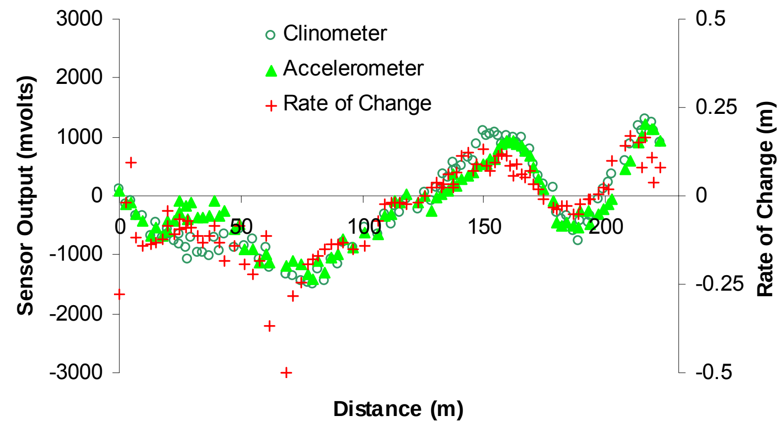

X

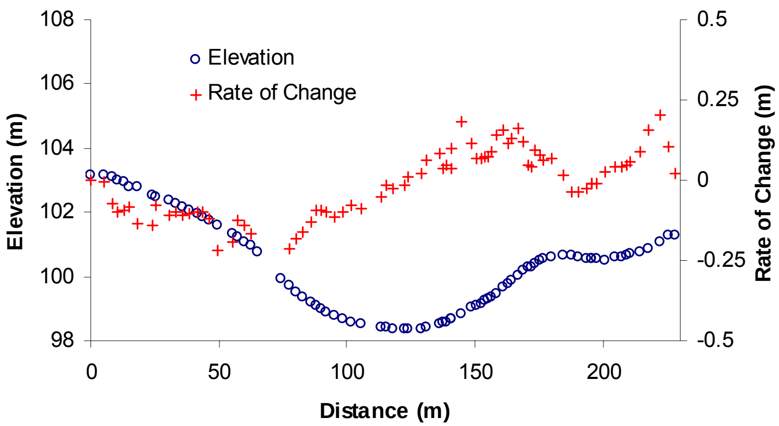

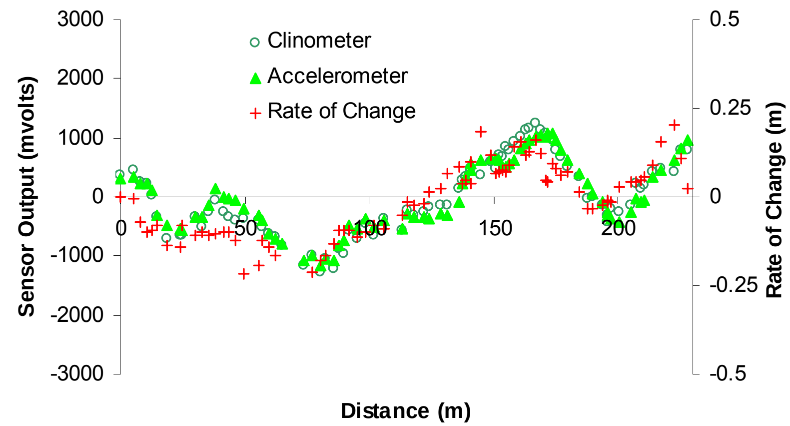

APPENDIX F

Electronic Drawing and Specifications

Material Specifications

Part	Value	Part	Value
C1	1uF	U$9	RIACON6
C2	1uF	U$12	5k
C3	1uF	U$15	5k
C4	1uF	U$18	5k
C5	4.7uF Tant.	U$37	20k
C6	0.1uF	U$38	20k
C7	0.1uF	U$48	RIACON6
C8	0.1uF	U$51	LCC-8
C9	0.47uF	U$54	5MM
C10	0.47uF	U$59	TC9401
C11	4.7uF Tant.	U$67	2k
C12	1.86nF	U$72	RIACON4
C13	1uF	U1	317LZ
C14	.01uF	U$5	5k
C15	1nF	U$3	5k
D1	1N914	U$2	SB1R555
D2	1N914	U$1	750L05
IC1	DIL8	R26	33k
IC2	DIL8	R25	1M
IC3	DIL8	R24	33k
IC4	DIL8	R23	2.2k
R1	10k	R22	100k
R2	30k	R21	10k
R3	8.2k	R20	1M
R4	10k	R19	240
R5	10k	R18	10k
R6	30k	R17	10k
R7	8.2k	R16	100k
R8	10k	R15	8.2k
R9	10k	R14	12.7k
R10	12.7k	R13	10k
R11	8.2k	R12	100

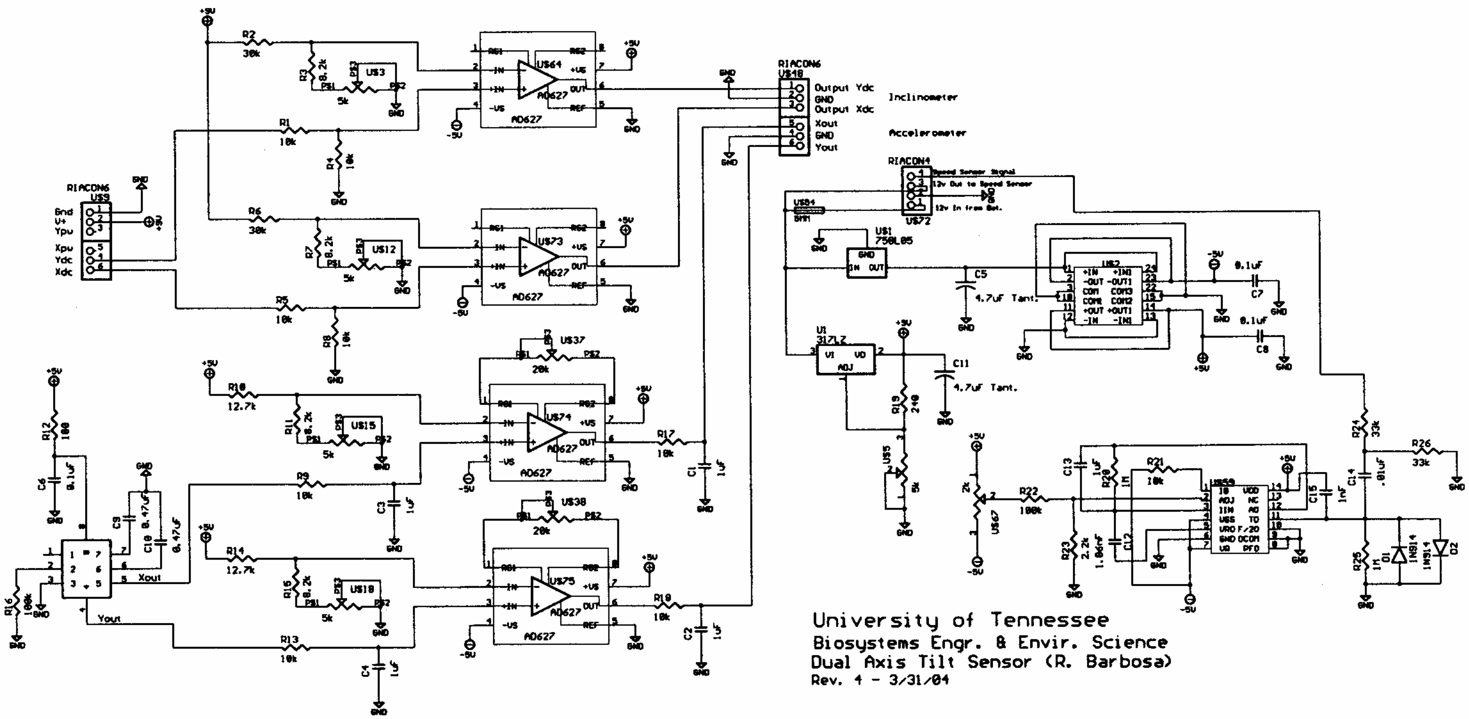
University of Tennessee
Biosystems Engr. & Envir. Science
Dual Axis Tilt Sensor (R. Barbosa)
Rev. 4 - 3/31/04
Inclinometer
Accelerometer
Output Ydc
GND
Output Xdc
Xout
GND
Yout
AD627
RIACON6
RIACON4
750L05
317LZ
4.7uF Tant.

APPENDIX G

Sensor Static Calibration Data

Data Used in the Sensor Calibration

X Axis:

Measured Angle (degrees)	Clinometer (mvolts)	Accelerometer (mvolts)
-16.7	-4504.3	-4040.8
-14.4	-3782.3	-3417.0
-10.8	-2761.7	-2486.3
-5.7	-1582.7	-1420.4
-2.8	-891.0	-797.3
2.1	773.5	635.5
3.5	1047.2	878.4
4.3	1164.5	991.1
5	1434.2	1248.2
6.4	1545.4	1429.7
7.9	2312.7	2020.1
9.3	2396.9	2179.5
12.2	3224.9	2924.2
12.2	3261.2	2867.7
15.9	4045.1	3554.1

Y Axis:

Measured Angle (degrees)	Clinometer (mvolts)	Accelerometer (mvolts)
-17.6	-4819.6	-4413.8
-15.0	-4078.8	-3738.3
-10.2	-2860.1	-2644.9
-7.7	-2219.5	-2061.5
-6.1	-1703.8	-1591.6
1.5	528.2	334.4
3.1	947.1	810.3
3.5	1097.0	852.7
6.6	1853.2	1628.4
8.7	2456.0	2064.1
10.8	3018.8	2621.8
11.3	3202.1	2687.1
13.9	3908.2	3371.4

RESULTS (X-AXIS CLINOMETER)

The SAS System   11:22 Thursday, April 15, 2004   7

The REG Procedure
Model: MODEL1
Dependent Variable: angle

Analysis of Variance

Source	DF	Sum of Squares	Mean Square	F Value	Pr > F
Model	1	1416.06573	1416.06573	8447.93	<.0001
Error	20	3.35246	0.16762		
Corrected Total	21	1419.41818			

Root MSE	0.40942	R-Square	0.9976
Dependent Mean	1.30909	Adj R-Sq	0.9975
Coeff Var	31.27496		

Parameter Estimates

Variable	DF	Parameter Estimate	Standard Error	t Value	Pr > |t|
Intercept	1	0.02201	0.08840	0.25	0.8059
volt	1	0.00378	0.00004115	91.91	<.0001

RESULTS (X-AXIS CLINOMETER)

The SAS System 11:22 Thursday, April 15, 2004 9

The REG Procedure
Model: MODEL1
Dependent Variable: angle

Output Statistics

Obs	Dependent Variable	Predicted Value	Std Error Mean Predict	95% CL Mean		Residual
1	-16.7000	-17.0157	0.2176	-17.4697	-16.5617	0.3157
2	-14.5000	-14.2847	0.1908	-14.6827	-13.8867	-0.2153
3	-10.8000	-10.4243	0.1546	-10.7469	-10.1017	-0.3757
4	-5.7000	-5.9646	0.1178	-6.2104	-5.7189	0.2646
5	-2.9000	-3.3482	0.1009	-3.5588	-3.1377	0.4482
6	2.2000	2.9478	0.0891	2.7620	3.1337	-0.7478
7	3.6000	3.9831	0.0920	3.7912	4.1750	-0.3831
8	4.3000	4.4268	0.0936	4.2314	4.6221	-0.1268
9	5.0000	5.4469	0.0982	5.2421	5.6518	-0.4469
10	6.5000	5.8676	0.1004	5.6581	6.0770	0.6324
11	7.9000	8.7699	0.1192	8.5213	9.0186	-0.8699
12	9.4000	9.0884	0.1216	8.8348	9.3420	0.3116
13	12.2000	12.3577	0.1486	12.0478	12.6675	-0.1577
14	12.3000	12.2204	0.1474	11.9130	12.5277	0.0796
15	16.0000	15.3228	0.1757	14.9563	15.6893	0.6772
16	0	-0.1584	0.0887	-0.3435	0.0267	0.1584
17	0	-0.1266	0.0887	-0.3116	0.0583	0.1266
18	0	-0.0971	0.0886	-0.2820	0.0877	0.0971
19	0	-0.1032	0.0886	-0.2881	0.0817	0.1032
20	0	-0.1970	0.0888	-0.3823	-0.0117	0.1970
21	0	-0.0673	0.0886	-0.2520	0.1175	0.0673
22	0	0.1559	0.0882	-0.0280	0.3399	-0.1559

Sum of Residuals	0
Sum of Squared Residuals	3.35246
Predicted Residual SS (PRESS)	4.13931

RESULTS (X-AXIS CLINOMETER)

The REG Procedure
Model: MODEL1
Dependent Variable: angle

Output Statistics

Obs	Dependent Variable	Predicted Value	Std Error Mean Predict	95% CL Predict		Residual
1	-16.7000	-17.0157	0.2176	-17.9829	-16.0485	0.3157
2	-14.5000	-14.2847	0.1908	-15.2270	-13.3425	-0.2153
3	-10.8000	-10.4243	0.1546	-11.3372	-9.5113	-0.3757
4	-5.7000	-5.9646	0.1178	-6.8533	-5.0759	0.2646
5	-2.9000	-3.3482	0.1009	-4.2278	-2.4686	0.4482
6	2.2000	2.9478	0.0891	2.0738	3.8218	-0.7478
7	3.6000	3.9831	0.0920	3.1078	4.8584	-0.3831
8	4.3000	4.4268	0.0936	3.5507	5.3029	-0.1268
9	5.0000	5.4469	0.0982	4.5687	6.3252	-0.4469
10	6.5000	5.8676	0.1004	4.9882	6.7469	0.6324
11	7.9000	8.7699	0.1192	7.8804	9.6594	-0.8699
12	9.4000	9.0884	0.1216	8.1975	9.9793	0.3116
13	12.2000	12.3577	0.1486	11.4492	13.2662	-0.1577
14	12.3000	12.2204	0.1474	11.3127	13.1280	0.0796
15	16.0000	15.3228	0.1757	14.3935	16.2521	0.6772
16	0	-0.1584	0.0887	-1.0323	0.7154	0.1584
17	0	-0.1266	0.0887	-1.0005	0.7472	0.1266
18	0	-0.0971	0.0886	-0.9709	0.7767	0.0971
19	0	-0.1032	0.0886	-0.9770	0.7706	0.1032
20	0	-0.1970	0.0888	-1.0709	0.6769	0.1970
21	0	-0.0673	0.0886	-0.9410	0.8065	0.0673
22	0	0.1559	0.0882	-0.7177	1.0295	-0.1559

Sum of Residuals	0
Sum of Squared Residuals	3.35246
Predicted Residual SS (PRESS)	4.13931

RESULTS (Y-AXIS CLINOMETER)

```
 The SAS System                                   10
                   11:22 Thursday, April 15, 2004

     The REG Procedure
       Model: MODEL1
Dependent Variable: angle

    Analysis of Variance
```

Source	DF	Sum of Squares	Mean Square	F Value	Pr > F
Model	1	1324.66211	1324.66211	28152.8	<.0001
Error	18	0.84695	0.04705		
Corrected Total	19	1325.50906			

Root MSE	0.21692	R-Square	0.9994
Dependent Mean	0.13650	Adj R-Sq	0.9993
Coeff Var	158.91283		

Parameter Estimates

Variable	DF	Parameter Estimate	Standard Error	t Value	Pr > |t|
Intercept	1	-0.06700	0.04852	-1.38	0.1842
volt	1	0.00360	0.00002145	167.79	<.0001

RESULTS (Y-AXIS CLINOMETER)

The SAS System 11
11:22 Thursday, April 15, 2004

The REG Procedure
Model: MODEL1
Dependent Variable: angle

Output Statistics

Obs	Dependent Variable	Predicted Value	Std Error Mean Predict	95% CL Predict		Residual
1	-6.2000	-6.1978	0.0615	-6.6715	-5.7241	-0.002204
2	-7.7000	-8.0534	0.0688	-8.5315	-7.5753	0.3534
3	-10.3000	-10.3585	0.0792	-10.8436	-9.8734	0.0585
4	-15.0000	-14.7438	0.1011	-15.2465	-14.2410	-0.2562
5	-17.7000	-17.4094	0.1153	-17.9255	-16.8933	-0.2906
6	3.1000	3.3410	0.0521	2.8723	3.8097	-0.2410
7	6.7000	6.6014	0.0619	6.1274	7.0753	0.0986
8	10.8000	10.7956	0.0799	10.3099	11.2812	0.004437
9	13.9000	13.9959	0.0958	13.4977	14.4941	-0.0959
10	1.5000	1.8336	0.0495	1.3662	2.3011	-0.3336
11	3.5800	3.8803	0.0534	3.4110	4.3497	-0.3003
12	11.3200	11.4551	0.0831	10.9671	11.9431	-0.1351
13	8.7300	8.7704	0.0707	8.2911	9.2498	-0.0404
14	0	-0.2386	0.0486	-0.7056	0.2284	0.2386
15	0	-0.2084	0.0485	-0.6754	0.2586	0.2084
16	0	-0.1803	0.0485	-0.6473	0.2866	0.1803
17	0	-0.1861	0.0485	-0.6531	0.2809	0.1861
18	0	-0.2753	0.0486	-0.7424	0.1917	0.2753
19	0	-0.1519	0.0485	-0.6189	0.3151	0.1519
20	0	0.0604	0.0485	-0.4066	0.5274	-0.0604

Sum of Residuals	0
Sum of Squared Residuals	0.84695
Predicted Residual SS (PRESS)	1.07384

RESULTS (Y-AXIS CLINOMETER)

The SAS System 12
11:22 Thursday, April 15, 2004

The REG Procedure
Model: MODEL1
Dependent Variable: angle

Output Statistics

Obs	Dependent Variable	Predicted Value	Std Error Mean Predict	95% CL Mean		Residual
1	-6.2000	-6.1978	0.0615	-6.3269	-6.0687	-0.002204
2	-7.7000	-8.0534	0.0688	-8.1980	-7.9089	0.3534
3	-10.3000	-10.3585	0.0792	-10.5248	-10.1922	0.0585
4	-15.0000	-14.7438	0.1011	-14.9561	-14.5314	-0.2562
5	-17.7000	-17.4094	0.1153	-17.6516	-17.1672	-0.2906
6	3.1000	3.3410	0.0521	3.2314	3.4505	-0.2410
7	6.7000	6.6014	0.0619	6.4712	6.7315	0.0986
8	10.8000	10.7956	0.0799	10.6276	10.9635	0.004437
9	13.9000	13.9959	0.0958	13.7947	14.1971	-0.0959
10	1.5000	1.8336	0.0495	1.7295	1.9377	-0.3336
11	3.5800	3.8803	0.0534	3.7682	3.9925	-0.3003
12	11.3200	11.4551	0.0831	11.2806	11.6297	-0.1351
13	8.7300	8.7704	0.0707	8.6219	8.9190	-0.0404
14	0	-0.2386	0.0486	-0.3407	-0.1366	0.2386
15	0	-0.2084	0.0485	-0.3104	-0.1064	0.2084
16	0	-0.1803	0.0485	-0.2823	-0.0784	0.1803
17	0	-0.1861	0.0485	-0.2881	-0.0841	0.1861
18	0	-0.2753	0.0486	-0.3774	-0.1733	0.2753
19	0	-0.1519	0.0485	-0.2539	-0.0500	0.1519
20	0	0.0604	0.0485	-0.0415	0.1623	-0.0604

Sum of Residuals	0
Sum of Squared Residuals	0.84695
Predicted Residual SS (PRESS)	1.07384

RESULTS (X-AXIS ACCELEROMETER)

The REG Procedure
Model: MODEL1
Dependent Variable: force

Analysis of Variance

Source	DF	Sum of Squares	Mean Square	F Value	Pr > F
Model	1	0.51722	0.51722	15161.7	<.0001
Error	21	0.00071638	0.00003411		
Corrected Total	22	0.51793			

Root MSE	0.00584	R-Square	0.9986
Dependent Mean	0.03636	Adj R-Sq	0.9986
Coeff Var	16.06133		

Parameter Estimates

Variable	DF	Parameter Estimate	Standard Error	t Value	Pr > |t|
Intercept	1	0.00140	0.00125	1.12	0.2748
volt	1	0.00007294	5.923879E-7	123.13	<.0001

RESULTS (X-AXIS ACCELEROMETER)

The REG Procedure
Model: MODEL1
Dependent Variable: force

Output Statistics

Obs	Dependent Variable	Predicted Value	Std Error Mean Predict	95% CL Predict		Residual
1	-0.0499	-0.0568	0.001434	-0.0693	-0.0442	0.006855
2	-0.1000	-0.1022	0.001658	-0.1148	-0.0896	0.002197
3	-0.1874	-0.1800	0.002138	-0.1929	-0.1670	-0.007423
4	-0.2874	-0.2933	0.002942	-0.3069	-0.2797	0.005987
5	-0.2499	-0.2478	0.002610	-0.2611	-0.2345	-0.002031
6	0.1625	0.1604	0.001580	0.1478	0.1730	0.002080
7	0.1125	0.1057	0.001342	0.0932	0.1182	0.006821
8	0.2124	0.2147	0.001892	0.2019	0.2275	-0.002349
9	0.0875	0.0924	0.001300	0.0800	0.1049	-0.004950
10	0.1374	0.1488	0.001522	0.1362	0.1613	-0.0113
11	0.0375	0.0478	0.001221	0.0353	0.0602	-0.0102
12	0.0750	0.0737	0.001255	0.0613	0.0861	0.001288
13	0.2113	0.2106	0.001867	0.1978	0.2233	0.000742
14	0.2750	0.2606	0.002191	0.2477	0.2736	0.0143
15	0.0624	0.0655	0.001241	0.0531	0.0779	-0.003036
16	0.3374	0.3408	0.002756	0.3274	0.3542	-0.003370
17	0	-0.002510	0.001258	-0.0149	0.009915	0.002510
18	0	-0.001286	0.001256	-0.0137	0.0111	0.001286
19	0	-0.001106	0.001255	-0.0135	0.0113	0.001106
20	0	-0.000617	0.001254	-0.0130	0.0118	0.000617
21	0	-0.001421	0.001256	-0.0138	0.0110	0.001421
22	0	-0.001291	0.001256	-0.0137	0.0111	0.001291
23	0	0.003818	0.001246	-0.008602	0.0162	-0.003818

Sum of Residuals	0
Sum of Squared Residuals	0.00071638
Predicted Residual SS (PRESS)	0.00089593

RESULTS (X-AXIS ACCELEROMETER)

The REG Procedure
Model: MODEL1
Dependent Variable: force

Output Statistics

Obs	Dependent Variable	Predicted Value	Std Error Mean Predict	95% CL Mean		Residual
1	-0.0499	-0.0568	0.001434	-0.0597	-0.0538	0.006855
2	-0.1000	-0.1022	0.001658	-0.1057	-0.0988	0.002197
3	-0.1874	-0.1800	0.002138	-0.1844	-0.1755	-0.007423
4	-0.2874	-0.2933	0.002942	-0.2995	-0.2872	0.005987
5	-0.2499	-0.2478	0.002610	-0.2533	-0.2424	-0.002031
6	0.1625	0.1604	0.001580	0.1571	0.1637	0.002080
7	0.1125	0.1057	0.001342	0.1029	0.1085	0.006821
8	0.2124	0.2147	0.001892	0.2108	0.2186	-0.002349
9	0.0875	0.0924	0.001300	0.0897	0.0952	-0.004950
10	0.1374	0.1488	0.001522	0.1456	0.1519	-0.0113
11	0.0375	0.0478	0.001221	0.0452	0.0503	-0.0102
12	0.0750	0.0737	0.001255	0.0711	0.0763	0.001288
13	0.2113	0.2106	0.001867	0.2067	0.2145	0.000742
14	0.2750	0.2606	0.002191	0.2561	0.2652	0.0143
15	0.0624	0.0655	0.001241	0.0629	0.0681	-0.003036
16	0.3374	0.3408	0.002756	0.3351	0.3465	-0.003370
17	0	-0.002510	0.001258	-0.005127	0.000106	0.002510
18	0	-0.001286	0.001256	-0.003897	0.001326	0.001286
19	0	-0.001106	0.001255	-0.003717	0.001504	0.001106
20	0	-0.000617	0.001254	-0.003225	0.001992	0.000617
21	0	-0.001421	0.001256	-0.004033	0.001191	0.001421
22	0	-0.001291	0.001256	-0.003903	0.001320	0.001291
23	0	0.003818	0.001246	0.001227	0.006410	-0.003818

Sum of Residuals	0
Sum of Squared Residuals	0.00071638
Predicted Residual SS (PRESS)	0.00089593

RESULTS (Y-AXIS ACCELEROMETER)

The SAS System 20
15:21 Thursday, April 15, 2004

The REG Procedure
Model: MODEL1
Dependent Variable: force

Analysis of Variance

Source	DF	Sum of Squares	Mean Square	F Value	Pr > F
Model	1	0.49781	0.49781	26318.2	<.0001
Error	19	0.00035939	0.00001892		
Corrected Total	20	0.49817			

Root MSE	0.00435	R-Square	0.9993
Dependent Mean	0.01826	Adj R-Sq	0.9992
Coeff Var	23.81857		

Parameter Estimates

Variable	DF	Parameter Estimate	Standard Error	t Value	Pr > |t|
Intercept	1	0.00430	0.00095295	4.51	0.0002
volt	1	0.00007053	4.347751E-7	162.23	<.0001

RESULTS (Y-AXIS ACCELEROMETER)

The REG Procedure
Model: MODEL1
Dependent Variable: force

Output Statistics

Obs	Dependent Variable	Predicted Value	Std Error Mean Predict	95% CL Predict		Residual
1	-0.1071	-0.1080	0.001227	-0.1174	-0.0985	0.000827
2	-0.1340	-0.1411	0.001366	-0.1506	-0.1316	0.007115
3	-0.1785	-0.1823	0.001558	-0.1919	-0.1726	0.003794
4	-0.2588	-0.2594	0.001957	-0.2694	-0.2494	0.000552
5	-0.3035	-0.3070	0.002218	-0.3172	-0.2968	0.003481
6	0.0536	0.0615	0.000986	0.0521	0.0708	-0.007901
7	0.1160	0.1192	0.001135	0.1097	0.1286	-0.003179
8	0.1874	0.1892	0.001418	0.1796	0.1988	-0.001842
9	0.2409	0.2421	0.001675	0.2323	0.2519	-0.001190
10	0.0267	0.0279	0.000951	0.0186	0.0372	-0.001189
11	0.0624	0.0644	0.000991	0.0551	0.0738	-0.002001
12	0.1963	0.1938	0.001439	0.1842	0.2034	0.002455
13	0.1518	0.1499	0.001249	0.1404	0.1594	0.001890
14	0.3303	0.3180	0.002077	0.3079	0.3281	0.0124
15	0	0.002487	0.000954	-0.006833	0.0118	-0.002487
16	0	0.002427	0.000954	-0.006892	0.0117	-0.002427
17	0	0.002490	0.000954	-0.006829	0.0118	-0.002490
18	0	0.002325	0.000954	-0.006994	0.0116	-0.002325
19	0	0.002724	0.000954	-0.006595	0.0120	-0.002724
20	0	0.001996	0.000954	-0.007324	0.0113	-0.001996
21	0	0.000742	0.000955	-0.008577	0.0101	-0.000742

Sum of Residuals	0
Sum of Squared Residuals	0.00035939
Predicted Residual SS (PRESS)	0.00050628

RESULTS (Y-AXIS ACCELEROMETER)

The REG Procedure
Model: MODEL1
Dependent Variable: force

Output Statistics

Obs	Dependent Variable	Predicted Value	Std Error Mean Predict	95% CL Mean		Residual
1	-0.1071	-0.1080	0.001227	-0.1105	-0.1054	0.000827
2	-0.1340	-0.1411	0.001366	-0.1440	-0.1382	0.007115
3	-0.1785	-0.1823	0.001558	-0.1855	-0.1790	0.003794
4	-0.2588	-0.2594	0.001957	-0.2635	-0.2553	0.000552
5	-0.3035	-0.3070	0.002218	-0.3117	-0.3024	0.003481
6	0.0536	0.0615	0.000986	0.0594	0.0635	-0.007901
7	0.1160	0.1192	0.001135	0.1168	0.1215	-0.003179
8	0.1874	0.1892	0.001418	0.1863	0.1922	-0.001842
9	0.2409	0.2421	0.001675	0.2386	0.2456	-0.001190
10	0.0267	0.0279	0.000951	0.0259	0.0299	-0.001189
11	0.0624	0.0644	0.000991	0.0624	0.0665	-0.002001
12	0.1963	0.1938	0.001439	0.1908	0.1968	0.002455
13	0.1518	0.1499	0.001249	0.1473	0.1525	0.001890
14	0.3303	0.3180	0.002077	0.3136	0.3223	0.0124
15	0	0.002487	0.000954	0.000490	0.004483	-0.002487
16	0	0.002427	0.000954	0.000431	0.004424	-0.002427
17	0	0.002490	0.000954	0.000493	0.004487	-0.002490
18	0	0.002325	0.000954	0.000328	0.004322	-0.002325
19	0	0.002724	0.000954	0.000728	0.004721	-0.002724
20	0	0.001996	0.000954	-1.712E-6	0.003993	-0.001996
21	0	0.000742	0.000955	-0.001257	0.002742	-0.000742

Sum of Residuals	0
Sum of Squared Residuals	0.00035939
Predicted Residual SS (PRESS)	0.00050628

APPENDIX H

Data Used in Vehicle Heading Calculation

Samples Used in Vehicle Heading Calculation.

Sample N#	Time	Easting	Northing
1	140645.5	784122.284	169500.179
1	140646.0	784122.728	169499.755
1	140646.5	784123.182	169499.329
1	140647.0	784123.602	169498.919
1	140647.5	784123.981	169498.545
1	140648.0	784124.324	169498.190
1	140648.5	784124.628	169497.847
1	140649.0	784124.970	169497.561
1	140649.5	784125.260	169497.214
1	140650.0	784125.551	169496.901
1	140650.5	784125.897	169496.565
1	140651.0	784126.260	169496.255
1	140651.5	784126.576	169495.851
1	140652.0	784126.922	169495.476
1	140652.5	784127.331	169495.041
1	140653.0	784127.721	169494.633
1	140653.5	784128.166	169494.267
1	140654.0	784128.603	169493.902
1	140654.5	784129.004	169493.432
1	140655.0	784129.436	169492.968
2	144655.0	784241.396	169404.177
2	144655.5	784240.927	169404.647
2	144656.0	784240.475	169405.076
2	144656.5	784240.099	169405.545
2	144657.0	784239.688	169405.975
2	144657.5	784239.314	169406.483
2	144658.0	784238.886	169406.901
2	144658.5	784238.417	169407.360
2	144659.0	784237.981	169407.793
2	144659.5	784237.524	169408.269
2	144700.0	784237.092	169408.706
2	144700.5	784236.620	169409.120
2	144701.0	784236.223	169409.559
2	144701.5	784235.802	169410.075
2	144702.0	784235.403	169410.566
2	144702.5	784234.986	169411.048
2	144703.0	784234.559	169411.531
2	144703.5	784234.116	169412.049
2	144704.0	784233.680	169412.544
2	144704.5	784233.222	169413.039

Samples Used in Vehicle Heading Calculation (continued).

Sample N#	Time	Easting	Northing
3	154509.5	784182.567	169532.380
3	154510.0	784183.089	169531.905
3	154510.5	784183.721	169531.494
3	154511.0	784184.328	169531.008
3	154511.5	784184.895	169530.482
3	154512.0	784185.469	169529.944
3	154512.5	784186.058	169529.509
3	154513.0	784186.646	169529.033
3	154513.5	784187.088	169528.707
3	154514.0	784187.584	169528.245
3	154514.5	784187.962	169527.782
3	154515.0	784188.397	169527.314
3	154515.5	784188.935	169526.956
3	154516.0	784189.408	169526.481
3	154516.5	784189.889	169526.046
3	154517.0	784190.375	169525.569
3	154517.5	784190.805	169525.078
3	154518.0	784191.274	169524.604
3	154518.5	784191.782	169524.200
3	154519.0	784192.230	169523.726
4	143006.5	784320.588	169458.810
4	143007.0	784320.215	169459.187
4	143007.5	784319.911	169459.542
4	143008.0	784319.535	169459.905
4	143008.5	784319.196	169460.318
4	143009.0	784318.803	169460.734
4	143009.5	784318.450	169461.201
4	143010.0	784318.053	169461.651
4	143010.5	784317.640	169462.066
4	143011.0	784317.239	169462.522
4	143011.5	784316.863	169462.990
4	143012.0	784316.489	169463.426
4	143012.5	784316.123	169463.849
4	143013.0	784315.765	169464.238
4	143013.5	784315.394	169464.585
4	143014.0	784315.022	169464.971
4	143014.5	784314.670	169465.411
4	143015.0	784314.349	169465.841
4	143015.5	784314.016	169466.277
4	143016.0	784313.684	169466.617
5	150035.0	784231.078	169580.338

Samples Used in Vehicle Heading Calculation (continued).

Sample N#	Time	Easting	Northing
5	150035.5	784231.311	169579.945
5	150036.0	784231.629	169579.563
5	150036.5	784231.944	169579.203
5	150037.0	784232.288	169578.878
5	150037.5	784232.593	169578.550
5	150038.0	784232.893	169578.223
5	150038.5	784233.195	169577.837
5	150039.0	784233.526	169577.532
5	150039.5	784233.813	169577.236
5	150040.0	784234.073	169576.894
5	150040.5	784234.374	169576.556
5	150041.0	784234.716	169576.153
5	150041.5	784235.024	169575.777
5	150042.0	784235.374	169575.262
5	150042.5	784235.687	169574.972
5	150043.0	784236.080	169574.523
5	150043.5	784236.375	169574.152
5	150044.0	784236.722	169573.642
5	150044.5	784237.118	169573.295
6	152003.0	784297.542	169519.701
6	152003.5	784297.233	169520.139
6	152004.0	784296.866	169520.549
6	152004.5	784296.440	169520.971
6	152005.0	784296.084	169521.408
6	152005.5	784295.749	169521.755
6	152006.0	784295.395	169522.117
6	152006.5	784295.056	169522.504
6	152007.0	784294.706	169522.913
6	152007.5	784294.376	169523.318
6	152008.0	784294.041	169523.707
6	152008.5	784293.643	169524.081
6	152009.0	784293.260	169524.445
6	152009.5	784292.917	169524.771
6	152010.0	784292.599	169525.136
6	152010.5	784292.275	169525.531
6	152011.0	784291.934	169525.864
6	152011.5	784291.578	169526.256
6	152012.0	784291.232	169526.611
6	152012.5	784290.842	169526.966
7	153459.0	784254.985	169575.722
7	153459.5	784254.567	169576.146

Samples Used in Vehicle Heading Calculation (continued).

Sample N#	Time	Easting	Northing
7	153500.0	784254.172	169576.667
7	153500.5	784253.782	169577.095
7	153501.0	784253.428	169577.602
7	153501.5	784253.063	169578.055
7	153502.0	784252.683	169578.550
7	153502.5	784252.330	169578.998
7	153503.0	784251.991	169579.477
7	153503.5	784251.597	169579.878
7	153504.0	784251.232	169580.290
7	153504.5	784250.871	169580.685
7	153505.0	784250.511	169581.087
7	153505.5	784250.062	169581.500
7	153506.0	784249.642	169581.935
7	153506.5	784249.240	169582.503
7	153507.0	784248.844	169582.995
7	153507.5	784248.468	169583.490
7	153508.0	784248.055	169584.008
7	153508.5	784247.647	169584.543
8	161150.5	784311.064	169543.342
8	161151.0	784311.442	169542.932
8	161151.5	784311.791	169542.447
8	161152.0	784312.074	169542.004
8	161152.5	784312.377	169541.564
8	161153.0	784312.691	169541.154
8	161153.5	784313.075	169540.727
8	161154.0	784313.475	169540.319
8	161154.5	784313.824	169539.854
8	161155.0	784314.183	169539.441
8	161155.5	784314.534	169539.016
8	161156.0	784314.895	169538.587
8	161156.5	784315.251	169538.142
8	161157.0	784315.635	169537.720
8	161157.5	784316.065	169537.311
8	161158.0	784316.495	169536.881
8	161158.5	784316.829	169536.380
8	161159.0	784317.169	169535.904
8	161159.5	784317.507	169535.493
8	161200.0	784317.875	169535.095
9	142642.5	784189.450	169440.198
9	142643.0	784189.033	169440.614
9	142643.5	784188.697	169441.086

Samples Used in Vehicle Heading Calculation (continued).

Sample N#	Time	Easting	Northing
9	142644.0	784188.343	169441.607
9	142644.5	784187.967	169441.999
9	142645.0	784187.611	169442.465
9	142645.5	784187.193	169442.812
9	142646.0	784186.779	169443.228
9	142646.5	784186.410	169443.663
9	142647.0	784186.032	169444.130
9	142647.5	784185.671	169444.589
9	142648.0	784185.279	169445.058
9	142648.5	784184.843	169445.463
9	142649.0	784184.449	169445.849
9	142649.5	784183.991	169446.222
9	142650.0	784183.562	169446.589
9	142650.5	784183.165	169446.984
9	142651.0	784182.758	169447.350
9	142651.5	784182.330	169447.804
9	142652.0	784181.953	169448.254
10	153939.5	784229.204	169482.188
10	153940.0	784229.642	169481.670
10	153940.5	784230.079	169481.174
10	153941.0	784230.523	169480.683
10	153941.5	784230.944	169480.201
10	153942.0	784231.426	169479.697
10	153942.5	784231.908	169479.122
10	153943.0	784232.407	169478.539
10	153943.5	784232.889	169478.022
10	153944.0	784233.379	169477.520
10	153944.5	784233.814	169477.045
10	153945.0	784234.251	169476.554
10	153945.5	784234.655	169476.080
10	153946.0	784235.083	169475.654
10	153946.5	784235.548	169475.195
10	153947.0	784236.006	169474.713
10	153947.5	784236.560	169474.278
10	153948.0	784237.073	169473.811
10	153948.5	784237.597	169473.296
10	153949.0	784238.038	169472.803

APPENDIX I

Computer Codes

MatLab® program used to calculate slope gradient and vehicle attitude in Chapter III tests.

```
 %% R = Rowe and Spencer's model (1976) %%
 %% Y = Yang's model (1997) %%
 %% S = Simplified model (2005) %%
clear;
clc;
%% Creates an array from -15 to 15 degrees %%
b = (-15:0.25:15);
a=nonzeros(b);
for i=1:120
   for j=1:120
%%CALCULATE SLOPE GRADIENT %%
      Slope_R(i,j) = asin(sqrt((sin (a(i)*pi/180)).^2+(sin(a(j)*pi/180)).^2))/pi*180;
      Slope_Y(i,j) = acos(sqrt((1+(tan(a(i)*pi/180).^2)+(tan(a(j)*pi/180).^2)).^-1))/pi*180;
      Slope_S(i,j) = sqrt(a(i).^2+a(j).^2);
%% CALCULATE DIFFERENCE BETWEEN MODELS %%
      Slope_dif_1(i,j) = Slope_R(i,j) - Slope_S(i,j);
      Slope_dif_2(i,j) = Slope_S(i,j) - Slope_Y(i,j);
      Slope_dif_3(i,j) = Slope_R(i,j) - Slope_Y(i,j);
%%CALCULATE VEHICLE ATTITUDE %%
      R_1(i,j) = asin(sin(a(j)*pi/180)/sqrt(sin(a(i)*pi/180).^2+sin(a(j)*pi/180).^2))/pi*180;
      Y_1(i,j) = atan(((tan(a(j)*pi/180)/tan(a(i)*pi/180))*(1+tan(a(j)*pi/180)*tan(a(j)*pi/180))+_
          (tan(a(j)*pi/180)*tan(a(i)*pi/180)))/sqrt(1+tan(a(j)*pi/180)*tan(a(j)*pi/180)+_
          tan(a(i)*pi/180)*tan(a(i)*pi/180)))/pi*180;
      S_1(i,j) = atan(a(j)/a(i))/pi*180;
      %% THE NEXT SERIES OF CONDITIONS CHANGES FROM -PI()/2 TO PI()/2 TO
      %% 0-360 %%
      if a(i)>0
         Att_R(i,j)= 180 - R_1(i,j);
      elseif a(j)>0
         Att_R(i,j)= R_1(i,j);
      else
         Att_R(i,j)= 360 + R_1(i,j);
      end
      if a(i)<0
         if a(j)<0
            Att_Y(i,j)= 360 - Y_1(i,j);
            Att_S(i,j)= 360 - S_1(i,j);
         else
            Att_Y(i,j)= abs(Y_1(i,j));
            Att_S(i,j) = abs(S_1(i,j));
         end
      else
         Att_Y(i,j)=180-Y_1(i,j);
         Att_S(i,j)=180-S_1(i,j);
      end
       Att_dif_1(i,j) = abs(Att_R(i,j) - Att_S(i,j));
       Att_dif_2(i,j) = abs(Att_Y(i,j) - Att_S(i,j));
       Att_dif_3(i,j) = abs(Att_R(i,j) - Att_Y(i,j));
   end
```

```
end
%% CALCULATES THE CORRELATION BETWEEN SURFACES %%
[R1,P1] = corrcoef(Slope_R,Slope_Y);
[R2,P2] = corrcoef(Slope_R,Slope_S);
[R3,P3] = corrcoef(Slope_Y,Slope_S);
[R4,P4] = corrcoef(Att_R,Att_Y);
[R5,P5] = corrcoef(Att_R,Att_S);
[R6,P6] = corrcoef(Att_Y,Att_S);
%%END%%
```

MatLab® program used to calculate the differences between inverse tangent and Maclaurin series.

```
%% COMPARISON BETWEEN OUTPUT OF ARCTAN FUNCTION AND APPROXIMATION %%
%% USING MACLAURIN SERIES %%
clear;
clc;
b = (-15:0.25:15);
a=nonzeros(b);
d= pi/4;
e = pi / 2;
for i=1:120
   for j=1:120
      sign(i,j) = a(j)/a(i);
      ratio(i,j) = abs (sign(i,j));
      inv_ratio(i,j) = 1 / ratio(i,j);
%% DIVIDE THE MACLAURIN ALGORITHM IN THREE PARTS %%
      if ratio(i,j) < 0.5
         Att_1(i,j) = ratio(i,j) - (ratio(i,j) ^ 3 / 3 ) + (ratio(i,j) ^ 5 / 5 ) - (ratio(i,j) ^ 7 / 7 ) +_
          (ratio(i,j) ^ 9 / 9 ) - (ratio(i,j) ^ 11 / 11) + (ratio(i,j) ^ 13 / 13);
      elseif ratio(i,j) >= 0.5 & ratio(i,j) <=3
         ratio2(i,j) = (ratio(i,j) - tan ( d ))/( 1 + ratio(i,j) * tan ( d ));
         Att_1(i,j) = d + ratio2(i,j) - (ratio2(i,j) ^ 3 / 3 ) + (ratio2(i,j) ^ 5 / 5 ) - (ratio2(i,j) ^ 7 / 7 ) +_
          (ratio2(i,j) ^ 9 / 9 ) ) - ( inv_ratio(i,j) ^ 11 / 11 ) + ( inv_ratio(i,j) ^ 13 / 13 ) );
      else
         Att_1(i,j) = e - ( inv_ratio(i,j) - ( inv_ratio(i,j) ^ 3 / 3 ) + ( inv_ratio(i,j) ^ 5 / 5 ) -_
          ( inv_ratio(i,j) ^ 7 / 7 ) + ( inv_ratio(i,j) ^ 9 / 9 ) - ( inv_ratio(i,j) ^ 11 / 11 ) +_
          ( inv_ratio(i,j) ^ 13 / 13 ) );
      end
 %% CORRECT FOR THE NEGATIVE SIGN IF NEEDED %%
      if sign(i,j) < 0
        Att_2(i,j) = Att_1(i,j) * - 1;
      else
        Att_2 (i,j) = Att_1(i,j);
      end
 %% OUTPUT A DIFFERENCE SURFACE %%
         Att_3(i,j) = Att_2(i,j) / pi * 180;
         True(i,j) = atan(sign(i,j)) / pi * 180;
         Diff(i,j) = Att_3(i,j) - True(i,j);
   end
```

Matlab® Code in Vehicle Heading Direction

```
%% PROGRAM TO CALCULATE LINEAR SLOPE OF GPS POINTS %%

clc;
clear;
data = dlmread ( 'one.txt' , '\t' ) ;
x = data ( : , 2 ) ;
y = data ( : , 3 ) ;
X = [ ones ( size ( x ) )  x ] ;
a = X \ y ;
slope = 90 - atan ( a ( 2 ) )  / pi * 180 ;

%% END %%
```

Visual Basic® Program Used in the Sensors' Calibration Procedure

```
Const BoardNum% = 1              ' Board number
Const NumPoints& = 2500          ' Number of data points to collect
Const FirstPoint& = 0            ' set first element in buffer to transfer to array
Const TotalPoint& = 150000
Dim ADData%(TotalPoint&)         ' NumPoints& dimension an array to hold the input values
Dim MemHandle&                   ' define a variable to contain the handle for
Dim strFilename1, strFilename2 ' memory allocated by Windows through cbWinBufAlloc%()
Dim fs As New FileSystemObject
Dim x&, y&

Private Sub cmdStart_Click()
   Call CreateFile
   txtDatafile.Text = strFilename2
End Sub

Private Function CreateFile()
   strFilename1 = InputBox("Enter a file name to store data", "File Name", , 500, 500)
   strFilename2 = "c:\barbosa\" + strFilename1
   Call OverWriteFile
End Function

Private Function OverWriteFile()
   If fs.FileExists(strFilename2) = True Then
      msgResult = MsgBox("File Already Exists. Overwrite?", vbQuestion + vbYesNo,
            "Overwrite?")
         If msgResult = vbYes Then
            Open strFilename2 For Output As #1
         Else
            Call CreateFile
         End If
   Else
      Open strFilename2 For Output As #1
   End If
End Function

Private Sub cmdStop_Click()
   Close #1
   ULStat% = cbWinBufFree(MemHandle&)        ' Free up memory for use by
  If ULStat% <> 0 Then Stop                  ' other programs
  End
End Sub

Private Sub Form_Load()
  ULStat% = cbDeclareRevision(CURRENTREVNUM)
  ULStat% = cbErrHandling(PRINTALL, DONTSTOP)
  If ULStat% <> 0 Then Stop
  MemHandle& = cbWinBufAlloc(TotalPoint&)      ' NumPoints& set aside memory to hold data
  If MemHandle& = 0 Then Stop
  Timer1.Interval = 1000
  Timer1.Enabled = False
End Sub
```

Visual Basic® Program Used in the Sensors' Calibration Procedure (continued)

```
Private Sub Timer1_Timer()
  y& = x& * NumPoints&
  LowChan% = 0                          ' first channel to acquire
  HighChan% = 4
  Debug.Print x&, y&
  CBCount& = NumPoints&                 ' total number of data points to collect
  CBRate& = 500                         ' sampling rate (samples per second)
  Options = CONVERTDATA                 ' return data as 12-bit values
  Gain = BIP5VOLTS                      ' set the gain
  If MemHandle& = 0 Then Stop           ' check that a handle to a memory buffer exists
  ULStat% = cbAInScan(BoardNum%, LowChan%, HighChan%, CBCount&, CBRate&, Gain,
            MemHandle&, Options)
  If ULStat% = 30 Then MsgBox "Change the Gain argument to one supported by this board.", 0,
            "Unsupported Gain"
  If ULStat% <> 0 And ULStat% <> 91 Then Stop
  ULStat% = cbWinBufToArray(MemHandle&, ADData%(y&), 0, NumPoints&)
  If ULStat% <> 0 Then Stop
  x& = x& + 1
End Sub


Private Sub txtText_KeyDown(KeyCode As Integer, Shift As Integer)
  If KeyCode = vbKeyF1 Then
     Timer1.Enabled = True
     x& = 0
  ElseIf KeyCode = vbKeyF2 Then
     Timer1.Enabled = False
     cmdStart.Enabled = True
     For z& = 0 To y& - 1 Step 5
        Print #1, ADData(z&), ",", ADData(z& + 1), ",", ADData(z& + 2), ",", ADData(z& + 3), ",",
            ADData(z& + 4)
     Next z&
   End If
End Sub
```

Visual Basic® Program Used in the Field Test

```
'THIS PROGRAM WAS WRITTEN TO SAMPLE 7 CHANNELS OF
' AN A/D BOARD 600 TIMES AND OUTPUT A SINGLE VALUE
' ALONG WITH GPS COORDINATES RECEIVED THROUGH COM 1
' 2 TIMES A SECOND
' JULY OF 2004
' WRITTEN BY ROBERTO BARBOSA

Const BoardNum% = 1
Dim DolarPos, LineFeedPos
Dim strGPS
Dim Lat, Lon, UTC, Alt
Dim buffer$
Dim Field
Dim Flag1 As String
Dim DumpArray(6, 599)
Dim ReadArray(6)
Dim FinalArray(6)
Dim OutArray()
Dim strFilename1, strFileName
Dim fs As New FileSystemObject
Public x
Public Flag2

Private Sub cmdStop_Click()
     If MSComm1.PortOpen = True Then
       MSComm1.PortOpen = False
   End If
   End
End Sub

Private Sub Form_Load()
   ULStat% = cbDeclareRevision(CURRENTREVNUM)
   ULStat% = cbErrHandling(PRINTALL, DONTSTOP)
   If ULStat% <> 0 Then Stop
   x = 0
End Sub

Private Sub MSComm1_OnComm()
buffer$ = MSComm1.Input
txtGPS.Text = buffer$
DolarPos = InStr(buffer$, "$") ' CHECKS THE POSITION OF THE $ IN THE STRING
LineFeedPos = InStr(buffer$, "*") ' CHECKS THE POSITION OF THE *
If DolarPos > 0 And LineFeedPos > 0 Then
   If LineFeedPos > DolarPos Then ' CHECK TO SEE IF THE SEQUENCE IS RIGHT
'EXTRACTS GPS INFO FROM $ TO THE END OF STRING
      strGPS = Mid(buffer$, DolarPos, LineFeedPos)
' THE FIELD COMMAND SPLITS A SEQUENTIAL STRING ACCORDING TO A COMMON
‘DELIMITER
      Field = Split(strGPS, ",")
      txtLat.Text = Field(2)
      txtLon.Text = Field(4)
      txtAlt.Text = Field(9)
```

```
        txtTime.Text = Field(1)
        txtQual.Text = Field(6)
        Call SampleData
        txtXINC.Text = FinalArray(0)
        txtYINC.Text = FinalArray(1)
        txtXACC.Text = FinalArray(2)
        txtYACC.Text = FinalArray(3)
        txtSPEED.Text = FinalArray(4)
        txtXACCRAW.Text = FinalArray(5)
        txtYACCRAW.Text = FinalArray(6)
        txtMarker.Text = x
        ReDim Preserve OutArray(11, x) ' RESIZED THE ARRAY W/O ERASING THE CONTENTS
        OutArray(0, x) = Field(1) 'UTC
        OutArray(1, x) = Field(2) 'LAT
        OutArray(2, x) = Field(4) 'LONG
        OutArray(3, x) = Field(9) 'HEIGHT
        OutArray(4, x) = Field(6) 'GPS QUALITY INDICATOR
        OutArray(5, x) = FinalArray(0) 'CHANNEL 1 (X INC)
        OutArray(6, x) = FinalArray(1) 'CHANNEL 2(Y INC)
        OutArray(7, x) = FinalArray(2) 'CHANNEL 3 (X ACC)
        OutArray(8, x) = FinalArray(3) 'CHANNEL 4 (Y ACC)
        OutArray(9, x) = FinalArray(4) 'CHANNEL 5 (SPEED)
        OutArray(10, x) = FinalArray(5) 'CHANNEL 6 (X ACC RAW)
        OutArray(11, x) = FinalArray(6) 'CHANNEL 7 (Y ACC RAW)
        x = x + 1 ' UPDATES THE COUNTER
    Else
        buffer$ = "" ' IF THE $ IS NOT THE FIRST CHARACTER LOOPS UNTIL GET IT
        MSComm1.PortOpen = False
        MSComm1.PortOpen = True
    End If
End If
End Sub

Private Sub SampleData()
    Gain = BIP5VOLTS
    'IN THIS FIRST LOOP 7 CHANNELS OF THE A/D CARD ARE READ AND THE VALUES
   ‘ARE ATTRIBUTED TO AN ARRAY
    For j = 0 To 599
        For Chan% = 0 To 6
            ULStat% = cbAIn(BoardNum%, Chan%, Gain, ReadArray(Chan%))
            If ULStat% <> 0 Then Stop
        Next Chan%
        DumpArray(0, j) = ReadArray(0)
        DumpArray(1, j) = ReadArray(1)
        DumpArray(2, j) = ReadArray(2)
        DumpArray(3, j) = ReadArray(3)
        DumpArray(4, j) = ReadArray(4)
        DumpArray(5, j) = ReadArray(5)
        DumpArray(6, j) = ReadArray(6)
    Next J
    'AFTER THE 600 VALUES ARE READ AN AVERAGE IS COMPUTED
    For i = 0 To 6
```

Visual Basic® Program Used in the Field Test (continued)

```
      Sum = 0
         For j = 0 To 599
            Sum = Sum + DumpArray(i, j)
         Next j
      FinalArray(i) = Sum / 600
   Next i
End Sub

Private Sub cmdStart_Click()
   Flag1 = 1 'The purpose of Flag1 is to keep tabs on the sequence of file numbers
   Flag2 = 0 'The pupose of Flag2 is to track weather F1 key has been pressed or not
   txtKEY.SetFocus
End Sub

Private Function CreateFile()
   strFilename1 = InputBox("Enter a new number for Flag1", "File Name", , 500, 500)
   Flag1 = strFilename1 ' Gives Flag1 a new number not to overwrite an exsting file
   strFileName = "c:\barbosa\" + Flag1 + ".txt"
   txtDatafile.Text = strFileName
   Call OverWriteFile
End Function

Private Function OverWriteFile()
'Checks to see if file exits to protect against overwriting
   If fs.FileExists(strFileName) = True Then
          msgResult = MsgBox("File Already Exists. Overwrite?", vbQuestion + vbYesNo,
               "Overwrite?")
         If msgResult = vbYes Then
            Open strFileName For Output As #1
            MSComm1.CommPort = 1
            MSComm1.PortOpen = True
            MSComm1.Settings = "4800,N,8,1"
            txtDatafile.Text = strFileName
            Flag2 = 1
         Else
            Call CreateFile
         End If
   Else
      Open strFileName For Output As #1 'If the file does not exists, create the sequence as usual
      MSComm1.CommPort = 1
      MSComm1.PortOpen = True
      MSComm1.Settings = "4800,N,8,1"
      txtDatafile.Text = strFileName
      Flag2 = 1 ' Flag2 set high (meaning F1 key has been pressed)
   End IF
   txtKEY.SetFocus
End Function

Private Sub txtKey_KeyDown(KeyCode As Integer, Shift As Integer)
  If KeyCode = vbKeyF1 Then
      If Flag2 = 1 Then   'If Flag2 is already high it means F1 was pressed accidently
         MSComm1.PortOpen = False ' Then the computer does nothing only closes and
```

Visual Basic® Program Used in the Field Test (continued)

```
        MSComm1.PortOpen = True ' opens COM 1
    ElseIf Flag2 = 0 Then   'If this is the first time pressing F1 then starts the
        If cmdStart.Enabled = True Then 'routine
            cmdStart.Enabled = False
        End If
        strFileName = "c:\barbosa\" + Flag1 + ".txt" 'Flag1 starts 1 and increments
        txtDatafile.Text = strFileName ' every time F2 is pressed to create a
        Call OverWriteFile  ' sequence of files
    End If

  ElseIf KeyCode = vbKeyF2 Then
    Flag1 = Flag1 + 1   'Increments FLag1 number
    Flag2 = 0   ' Zeros Flag2
    MSComm1.PortOpen = False
    For j = 0 To x - 1
        Print #1, OutArray(0, j); ","; OutArray(1, j); ","; OutArray(2, j); ","; OutArray(3, j); ",";
              OutArray(4, j); ","; OutArray(5, j); ","; OutArray(6, j); ","; OutArray(7, j); ","; OutArray(8,
              j); ","; OutArray(9, j); ","; OutArray(10, j); ","; OutArray(11, j)
    Next j
    x = 0
    Close #1
    txtGPS.Text = "" 'Clears the screen
    txtMarker.Text = ""
    txtLat.Text = ""
    txtLon.Text = ""
    txtAlt.Text = ""
    txtQual.Text = ""
    txtTime.Text = ""
    txtXINC.Text = ""
    txtYINC.Text = ""
    txtXACC.Text = ""
    txtYACC.Text = ""
    txtSPEED.Text = ""
    txtXACCRAW.Text = ""
    txtYACCRAW.Text = ""
    txtDatafile.Text = ""
  End If
End Sub
```

Matlab® Program Used to Compute Slope

```
%% PROGRAM TO CALCULATE SLOPE GRADIENT AND ASPECT %%
%% WRITTEN BY ROBERTO BARBOSA %%
%% FILENAME CEBOLA.M %%
clc;
clear;

%% TRUE ELEVATION MUST CONTAIN ELEVATION DATA %%
a=dlmread('true_elev.txt','\t');

%% GRID DISTANCE IN METERS %%
d=input('What is the distance?  ');

%% WINDOW SIZE FOR FILTERING %%
windowsize = input('What is the window size?  ');
[m,n]=size(a);

%% TRUE SLOPE CALCULATION %%
for i=1 : m - 1
   for j=1 : n - 1
      if a(i,j) == NaN | a(i+1,j) == NaN | a(i,j+1) == NaN | a(i+1,j+1) == NaN
         slope(i,j) = NaN;
         att(i,j) = NaN;
      else
      x(i,j) = ( ( a(i,j+1) - a(i,j) ) / d + ( a(i+1,j+1) - a(i+1,j) ) / d ) / 2;
      y(i,j) = ( ( a(i+1,j) - a(i,j) ) / d + ( a(i+1,j+1) - a(i,j+1) ) / d ) / 2;
      slope(i,j) = atan ( sqrt ( x(i,j) * x(i,j) + y(i,j) * y(i,j) ) ) / pi * 180;
%% ASPECT CALCULATION %%
      att(i,j) = atan ( y(i,j) / x(i,j) ) / pi *180;
          if x(i,j) > 0
            aspect(i,j) = 270 + att (i,j);
         elseif x(i,j) < 0
            aspect (i,j) = 90 + att(i,j);
         else
            aspect(i,j) = NaN;
         end
      end
   end
end

%% INPUT SENSOR DATA %%
s1 = dlmread('s1.txt', '\t');
s2 = dlmread('s2.txt', '\t');
s3 = dlmread('s3.txt', '\t');
s4 = dlmread('s4.txt', '\t');

%% INPUT GIS DATA %%
slope_gis = dlmread ('slope.txt' , '\t' );
aspect_gis = dlmread('aspect.txt' , '\t');

%% PREPARES SENSOR DATA FOR FILTERING %%
s1_inv = s1';
```

Matlab® Program Used to Compute Slope (continued)

```
s1_filt = filter(ones(1,windowsize) / windowsize,1,s1_inv);
s1_filt = s1_inv';
s2_filt = filter(ones(1,windowsize) / windowsize,1,s2);
s3_inv = s3';
s3_filt = filter(ones(1,windowsize) / windowsize,1,s3_inv);
s3_filt = s3_inv';
s4_filt = filter(ones(1,windowsize) / windowsize,1,s4);
[m,n] = size(s1);

%% ALIGNS THE DATA AFTER FILTERING %%
TF = isnan (s1_filt);
TF2 = isnan (s2_filt);
TF3 = isnan (s3_filt);
TF4 = isnan (s4_filt);
for i=1:m
   for j=1:n
      if TF(i,j) == 0
         s1_new(i,j) = s1_filt(i,j);
      else
         s1_new(i,j) = s1(i,j);
      end
      if TF2(i,j) == 0
         s2_new(i,j) = s2_filt(i,j);
      else
         s2_new(i,j) = s2(i,j);
      end
      if TF3(i,j) == 0
         s3_new(i,j) = s3_filt(i,j);
      else
         s3_new(i,j) = s3(i,j);
      end
      if TF4(i,j) == 0;
         s4_new(i,j) = s4_filt(i,j);
      else
         s4_new(i,j) = s4(i,j);
      end
   end
end

%% CALCULATES SLOPE GRADIENT AND ASPECT FROM SENSOR%%
%% USING SIMPLIFIED MODEL %%
for i = 1 : m
   for j = 1 : n
      if s1_new(i,j) == NaN
         x_inc(i,j) = NaN;
         y_inc(i,j) = NaN;
         x_acc(i,j) = NaN;
         y_acc(i,j) = NaN;
      else
%% CONVERTS FROM MILVOLTS TO DEGREES %%
         x_inc(i,j) = s1_new(i,j) * 0.00378 + 0.02201;
```

```
        y_inc(i,j) = s2_new(i,j) * 0.0036 - 0.067;
        x_acc(i,j) = asin ( s3_new(i,j) * 0.00007294 + 0.0014 ) / pi * 180;
        y_acc(i,j) = asin ( s4_new(i,j) * 0.00007053 + 0.0043 ) / pi * 180;
%% SLOPE GRADIENT %%
        slope_inc(i,j) = sqrt ( x_inc(i,j) * x_inc(i,j) + y_inc(i,j) * y_inc(i,j) );
        slope_acc(i,j) = sqrt ( x_acc(i,j) * x_acc(i,j) + y_acc(i,j) * y_acc(i,j) );
%% VEHICLE ATTITUDE%%
        att_inc(i,j) = atan ( y_inc(i,j) / x_inc(i,j) ) / pi * 180 ;
        att_acc(i,j) = atan ( y_acc(i,j) / x_acc(i,j) ) / pi * 180 ;
%%CONVERSION TO 0-360 DEGREES %%
          if x_inc(i,j) > 0
            att_2_inc(i,j) = 180 - att_inc(i,j);
          elseif y_inc(i,j) < 0
            att_2_inc(i,j) = 360 - att_inc(i,j);
          else
            att_2_inc(i,j) = abs ( att_inc(i,j) );
          end
          if x_acc(i,j) > 0
            att_2_acc(i,j) = 180 - att_acc(i,j);
          elseif y_acc(i,j) < 0
            att_2_acc(i,j) = 360 - att_acc(i,j);
          else
            att_2_acc(i,j) = abs ( att_acc(i,j) );
          end
%%COVERSION TO NORTH USING BIAS %%
          if att_2_inc(i,j) < 223
            aspect_inc(i,j) = att_2_inc(i,j) + 137 ;
          else
            aspect_inc(i,j) = att_2_inc(i,j) + 137 - 360 ;
          end
          if att_2_acc(i,j) < 223
            aspect_acc(i,j) = att_2_acc(i,j) + 137 ;
          else
            aspect_acc(i,j) = att_2_acc(i,j) + 137 - 360 ;
          end
      end
   end
end

%%CLASSIFY ASPECT RESULTS IN 8 GROUPS %%
for i=1:m
   for j=1:n
%% TRUE ASPECT %%
      if aspect (i,j) >= 337.5 | aspect(i,j) <= 22.5
         region(i,j) = 1; %% NORTH %%
      elseif aspect(i,j) <= 67.5
         region(i,j) = 2; %% NORTHEAST %%
      elseif aspect(i,j) <= 112.5
         region(i,j) = 3; %% EAST %%
      elseif aspect(i,j) <= 157.5
         region(i,j) = 4; %% SOUTHEAST %%
      elseif aspect(i,j) <= 202.5
```

```
        region(i,j) = 5; %% SOUTH %%
    elseif aspect(i,j) <= 247.5
        region(i,j) = 6; %% SOUTHWEST %%
    elseif aspect(i,j) <= 292.5
        region(i,j) = 7; %% WEST %%
    elseif aspect(i,j) < 337.5
        region(i,j) = 8; %% NORTHWEST %%
    else
        region(i,j) = NaN;
    end
%% GIS ASPECT %%
    if aspect_gis (i,j) >= 337.5 | aspect_gis(i,j) <= 22.5
        region_gis(i,j) = 1;
    elseif aspect_gis(i,j) <= 67.5
        region_gis(i,j) = 2;
    elseif aspect_gis(i,j) <= 112.5
        region_gis(i,j) = 3;
    elseif aspect_gis(i,j) <= 157.5
        region_gis(i,j) = 4;
    elseif aspect_gis(i,j) <= 202.5
        region_gis(i,j) = 5;
    elseif aspect_gis(i,j) <= 247.5
        region_gis(i,j) = 6;
    elseif aspect_gis(i,j) <= 292.5
        region_gis(i,j) = 7;
    elseif aspect_gis(i,j) < 337.5
        region_gis(i,j) = 8;
    else
        region_gis(i,j) = NaN;
    end
%% CLINOMETER ASPECT %%
    if aspect_inc (i,j) >= 337.5 | aspect_inc(i,j) <= 22.5
        region_inc(i,j) = 1;
    elseif aspect_inc(i,j) <= 67.5
        region_inc(i,j) = 2;
    elseif aspect_inc(i,j) <= 112.5
        region_inc(i,j) = 3;
    elseif aspect_inc(i,j) <= 157.5
        region_inc(i,j) = 4;
    elseif aspect_inc(i,j) <= 202.5
        region_inc(i,j) = 5;
    elseif aspect_inc(i,j) <= 247.5
        region_inc(i,j) = 6;
    elseif aspect_inc(i,j) <= 292.5
        region_inc(i,j) = 7;
    elseif aspect_inc(i,j) < 337.5
        region_inc(i,j) = 8;
    else
        region_inc(i,j) = NaN;
    end
%% ACCELEROMETER ASPECT %%
    if aspect_acc (i,j) >= 337.5 | aspect_acc(i,j) <= 22.5
```

Matlab® Program Used to Compute Slope (continued)

```
        region_acc(i,j) = 1;
    elseif aspect_acc(i,j) <= 67.5
        region_acc(i,j) = 2;
    elseif aspect_acc(i,j) <= 112.5
        region_acc(i,j) = 3;
    elseif aspect_acc(i,j) <= 157.5
        region_acc(i,j) = 4;
    elseif aspect_acc(i,j) <= 202.5
        region_acc(i,j) = 5;
    elseif aspect_acc(i,j) <= 247.5
        region_acc(i,j) = 6;
    elseif aspect_acc(i,j) <= 292.5
        region_acc(i,j) = 7;
    elseif aspect_acc(i,j) < 337.5
        region_acc(i,j) = 8;
    else
        region_acc(i,j) = NaN;
    end

%% CLASSIFY SLOPE IN 6 GROUPS %%
%% TRUE SLOPE %%
    if slope(i,j) <= 1.14
        slope_region(i,j) = 1; %% 0 TO 2 PERCENT %%
    elseif slope(i,j) <= 2.86
        slope_region(i,j) = 2; %% 2 TO 5 PERCENT %%
    elseif slope(i,j) <=6.84
        slope_region(i,j) = 3; %% 5 TO 12 PERCENT %%
    elseif slope(i,j) <= 11.31
        slope_region(i,j) = 4; %% 12 TO 20 PERCENT %%
    elseif slope(i,j) <= 16.7
        slope_region(i,j) = 5; %% 20 TO 30 PERCENT %%
    elseif slope(i,j) < 99
        slope_region(i,j) = 6; %% GREATER THAN 30 PERCENT %%
    else
        slope_region(i,j) = NaN;
    end
%% GIS SLOPE %%
    if slope_gis(i,j) <= 1.14
        slope_region_gis(i,j) = 1; %% 0 TO 2 PERCENT %%
    elseif slope_gis(i,j) <= 2.86
        slope_region_gis(i,j) = 2; %% 2 TO 5 PERCENT %%
    elseif slope_gis(i,j) <=6.84
        slope_region_gis(i,j) = 3; %% 5 TO 12 PERCENT %%
    elseif slope_gis(i,j) <= 11.31
        slope_region_gis(i,j) = 4; %% 12 TO 20 PERCENT %%
    elseif slope_gis(i,j) <= 16.7
        slope_region_gis(i,j) = 5; %% 20 TO 30 PERCENT %%
    elseif slope_gis(i,j) < 99
        slope_region_gis(i,j) = 6; %% GREATER THAN 30 PERCENT %%
    else
        slope_region_gis(i,j) = NaN;
    end
```

Matlab® Program Used to Compute Slope (continued)

```
%% CLINOMETER SLOPE %%
      if slope_inc(i,j) <= 1.14
         slope_region_inc(i,j) = 1; %% 0 TO 2 PERCENT %%
      elseif slope_inc(i,j) <= 2.86
         slope_region_inc(i,j) = 2; %% 2 TO 5 PERCENT %%
      elseif slope_inc(i,j) <=6.84
         slope_region_inc(i,j) = 3; %% 5 TO 12 PERCENT %%
      elseif slope_inc(i,j) <= 11.31
         slope_region_inc(i,j) = 4; %% 12 TO 20 PERCENT %%
      elseif slope_inc(i,j) <= 16.7
         slope_region_inc(i,j) = 5; %% 20 TO 30 PERCENT %%
      elseif slope_inc(i,j) < 99
         slope_region_inc(i,j) = 6; %% GREATER THAN 30 PERCENT %%
      else
         slope_region_inc(i,j) = NaN;
      end
%% ACCELEROMETER SLOPE %%
      if slope_acc(i,j) <= 1.14
         slope_region_acc(i,j) = 1; %% 0 TO 2 PERCENT %%
      elseif slope_acc(i,j) <= 2.86
         slope_region_acc(i,j) = 2; %% 2 TO 5 PERCENT %%
      elseif slope_acc(i,j) <=6.84
         slope_region_acc(i,j) = 3; %% 5 TO 12 PERCENT %%
      elseif slope_acc(i,j) <= 11.31
         slope_region_acc(i,j) = 4; %% 12 TO 20 PERCENT %%
      elseif slope_acc(i,j) <= 16.7
         slope_region_acc(i,j) = 5; %% 20 TO 30 PERCENT %%
      elseif slope_acc(i,j) < 99
         slope_region_acc(i,j) = 6; %% GREATER THAN 30 PERCENT %%
      else
         slope_region_acc(i,j) = NaN;
      end
   end
end

%% REMOVES NaN FROM MATRIX %%
slope_region_n = slope_region (~isnan (slope_region) );
slope_region_gis_n = slope_region_gis (~isnan (slope_region_gis) );
slope_region_inc_n = slope_region_inc (~isnan (slope_region_inc) );
slope_region_acc_n = slope_region_acc (~isnan (slope_region_acc) );

%% INDICATES RIGHT SLOPE CLASSIFICATION WITH NUMBER ONE %%
[g h] = size(slope_region_n);
for i=1:g
   if slope_region_gis_n(i) == slope_region_n(i)
      slope_gis_region_corr_n(i) = 1;
   else
      slope_gis_region_corr_n(i) = 0;
   end
   if slope_region_inc_n(i) == slope_region_n(i)
      slope_inc_region_corr_n(i) = 1;
   else
```

```
            slope_inc_region_corr_n(i) = 0;
    end
    if slope_region_acc_n(i) == slope_region_n(i)
        slope_acc_region_corr_n(i) = 1;
    else
        slope_acc_region_corr_n(i) = 0;
    end
end

%% CALCULATES THE % CLASSIFIED RIGHT SLOPE REGION %%
slope_gis_region_corr = ( sum ( slope_gis_region_corr_n ) / g ) * 100 ;
slope_inc_region_corr = ( sum ( slope_inc_region_corr_n ) / g ) * 100;
slope_acc_region_corr = ( sum ( slope_acc_region_corr_n ) / g ) * 100;

%% CALCULATE THE MEAN ABSOLUTE ERROR %%
inc_dif = abs ( slope - slope_inc );
inc_dif = inc_dif ( ~isnan ( inc_dif ) );
acc_dif = abs ( slope - slope_acc );
acc_dif = acc_dif ( ~isnan ( acc_dif ) );
gis_dif = abs ( slope - slope_gis );
gis_dif = gis_dif ( ~isnan ( gis_dif ) );
mae_inc = mean ( inc_dif );
mae_acc = mean ( acc_dif );
mae_gis = mean ( gis_dif );

%% CALCULATE THE COEFFICIENT OF LINEAR CORRELATION %%

%% SLOPE %%
slope_n = slope ( ~isnan ( slope ) );
slope_inc_n = slope_inc ( ~isnan ( slope_inc ) );
slope_acc_n = slope_acc ( ~isnan ( slope_acc ) );
slope_gis_n = slope_gis ( ~isnan ( slope_gis ) );
rs_inc = corrcoef ( slope_n, slope_inc_n );
rs_acc = corrcoef ( slope_n, slope_acc_n );
rs_gis = corrcoef ( slope_n, slope_gis_n );

%% ASPECT %%
region_n = region ( ~isnan ( region ) );
region_inc_n = region_inc ( ~isnan ( region_inc ) );
region_acc_n = region_acc ( ~isnan ( region_acc ) );
region_gis_n = region_gis ( ~isnan ( region_gis ) );
ra_inc = corrcoef ( region_n, region_inc_n );
ra_acc = corrcoef ( region_n, region_acc_n );
ra_gis = corrcoef ( region_n, region_gis_n );

%% CALCULATE MODEL EFFICIENCY %%

%% CLINOMETER %%
inc_dif_sq = inc_dif.^2 ;
mean_slope = mean ( slope_n );
slope_2 = sum ( ( slope_n - mean_slope ).^2 ) ;
sum_inc_dif = sum ( inc_dif_sq ) ;
```

```
eff_inc = 1 - ( sum_inc_dif / slope_2 ) ;

%% ACCELEROMETER %%
acc_dif_sq = acc_dif.^2 ;
sum_acc_dif = sum ( acc_dif_sq );
eff_acc = 1 - ( sum_acc_dif / slope_2 ) ;

%% GIS %%
gis_dif_sq = gis_dif.^2 ;
sum_gis_dif = sum ( gis_dif_sq );
eff_gis = 1 - ( sum_gis_dif / slope_2 ) ;

%% LINEAR REGRESSION CALCULATION %%
reg_inc = [ones( size(slope_inc_n) ) slope_inc_n ];
lin_reg_inc = reg_inc \ slope_n;
reg_acc = [ones( size(slope_acc_n) ) slope_acc_n ];
lin_reg_acc = reg_acc \ slope_n;
reg_gis = [ones( size(slope_gis_n) ) slope_gis_n ];
lin_reg_gis = reg_gis \ slope_n;

%% COMPARISON ASPECT CALCULATION %%
for i=1:m
   for j=1:n
      if region_gis(i,j) == region (i,j)
         region_corr_gis(i,j) = 1;
      else
         region_corr_gis(i,j) = NaN;
      end
      if region_inc(i,j) == region(i,j)
         region_corr_inc(i,j) = 1;
      else
         region_corr_inc(i,j) = NaN;
      end
      if region_acc(i,j) == region(i,j)
         region_corr_acc(i,j) = 1;
      else
         region_corr_acc(i,j) = NaN;
      end
   end
end

% GETS THE TOTAL SIZE OF THE MATRIX %%
[e f] = size ( region_n );

%%CALCULATES THE % RIGHT ASPECT CLASSIFICATION %%
region_corr_gis2 = region_corr_gis ( ~ isnan ( region_corr_gis ) );
total_gis_asp = ( sum ( region_corr_gis2 ) / e ) * 100 ;
region_corr_inc2 = region_corr_inc ( ~ isnan ( region_corr_inc ) );
total_inc_asp = ( sum ( region_corr_inc2 ) / e ) * 100 ;
region_corr_acc2 = region_corr_acc ( ~ isnan ( region_corr_acc ) );
total_acc_asp = ( sum ( region_corr_acc2 ) / e ) * 100 ;
```

Matlab® Program Used to Compute Slope (continued)

```
%% PACK ASPECT CALCULATIONS %%
% aspect_n = aspect (~isnan (aspect) );
% aspect_gis_n = aspect_gis (~isnan (aspect_gis) );
% aspect_inc_n = aspect_inc (~isnan (aspect_inc) );
% aspect_acc_n = aspect_acc (~isnan (aspect_acc) );

%% WRITE THE RESULTS TO A FILE %%
res_out = [rs_gis(2,1) mae_gis  eff_gis  lin_reg_gis(1) lin_reg_gis(2) slope_gis_region_corr
ra_gis(2,1) total_gis_asp; rs_inc(2,1) mae_inc eff_inc lin_reg_inc(1) lin_reg_inc(2)
slope_inc_region_corr ra_inc(2,1) total_inc_asp; rs_acc(2,1) mae_acc eff_acc lin_reg_acc(1)
lin_reg_acc(2) slope_acc_region_corr ra_acc(2,1) total_acc_asp];
csvwrite('res_out.csv', res_out);
%% END %%
```

Matlab® Program Used to Compute Curvature

```
%% PROGRAM TO CALCULATE CURVATURE BASED ON SLOPE VALUES %%
%% CALCULATED WITH THE PROGRAM CEBOLA.M %%
%% PROGRAM NAME IS CURV.M %%
%% WRITEEN BY ROBERTO BARBOSA %%
%% FEBRUARY 2005 %%

[m,n] = size(slope);

%% CALCULATE SLOPE CHANGE %%
%% X %%
for i = 1 : m
   for j = 1 : n - 1
      if slope(i,j) == NaN | slope(i,j+1) == NaN
         curv_x(i,j) = NaN;
         curv_gis_x(i,j) = NaN;
         curv_inc_x(i,j) = NaN;
         curv_acc_x(i,j) = NaN;

      else
      curv_x(i,j) = ( slope(i,j+1) - slope(i,j) ) / d;
      curv_gis_x(i,j) = ( slope_gis(i,j+1) - slope_gis(i,j) ) / d;
      curv_inc_x(i,j) = ( slope_inc(i,j+1) - slope_inc(i,j) ) / d;
      curv_acc_x(i,j) = ( slope_acc(i,j+1) - slope_acc(i,j) ) / d;

      end
   end
end

%% Y %%
for i=2 : m
   for j=1 : n
      if slope_inc(i,j) == NaN | slope_inc(i-1,j) == NaN
         curv_y(i-1,j) = NaN;
         curv_gis_y(i-1,j) = NaN;
         curv_inc_y(i-1,j) = NaN;
         curv_acc_y(i-1,j) = NaN;
      else
      curv_y(i-1,j) = ( slope(i-1,j) - slope(i,j) ) / d;
      curv_gis_y(i-1,j) = ( slope_gis(i-1,j) - slope_gis(i,j) ) / d;
      curv_inc_y(i-1,j) = ( slope_inc(i-1,j) - slope_inc(i,j) ) / d;
      curv_acc_y(i-1,j) = ( slope_acc(i-1,j) - slope_acc(i,j) ) / d;
      end
   end
end

%% SURFACE DIFFERENCES %%
x_diff_gis = curv_gis_x - curv_x;
y_diff_gis = curv_gis_y - curv_y;
x_diff_inc = curv_inc_x - curv_x;
y_diff_inc = curv_inc_y - curv_y;
x_diff_acc = curv_acc_x - curv_x;
y_diff_acc = curv_acc_y - curv_y;
```

Matlab® Program Used to Compute Curvature (continued)

```
%% ELIMINATE NaN FROM MATRIX %%
x_diff_gis2 = x_diff_gis (~isnan(x_diff_gis));
y_diff_gis2 = y_diff_gis (~isnan(y_diff_gis));
x_diff_inc2 = x_diff_inc (~isnan(x_diff_inc));
y_diff_inc2 = y_diff_inc (~isnan(y_diff_inc));
x_diff_acc2 = x_diff_acc (~isnan(x_diff_acc));
y_diff_acc2 = y_diff_acc (~isnan(y_diff_acc));

%% CALCULATE MEAN ABSOLUTE VALUES %%
x_diff_gis3 = mean(abs(x_diff_gis2));
y_diff_gis3 = mean(abs(y_diff_gis2));
x_diff_inc3 = mean(abs(x_diff_inc2));
y_diff_inc3 = mean(abs(y_diff_inc2));
x_diff_acc3 = mean(abs(x_diff_acc2));
y_diff_acc3 = mean(abs(y_diff_acc2));

%% CALCULATE MEAN DIFFERENCE SURFACE %%
for i=2:m-1
   for j=2:n-1
      acd_calc(i,j) = ((slope(i,j) - slope(i-1,j-1)) + (slope(i,j) - slope(i,j-1)) + (slope(i,j) - slope(i+1,j-
1)) + (slope(i,j) - slope(i-1,j)) + (slope(i,j) - slope(i+1,j)) + (slope(i,j) - slope(i-1,j+1)) + (slope(i,j) -
slope(i,j+1)) + (slope(i,j) - slope(i+1,j+1))) / 8;
      acd_gis(i,j) = ((slope_gis(i,j) - slope_gis(i-1,j-1)) + (slope_gis(i,j) - slope_gis(i,j-1)) +
(slope_gis(i,j) - slope_gis(i+1,j-1)) + (slope_gis(i,j) - slope_gis(i-1,j)) + (slope_gis(i,j) -
slope_gis(i+1,j)) + (slope_gis(i,j) - slope_gis(i-1,j+1)) + (slope_gis(i,j) - slope_gis(i,j+1)) +
(slope_gis(i,j) - slope_gis(i+1,j+1))) / 8;
      acd_inc(i,j) = ((slope_inc(i,j) - slope_inc(i-1,j-1)) + (slope_inc(i,j) - slope_inc(i,j-1)) +
(slope_inc(i,j) - slope_inc(i+1,j-1)) + (slope_inc(i,j) - slope_inc(i-1,j)) + (slope_inc(i,j) -
slope_inc(i+1,j)) + (slope_inc(i,j) - slope_inc(i-1,j+1)) + (slope_inc(i,j) - slope_inc(i,j+1)) +
(slope_inc(i,j) - slope_inc(i+1,j+1))) / 8;
      acd_acc(i,j) = ((slope_acc(i,j) - slope_acc(i-1,j-1)) + (slope_acc(i,j) - slope_acc(i,j-1)) +
(slope_acc(i,j) - slope_acc(i+1,j-1)) + (slope_acc(i,j) - slope_acc(i-1,j)) + (slope_acc(i,j) -
slope_acc(i+1,j)) + (slope_acc(i,j) - slope_acc(i-1,j+1)) + (slope_acc(i,j) - slope_acc(i,j+1)) +
(slope_acc(i,j) - slope_acc(i+1,j+1))) / 8;
   end
end
acd_calc(1,:)=[];
acd_calc(:,1)=[];
acd_gis(1,:)=[];
acd_gis(:,1)=[];
acd_inc(1,:)=[];
acd_inc(:,1)=[];
acd_acc(1,:)=[];
acd_acc(:,1)=[];

%% END %%
```

Matblab Program Used to Compute Correlation Coefficient Between Sensor Data and RTK GPS Elevation Data

```
%% PROGRAM USED TO CALCULATE CORRELATION COEFFICIENT %%
%% BETWEEN RTK-GPS AND SENSOR DATA %%
%% WRITTEN BY ROBERTO BARBOSA %%
%% 2004 %%
clc;
clear;
filename = input('What is the file name?  ', 's');
outname = input('What is the output filename?   ', 's');
a=dlmread(filename, '\t');
%% Elev is the RTK GPS reading %%
Elev = a(:,3);
%% Dist was calculated based on GPS coordinates %%
Dist=a(:,4);
%% S1 is the clinometer data %%
s1=a(:,6);
%% S3 is the accelerometer data %%
s3=a(:,8);
[m n]=size(Elev);
for i=1:m-1
   Dif_Elev(i) = abs(Elev(i+1) - Elev(i));
end
mde = mean(Dif_Elev);
Grad = gradient(Elev);
%% Calculates the correlation coefficient %%
R_s1 = corrcoef(s1, Grad);
R_s3 = corrcoef(s3, Grad);
%% Filter grad of elev, S1 and S3 using 5 points %%
grad_f_5 = filter(ones(1,5) / 5, 1, Grad);
s1_f_5 = filter(ones(1,5) / 5, 1, s1);
s3_f_5 = filter(ones(1,5) / 5, 1, s3);
%% Calculates the correlation coefficient %%
R_s1_5 = corrcoef(s1_f_5,grad_f_5);
R_s3_5 = corrcoef(s3_f_5,grad_f_5);
%% Filter grad of elev, S1 and S3 using 10 points %%
grad_f_10 = filter(ones(1,10) / 10, 1, Grad);
s1_f_10 = filter(ones(1,10) / 10, 1, s1);
s3_f_10 = filter(ones(1,10) / 10, 1, s3);
%% Calculates the correlation coefficient %%
R_s1_10 = corrcoef(s1_f_10,grad_f_10);
R_s3_10 = corrcoef(s3_f_10,grad_f_10);
% Filter grad of elev, S1 and S3 using 15 points %%
grad_f_15 = filter(ones(1,15) / 15, 1, Grad);
s1_f_15 = filter(ones(1,15) / 15, 1, s1);
s3_f_15 = filter(ones(1,15) / 15, 1, s3);
%% Calculates the correlation coefficient %%
R_s1_15 = corrcoef(s1_f_15,grad_f_15);
R_s3_15 = corrcoef(s3_f_15,grad_f_15);
% Filter grad of elev, S1 and S3 using 20 points %%
grad_f_20 = filter(ones(1,20) / 20, 1, Grad);
s1_f_20 = filter(ones(1,20) / 20, 1, s1);
s3_f_20 = filter(ones(1,20) / 20, 1, s3);
```

```
%% Calculates the correlation coefficient %%
R_s1_20 = corrcoef(s1_f_20,grad_f_20);
R_s3_20 = corrcoef(s3_f_20,grad_f_20);
%% Calculates the coefficient of variation %%
coef_var = std(Elev) / mean(Elev);
cv_s1 = std(s1) / mean(s1);
cv_s3 = std(s3) / mean(s3);
%% output the results in a file %%
res_out = [coef_var mde cv_s1 cv_s3 R_s1(2,1) R_s1_5(2,1) R_s1_10(2,1) R_s1_15(2,1)
R_s1_20(2,1) R_s3(2,1) R_s3_5(2,1) R_s3_10(2,1) R_s3_15(2,1) R_s3_20(2,1)];
csvwrite(outname, res_out);
s1_out = [s1_f_5 s1_f_10 s1_f_15 s1_f_20];
csvwrite('s1_out.csv', s1_out);
s3_out = [s3_f_5 s3_f_10 s3_f_15 s3_f_20];
csvwrite('s3_out.csv', s3_out);
grad_out = [Grad grad_f_5 grad_f_10 grad_f_15 grad_f_20];
csvwrite('grad_out.csv', grad_out);
%% end %%
```

APPENDIX J

Error Distribution Analysis of Field #9 Data

Error distribution (%) in slope gradient estimation according to slope class, spatial resolution, and sensor

- **Spatial resolution: 4 m^2**

Slope Class: 0 to 2 degrees (n = 2,886)

Error (degrees)	Error Distribution (%)		
	GIS	Clinometer	Accelerometer
-5	0.0	0.0	0.0
-4	0.0	0.0	0.0
-3	0.0	0.0	0.0
-2	0.0	0.0	0.0
-1	0.5	1.8	1.4
0	43.1	20.2	16.4
1	51.1	34.8	32.6
2	3.1	25.3	27.9
3	1.4	12.7	14.1
4	0.7	3.2	5.0
5	0.1	1.0	1.6

Slope Class: 2 to 4 degrees (n = 3,037)

Error (degrees)	Error Distribution (%)		
	GIS	Clinometer	Accelerometer
-5	0.0	0.0	0.0
-4	0.0	0.0	0.0
-3	0.0	0.0	0.0
-2	0.7	2.4	1.5
-1	4.7	14.1	6.6
0	42.8	24.3	23.4
1	41.3	25.3	33.3
2	5.8	15.9	20.9
3	2.5	10.3	8.3
4	1.4	4.2	4.0
5	0.6	1.9	1.4

Error distribution (%) in slope gradient estimation according to slope class, resolution, and sensor (continued)

- **Spatial resolution: 4 m^2**

Slope Class: 4 to 6 degrees (n = 1,901)

Error (degrees)	Error Distribution (%)		
	GIS	Clinometer	Accelerometer
-5	0.0	0.0	0.1
-4	0.2	0.5	1.0
-3	1.8	2.0	2.6
-2	3.1	6.7	5.1
-1	7.5	14.0	12.2
0	35.7	16.3	21.9
1	33.2	14.7	22.0
2	13.2	16.1	17.7
3	4.1	15.1	9.2
4	1.0	8.3	5.3
5	0.4	4.7	2.5

Slope Class: Above 6 degrees (n = 1,523)

Error (degrees)	Error Distribution (%)		
	GIS	Clinometer	Accelerometer
-5	6.9	6.0	13.2
-4	5.3	4.2	8.5
-3	6.7	8.9	12.5
-2	10.0	13.5	18.7
-1	23.1	19.4	21.1
0	45.4	20.7	22.1
1	26.2	17.7	16.9
2	6.0	18.0	10.6
3	1.2	13.5	4.8
4	0.4	6.6	2.3
5	0.1	1.9	0.6

Error distribution (%) in slope gradient estimation according to slope class, resolution, and sensor

- **Spatial resolution: 16 m^2**

Slope Class: 0 to 2 degrees (n = 658)

Error (degrees)	Error Distribution (%)		
	GIS	Clinometer	Accelerometer
-5	0.0	0.0	0.0
-4	0.0	0.0	0.0
-3	0.0	0.0	0.0
-2	0.0	0.0	0.0
-1	0.6	0.5	1.1
0	48.6	40.1	33.9
1	48.8	54.7	60.3
2	1.8	4.0	3.6
3	0.2	0.8	0.9
4	0.0	0.0	0.2
5	0.0	0.0	0.0

Slope Class: 2 to 4 degrees (n = 736)

Error (degrees)	Error Distribution (%)		
	GIS	Clinometer	Accelerometer
-5	0.0	0.0	0.0
-4	0.0	0.0	0.0
-3	0.0	0.1	0.1
-2	0.5	0.5	2.3
-1	5.0	3.9	5.0
0	54.3	42.1	27.0
1	39.0	46.6	59.9
2	1.1	5.7	4.8
3	0.0	0.8	0.7
4	0.0	0.1	0.1
5	0.0	0.0	0.0

Error distribution (%) in slope gradient estimation according to slope class, resolution, and sensor (continued)

- **Spatial resolution: 16 m^2**

Slope Class: 4 to 6 degrees (n = 505)

Error (degrees)	Error Distribution (%)		
	GIS	Clinometer	Accelerometer
-5	0.0	0.0	0.2
-4	0.0	0.2	1.4
-3	0.8	1.2	3.4
-2	2.6	1.8	5.7
-1	4.8	3.4	7.5
0	48.7	26.7	35.8
1	41.0	50.5	36.6
2	2.2	13.5	8.5
3	0.0	2.2	0.6
4	0.0	0.6	0.2
5	0.0	0.0	0.0

Slope Class: Above 6 degrees (n = 373)

Error (degrees)	Error Distribution (%)		
	GIS	Clinometer	Accelerometer
-5	0.5	0.3	3.2
-4	0.8	1.6	9.4
-3	1.9	2.1	14.7
-2	2.9	4.3	9.7
-1	11.3	4.8	10.7
0	51.5	31.9	32.4
1	30.3	42.4	18.5
2	0.8	11.8	1.3
3	0.0	0.8	0.0
4	0.0	0.0	0.0
5	0.0	0.0	0.0

Error distribution (%) in slope gradient estimation according to slope class, resolution, and sensor

- **Spatial resolution: 100 m^2**

Slope Class: 0 to 2 degrees (n = 102)

Error (degrees)	Error Distribution (%)		
	GIS	Clinometer	Accelerometer
-5	0.0	0.0	0.0
-4	0.0	0.0	0.0
-3	0.0	0.0	0.0
-2	0.0	0.0	0.0
-1	0.0	0.0	1.0
0	52.9	43.1	35.3
1	47.1	56.9	62.7
2	0.0	0.0	1.0
3	0.0	0.0	0.0
4	0.0	0.0	0.0
5	0.0	0.0	0.0

Slope Class: 2 to 4 degrees (n = 109)

Error (degrees)	Error Distribution (%)		
	GIS	Clinometer	Accelerometer
-5	0.0	0.0	0.0
-4	0.0	0.0	0.0
-3	0.0	0.0	0.0
-2	0.0	0.0	3.7
-1	0.9	2.8	1.8
0	72.5	34.9	21.1
1	26.6	61.5	72.5
2	0.0	0.9	0.9
3	0.0	0.0	0.0
4	0.0	0.0	0.0
5	0.0	0.0	0.0

Error distribution (%) in slope gradient estimation according to slope class, resolution, and sensor (continued)

- **Spatial resolution: 100 m^2**

Slope Class: 4 to 6 degrees (n = 74)

Error (degrees)	Error Distribution (%)		
	GIS	Clinometer	Accelerometer
-5	0.0	0.0	0.0
-4	0.0	0.0	2.7
-3	0.0	0.0	1.4
-2	1.4	0.0	4.1
-1	1.4	4.1	6.8
0	58.1	14.9	35.1
1	39.2	68.9	47.3
2	0.0	10.8	2.7
3	0.0	1.4	0.0
4	0.0	0.0	0.0
5	0.0	0.0	0.0

Slope Class: Above 6 degrees (n = 51)

Error (degrees)	Error Distribution (%)		
	GIS	Clinometer	Accelerometer
-5	0.0	0.0	0.0
-4	0.0	0.0	9.8
-3	0.0	0.0	11.8
-2	0.0	3.9	15.7
-1	7.8	7.8	11.8
0	84.3	11.8	23.5
1	7.8	66.7	25.5
2	0.0	9.8	2.0
3	0.0	0.0	0.0
4	0.0	0.0	0.0
5	0.0	0.0	0.0

APPENDIX K

Correlation Matrix of Results in Different Spatial Resolutions

Resolution: 4 m^2

The CORR Procedure

4 Variables: CALC GIS CLIN ACC

Simple Statistics

Variable	N	Mean	Std Dev	Sum	Minimum	Maximum
CALC	9347	3.51095	2.31842	32817	0.06993	15.62400
GIS	9347	3.42539	2.14185	32017	0.01880	10.48100
CLIN	9347	4.06950	2.52646	38038	0.03511	12.47400
ACC	9347	3.89466	2.10034	36403	0.03220	11.98600

Pearson Correlation Coefficients, N = 9347
Prob > |r| under H0: Rho=0

	CALC	GIS	CLIN	ACC
CALC	1.00000	0.85434	0.71138	0.62918
		<.0001	<.0001	<.0001
GIS	0.85434	1.00000	0.78450	0.70013
	<.0001		<.0001	<.0001
CLIN	0.71138	0.78450	1.00000	0.79109
	<.0001	<.0001		<.0001
ACC	0.62918	0.70013	0.79109	1.00000
	<.0001	<.0001	<.0001	

Resolution: 16 m^2

The CORR Procedure

4 Variables: CALC GIS CLIN ACC

Simple Statistics

Variable	N	Mean	Std Dev	Sum	Minimum	Maximum
CALC	2272	3.53865	2.15002	8040	0.04000	11.99300
GIS	2272	3.38617	2.08058	7693	0.08540	9.46680
CLIN	2272	3.64136	2.25086	8273	0.11793	9.65850
ACC	2272	3.30650	1.89942	7512	0.07778	9.10650

Pearson Correlation Coefficients, N = 2272
Prob > |r| under H0: Rho=0

	CALC	GIS	CLIN	ACC
CALC	1.00000	0.95412	0.93229	0.82744
		<.0001	<.0001	<.0001
GIS	0.95412	1.00000	0.94460	0.82079
	<.0001		<.0001	<.0001
CLIN	0.93229	0.94460	1.00000	0.88232
	<.0001	<.0001		<.0001
ACC	0.82744	0.82079	0.88232	1.00000
	<.0001	<.0001	<.0001	

Resolution: 100 m^2

The CORR Procedure

4 Variables: CALC GIS CLIN ACC

Simple Statistics

Variable	N	Mean	Std Dev	Sum	Minimum	Maximum
CALC	336	3.42043	2.10883	1149	0.07375	8.19210
GIS	336	3.28945	2.02686	1105	0.28508	7.85350
CLIN	336	3.58100	2.24093	1203	0.32214	8.83730
ACC	336	3.22462	1.86790	1083	0.10430	8.21570

Pearson Correlation Coefficients, N = 336
Prob > |r| under H0: Rho=0

	CALC	GIS	CLIN	ACC
CALC	1.00000	0.98675	0.97206	0.85938
	<.0001	<.0001	<.0001	
GIS	0.98675	1.00000	0.96350	0.83696
	<.0001		<.0001	<.0001
CLIN	0.97206	0.96350	1.00000	0.88391
	<.0001	<.0001		<.0001
ACC	0.85938	0.83696	0.88391	1.00000
	<.0001	<.0001	<.0001	

APPENDIX L

Permission to Use Figure 1

Dear Roberto,

You are very welcome to use this or other graphics as you need. We would
appreciate a proper citation as shown on the first page of the
Acknowledgements (page i) of the Field Book.

We wish you well in your professional pursuits and are gratified that our
work is of some use to you.

Sincerely,

Dr. Philip J. Schoeneberger

-----Original Message-----
From: rbarbosa@utk.edu [mailto:rbarbosa@utk.edu]
Sent: Wednesday, February 23, 2005 7:41 AM
To: Doug Wysocki; Philip Schoeneberger
Subject: Permission to use figure

Dear Sir(s),

I am writing my dissertation and I would like to use the figure exemplifying
the nine possible slope shapes, created by you and printed on the NSSC -
NRCS Field Book for Describing and Sampling Soils (p. 3-38).

I hereby ask your permission for such use, assuring that acknowledgement
will be given in the document, citing proper sources.

Sincerely,

____
****

Roberto N Barbosa
Biosystems Engineering Department
University of Tennessee
Phone: 865/974-2676
Fax: 865/974-4514
Email: rbarbosa@utk.edu

____
****

VITA

Roberto Negrão Barbosa was born May 26, 1967 in São Paulo, Brazil. He graduated in Agronomy at the State University of Londrina in 1990. In 1994, Roberto received a Fulbright Scholarship to pursue advanced studies in the United States. He received a Master of Science degree with a major in Agricultural Engineering Technology from The University of Tennessee in 1996.

In 2001, Roberto returned to the United States to pursue a doctoral degree, upon invitation of the Biosystems Engineering Department. In the spring of 2005 Roberto was invited by the Biological and Agricultural Department of The Louisiana State University for an Assistant Professor position, which started in the fall of 2005.